6-22-2018

Impact of San-mediated Signaling on Glioblastoma and Neuroblastoma Metabolism

Monica Rodriguez Silva
Florida International University, mrodr204@fiu.edu

DOI: 10.25148/etd.FIDC006885

FLORIDA INTERNATIONAL UNIVERSITY

Miami, Florida

IMPACT OF SAB-MEDIATED SIGNALING ON GLIOBLASTOMA AND NEUROBLASTOMA METABOLISM

A dissertation submitted in partial fulfillment of the

requirements for the degree of

DOCTOR OF PHILOSOPHY

in

BIOMEDICAL SCIENCES

by

Monica Rodriguez Silva

2018

To: Dean John Rock
Herbert Wertheim College of Medicine

This dissertation, written by Monica Rodriguez Silva, and entitled Impact of Sab-mediated Signaling on Glioblastoma and Neuroblastoma Metabolism, having been approved in respect to style and intellectual content, is referred to you for judgment.

We have read this dissertation and recommend that it be approved.

_____
Ralph DeBerardinis

_____
Nazira El-Hage

_____
Lidia Kos

_____
Helen Tempest

_____
Jeremy W. Chambers, Major Professor

Date of Defense: June 22, 2018

The dissertation of Monica Rodriguez Silva is approved

_____
Dean Jonh Rock
Herbert Wertheim College of Medicine

_____
Andres G. Gil
Vice President for Research and Economic Development
And Dean of the University Graduate School

Florida International University, 2018

DEDICATION

To my cousin Eduardo

Thank you for sending me on this fantastic journey

ACKNOWLEDGMENTS

At many points during this journey I was convinced this day would never come, that all the challenges I was facing was the Universe's way of telling me that "this road was not for me" and I needed to move on. Like raising a small child, perhaps a scientific one, it took a village to get me here and I couldn't have done it alone.

I want to thank my advisor Dr. Jeremy Chambers, Jimmy, I know he believes in actions more than words, so I hope that whatever I do next will be a reflection of how grateful I am. There are simply no words, you took me in your lab at one of my lowest points, you gave me a chance when nobody else would, and more importantly you believed in me (I had forgotten what that was like). These few years in the lab have been a tremendous learning experience, both personally and scientifically, thank you so much for the support, all the opportunities, the advice, the laughs, and especially thank you for helping me reconnect with my passion for science, before I came to your lab I thought I had lost it forever.

I definitely wouldn't be here if it wasn't for you Ivan, thank you for not letting me quit, for pushing me to be better, for making me laugh even when I didn't want to, for always being there. These past few years have been rough, and you've have been such a rock, I can't wait to see what the future holds for us, we got this! And I'm only going to say this once, you were right I would've regretted quitting, so thank you!!!!

I want to thank my lab mates, specially Arlet, I've learned a lot from you and it has been fun having another cancer person in the lab, you've made me laugh and more importantly you have that calming energy I needed so many days when I was so

stressed out. Tony, I don't think I've ever laughed so much in the lab, also thank you for all those awesome boss' stories. I can't forget my ladies from upstairs, Jen, KK, Mer and Deb, you ladies rock! Thank you for teaching so many new things and for all your support both inside and outside the lab.

And last but not least, my family. My parents for all the support throughout the years, I know this took a little longer than expected, but they managed to keep the when are you going to finish? questions to a minimum. Mi Lala, you know me better than most people, and know exactly what to say whenever I call you, just by saying hello you can tell what I need, thank you for all the vamos Monica, tienes que terminar. My sisters, the blood-related ones, Vero and Tina, and the one that life gave me, Vane, you guys can't even imagine how important you're for me, thank you for the support, the laughter, the tears and the tough love through the years. My furry children, Mali, Olivia, Kira and Bonz, thank you for helping keep my sanity and teaching me to be patient, enjoy the little things and live in the moment.

I can't forget to thank my cousin Eduardo and mi Lalo, I decided to be scientist when I was 13 years old, and I did it because of you guys. Thank you for being my guardian angels and for being that guiding star that kept me going when things got tough. I miss you guys every day.

I would like to extend our gratitude to Dr. William Reinhold at NCI for providing the NCI60 GBM cell lines used for this project. M.R.S was supported by NIH/NIGMS R25 GM06134.

ABSTRACT OF THE DISSERTATION

IMPACT OF SAB-MEDIATED SIGNALING ON GLIOBLASTOMA AND NEUROBLASTOMA METABOLISM

by

Monica Rodriguez Silva

Florida International University, 2018

Miami, Florida

Professor Jeremy W. Chambers, Major Professor

Glioblastoma (GBM) is the most common and aggressive type of brain cancer, with an average life expectancy of 15 months. The standard of care for GBM, surgery accompanied by radiation and chemotherapy (temozolomide-TMZ), has not changed in over 10 years illustrating the need for new and efficacious treatments. Therefore, it is imperative to improve our knowledge of GBM physiology to understand the mechanisms driving recurrence and chemoresistance so that more effective therapeutic options can be developed. Mitochondria-cell communication is key to monitor and maintain both mitochondrial and cellular health, and signaling events on the outer mitochondrial membrane (OMM) have emerged as a crucial signal integration site for cellular responses. Consequently, proteins on the OMM are crucial to determining cellular survival and dictating organelle physiology. Thus, the goal of our current study is to evaluate OMM proteins to determine how alterations in organelle regulation may impact CNS tumor biology. We first measured the concentrations of Bcl-2 family proteins on mitochondria from ten continuous GBM cell lines and correlated the protein

levels to IC_{50} values of genotoxic agents TMZ and irinotecan. We found that Bcl-2 levels corresponded to chemoresistance, while increased Bim concentrations promoted chemosensitivity. In contrast to our studies in gynecological cancers, the concentrations of the pro-dysfunction OMM scaffold protein Sab had no impact on chemosensitivity of the GBM cell lines, despite diminished Sab expression in GBM patients. However, we identified a novel truncated variant of Sab in the GBM cell lines. We found that GBM cells expressing only full-length Sab had a slower proliferation rate than those with the variant, which could be attributed to increased glycolysis in GBM cells expressing the Sab variant. To determine if the lack of Sab-mediated apoptosis was consistent across CNS tumors, we analyzed publicly-available patient data and found that Sab expression is down-regulated in neuroblastoma patients, a pediatric malignancy responsible for 12% of childhood cancer deaths. We found that that inhibiting Sab-mediated signaling in human neuroblastoma (SH-SY5Y cells) enhanced oxidative phosphorylation in a pyruvate dehydrogenase-dependent manner, increased BCl-2 levels (pro-survival), decreased Bim concentrations (pro-apoptotic), and promoted chemoresistance. Furthermore, examination of additional neuroblastoma cells derived from CNS tumors revealed that Sab levels correspond to proliferation rate, metabolic phenotype, and chemosensitivity. Our studies demonstrate the importance of OMM signaling in CNS tumor physiology and emphasizes the importance of cellular context to the outcomes of OMM signaling events.

TABLE OF CONTENTS

LIST OF TABLES

TABLE PAGE

LIST OF FIGURES

FIGURE PAGE

ABBREVIATIONS AND ACRONYMS

A1	Bcl-2-related gene A1
ABTA	American Brain Tumor Association
ACS	American Cancer Society
ADP	Adenosine diphosphate
AICAR	Aminoimidazole-4-carboxamide ribotide
AKT	AKT serine/threonine kinase 1
ALK	Anaplastic lymphoma kinase
ASCL1	Achaete-scute family bHLH transcription factor 1
ATP	Adenosine triphosphate
ATRX	Alpha thalassemia/mental retardation syndrome X-linked
BAD	Bcl-2 associated agonist of cell death
BAK	Bcl-2 antagonist killer 1
BAX	Bcl-2 associated X protein
Bcl-2	B-cell lymphoma-2
Bcl-xL	Bcl-2-related gene, long isoform
BH	Bcl-2 homology
BID	Bcl-2 interacting domain agonist
BIK	BCL-2 interacting killer
BIM	Bcl-2 interacting mediator of cell death
BITCs	Brain tumor initiating cells
BMF	BCL-2 modifying factor
BTSC	Brain tumor stem cells

CCND1	Cyclin D1
CDK4	Cyclin dependent kinase 4
CDK6	Cyclin dependent kinase 6
CDKN1A	Cyclin dependent kinase inhibitor 1A
CDKN2A	Cyclin dependent kinase inhibitor 2A
CHI3L-1	Chitinase 3 like 1
CNS	Central nervous system
COI	Cytochrome C oxidase I
COL5A	Collagen, type 5, alpha 1
COX	Cyclooxygenase
DCA	Dichloroacetate
2-DG	2-deoxyglucose
DLL3	Delta like canonical Notch ligand 3
DNA	Deoxyribonucleic acid
DROSHA	Drosha ribonuclease III
EGF	Epidermal growth factor
EGFR	Epidermal growth factor receptor
EMT	Epithelial to mesenchymal transition
ERK	Extracellular signal-regulated kinase
FABP3	Fatty acid-binding protein 3
FABP7	Fatty acid-binding protein 7
FBP	Fructose-1,6-biphosphate
FH	Fumarate hydratase

G6PC	Glucose-6-phosphatase complex
GABA	gamma-aminobutiric acid
GABRA1	gamma-aminobutyric acid type A receptor alpha1 subunit
GAC	Glutaminase C
GBM	Glioblastoma
G-CIMP	Glioma-CpG island methylator phenotype
GICs	Glioma-initiating cells
GLS	Glutaminase
GLUD	Glutamate dehydrogenase
GLUT1	Glucose transporter I
GM-CSF	Granolucyte-macrophage colony stimulating factor
GRIM-19	Gene associated with retinoid-interferon-induced mortality-19
GS	Glutamine synthase
HDAC	Histone deacetylases
2-HG	2-Hydroxyglutarate
HIF1-α	Hypoxia-inducible factor 1-alpha
HK	Hexokinase
HOG	Human oligodendroglioma
HRK	Harakiri
HtrA2	HtrA serine peptidase 2
IDH	Isocitrate dehydrogenase
IDRFs	Image-defined risk factors
IGFBP2	Insulin-like growth factor binding protein 2

IGFR1	Insulin-like growth factor receptor 1
IL-2	Interleukin-2
IMP	Inosine monophosphate
IMS	Inter-membrane space
iNOS	Inducible nitric oxide synthase
INRG	International Neuroblastoma Risk Group
INSS	International Neuroblastoma Staging System
IRF3	Interferon regulatory factor 3
JNK	c-Jun N-Terminal Kinase
α-KG	alpha-ketoglutarate
KDM1B	Lysine demethylase 1B
KIM	Kinase interaction motif
LD	Lipid droplets
LDHA	Lactate dehydrogenase A
MAPK	Mitogen activated protein kinase
Mcl-1	Myeloid cell leukemia
MEK	MAPK/ERK kinase
MERTK	MER proto-oncogene, tyrosine kinase
MET	Mesenchymal epithelial transition
MGMT	O-6-methylguanine-DNA-methyltransferase
MOM	Mitochondrial outer membrane
MOMP	Mitochondrial outer membrane permeabilization
MRS	Magnetic resonance spectroscopy

MSO	L-methionine sufoximine
mtDNA	Mitochondrial DNA
mTOR	Mammalian target of rapamycin
mtPTP	Mitochondrial permeability transition pore
MYC	MYC proto-oncogene, bHLH transcription factor
MYCN	MYCN proto-oncogene, bHLH transcription factor
NADP	Nicotinamide adenine dinucleotide phosphate
NCI	National Cancer Institute
ND3	NADH:ubiquinone oxidoreductase core subunit 3
NEFL	Neurofilament light
NF1	Neurofibromin 1
NKX2-2	NK2 homeobox 2
NMR	Nuclear magnetic resonance
N-Myc	N-myc proto-oncogene protein
OAA	Oxaloacetate
ODD	Oxygen-depedent degradation
OLIG2	Oligodendrocyte transcription factor 2
PAR	Poly-ADP-ribose
PARP1	Poly-ADP-ribose polymerase-1
PC	Pyruvate carboxylase
PDC	Pyruvate dehydrogenase complex
PDGFRA	Platelet derived growth factor alpha
PDH	Pyruvate dehydrogenase

PDK1	Pyruvate dehydrogenase kinase 1
PEP	Phosphoenolpyruvate
PFK1	Phosphofructokinase
PHD	Prolyl-hydroxylases
PHOX2B	Paired-like homeobox 2B
PI3K	Phosphatidyl inositol 3-kinase
PIK3CA	phosphatidylinositol-4,5-bisphosphate 3-kinase catalytic subunit alpha
PIK3R1	phosphoinositide-3-kinase regulatory subunit 1
PIN1	Peptidyl-prolyl Cis/Trans Isomerase, NIMA-Interacting 1
PK	Pyruvate kinase
PKC-δ	Protein kinase C-delta
PKM2	Pyruvate kinase M2
PPP	Pentose phosphate pathway
PTEN	Phosphatase and tensin homolog
PUMA	p53 modulator of apoptosis
pVHL	Von Hippel-Lindau tumor suppressor
Rb	Retinoblastoma
Redox	Reduction-oxidation
RELB	RELB proto-oncogene, NF-kB subunit
ROS	Reactive oxygen species
RTK	Receptor tyrosine kinase
SAICAR	Succinyl-5-aminoimidazole-4-carboxamide-1-ribose-5'-phosphate

SCT	Stem cell transplantation
SDH	Succinate dehydrogenase
shRNA	Short hairpin ribonucleic acid
SHMT2	Serine hydroxymethyltransferase
siRNA	Small interference RNA
SLC12A5	Solute carrier family 12 member 5
SMAC	Second mitochondria-derived activator of caspase
SOX	SRY-boxes
STAT3	Signal transducers and activators of transcription
SYT1	Synaptotagmin 1
TCA	Tricarboxylic acid
TCF4	Transcription factor 4
TCGA	The Cancer Genome Atlas
TERT	Telomerase reverse transcriptase
TIGAR	TP53-induced glycolysis and apoptosis regulator
TMZ	Temozolomide
TNFRSF1A	TNF receptor superfamily member 1A
TRADD	TNFRSF1A associated via death domain
TTFields	Tumor treating fields
VEGF	Vascular endothelial growth factor
WHO	World Health Organization
ZEB1	Zinc finger E-box binding homeobox 1

CHAPTER I

Literature Review

Central Nervous System Malignancies

Cancers that affect brain and spinal cord tissue are considered central nervous system (CNS) tumors. Using an integrated system of both phenotypic and genotypic characteristics, CNS tumors can be classified as diffused astrocytic and oligodendroglial tumors, neuronal and mixed neuronal glial tumors, tumors of the pineal region, embryonal tumors, ependymal tumors, choroid plexus tumors, meningiomas, cranial and paraspinal nerves tumors, melanocytic tumors, lymphomas, mesenchymal non-meningothelial tumors, histiocytic tumors, germ cell tumors, tumors of the sellar region and metastatic tumors. For the purpose of our research, the focus will be on glioblastoma (GBM), a type of diffused astrocytic and oligodendroglial tumor, and neuroblastoma a kind of embryonal tumor (Louis et al., 2016).

1. Glioblastoma

Glioblastoma (GBM) is the most aggressive and common type of primary brain tumor in adults, patient survival is generally less than 15 months following diagnosis (Ostrom et al., 2016). GBM is notorious for the extensive cellular heterogeneity within a tumor, which is even more complex when one considers that the etiology of GBM is unknown. GBMs are believed to originated from either adult neural stem cells or glial cells, specifically astrocytes (Alcantara Llaguno et al., 2016; Phillips et al., 2006). The clinical presentation of GBM varies depending on size, location, and regions of the brain affected. The areas of the brain impacted by GBM lead to clinical symptoms that often precipitate a diagnosis, but only after the tumor has grown significantly. Most patients will present headaches, increased

intercranial pressure and focal or progressive neurological deficits (M. E. Davis, 2016).

1.1 Statistics

The National Cancer Institute (NCI) estimates that brain tumors account for 85%-90% of all primary CNS tumors, anaplastic astrocytomas and glioblastomas are the most common and represent 38% of cases of primary brain tumors (Noone et al., 2018). GBM commonly affects older adults, with the median age of diagnosis being 64 years old, and rarely affects children (Thakkar et al., 2014). The American Brain Tumor Association (ABTA) estimates the median survival for patients treated concurrently with temozolomide (TMZ) and radiotherapy to be 14.6 months, two-year survival is around 30%, however less than 10% of patients will survive five years or longer (Stupp et al., 2015). Thus, it is imperative to improve the collective knowledge regarding GBM pathogenesis from both the basic science and clinical perspective to improve diagnostic strategies and develop more efficacious treatment options for GBM patients.

1.2 GBM stages and classification

The World Health Organization (WHO) classifies CNS tumors according to a malignancy scale based on the tumor's histologic features. CNS tumor grades are defined as follows (Kleihues et al., 1993):

a. Grade I: slow proliferating tumors that have low invasive potential, tumors are localized, and surgical resection alone is sufficient treatment.

b. Grade II: tumors show slow proliferating rates but have more invasive potential than grade I tumors, overtime tumors are more likely to recur and become more aggressive.
c. Grade III: tumors are highly proliferative, have increased invasive potential and show histologic evidence of malignancy, such as nuclear atypia.
d. Grade IV: tumors are highly proliferative, prone to necrosis, and show rapid preoperative progression and postoperative reoccurrence. All GBM tumors are considered to be grade IV.

GBMs can be further classified into four subtypes based on gene expression patterns and genomic alterations, this classification is clinically relevant and allows better patient stratification for targeted therapies. The four molecular subtypes are described below (Table 1) (Verhaak et al., 2010).

1.3 GBM features

GBMs exhibits common hallmarks of cancer including genomic instability, ability to diffusely infiltrate tissue, increased resistance to apoptosis, unrestricted proliferation, and dysregulated angiogenesis (Hanahan and R. A. Weinberg, 2011). These characteristics, combined with significant tumor heterogeneity, and the constant presence of cancer stem cells, make GBMs a particularly complex and difficult disease to treat malignancy (Furnari et al., 2007) Specific genetic modifications that occur in GBMs sustain tumor biology and alter metabolism, collectively, these alterations enhance the survival of GBM tumor cells in the stressful tumor microenvironment.

Comprehensive genomic analysis of GBM samples for The Cancer Genome Atlas (TCGA) project determine alterations in the three main pathways, namely aberrant activation of receptor tyrosine kinase (RTK)/ Ras/phosphatidyl inositol 3-kinase

Table 1. Gene expression based molecular classification of GBM subtypes. (Adapted from (Verhaak et al., 2010)

GBM SUBTYPE	MOLECULAR SIGNATURE
Classical	Chromosome 7 amplification paired with chromosome 10 loss High level EGFR amplification No TP53 mutations Focal 9p21.3 homozygous deletion, target CDKN2A High expression of stem cell marker Nes, and signaling pathways Notch and Sonic hedgehog
Mesenchymal	Focal 17q11.2 hemizygous deletion, target NF1 Expression of mesenchymal marker CHI3L Expression of astrocytic markers CD44 and MERTK Increased expression of TRADD, RELB, TNFRSF1A (NF-κB pathway)
Proneural	PDGFRA alterations, focal amplifications at 4q12 and high PDGFRA expression IDH1 point mutations TP53 loss of heterozygosity and mutations High expression of oligodendrocytic development genes PDGFRA, NKX2-2, OLIG2 Low expression of CDKN1A PIK3CA/PIK3R1 mutations Expression of proneural development genes SOX, DCS, DLL3, ASCL1, TCF4
Neural	Expression of neuron markers NEFL, GABRA1, SYT1 and SLC12A5

(PI3K) signaling, and inactivation of tumor suppressor pathways p53 and retinoblastoma (Rb) (Cancer Genome Atlas Research Network, 2008). Moreover, amplifications on chromosome 7 (epidermal growth factor receptor - EGFR, mesenchymal epithelial transition - MET and cyclin dependent kinase 6 - CDK6), chromosome 12 (cyclin dependent kinase 4 - CDK4 and E3 ubiquitin-protein ligase MDM2) and chromosome 4 (platelet derived growth factor alpha - PDGFRA) are the most common, and mutations on the telomerase reverse transcriptase (TERT) promoter enhance telomere maintenance, promoting sustained cell survival (Brennan et al., 2013).

Mutations in certain metabolic enzymes, such as isocitrate dehydrogenase (IDH) or pyruvate kinase M2 (PKM2), facilitate the use of aerobic glycolysis by GBM tumors. Furthermore, the distinctive metabolites produced by the mutated enzymes can induce oncogenic changes by affecting epigenetics (Agnihotri and Zadeh, 2016; Wolf et al., 2010).

Isocitrate dehydrogenases (IDH1, IDH2) produce α-ketoglutarate (α-KG) from isocitrate and reduce $NADP^+$ to NADPH (Krell et al., 2011). Mutations on the IDH active site results in 80% reduction of enzymatic activity, decreased levels of α-KG and a gain of alternative function for the enzyme, which now reduces α-KG in an NADP-dependent manner to produce 2-hydroxyglutarate (2-HG) (Dang et al., 2009; Zhao et al., 2009). 2-HG acts as an oncometabolite by inhibiting α-KG-dependent histone demethylases resulting in hypermethylation at a large number of genetic loci, collectively known as the glioma-CpG island methylator phenotype (G-CIMP) (Noushmehr et al., 2010; Xu et al., 2011). Decreased levels of α-KG

result in stabilization and increased levels of hypoxia-inducible factor 1-alpha (HIF1-α), which orchestrates a concerted response within mammalian cells under hypoxic conditions by inducing the expression of genes involved in angiogenesis and glucose metabolism (Semenza, 1999; Zhao et al., 2009). Furthermore, interaction of HIF1-α with nuclear PKM2 promotes transactivation of HIF1-α target genes such as glucose transporter (GLUT1), lactate dehydrogenase A (LDHA), and pyruvate dehydrogenase kinase 1 (PDK1). HIF1-α also promotes the transcription of PKM2 creating a feedforward loop that amplifies the HIF1-α metabolic reprogramming (Luo et al., 2011).

1.4 Standard of care and current therapies

Treatment for newly diagnosed GBM patients is surgery follow by a combination of radiotherapy and chemotherapy with temozolomide (TMZ), a DNA alkylating agent. Promoter methylation status for O-6-methylguanine-DNA-methyltransferase (MGMT) serves as a predictor for patients that would benefit from TMZ treatment (Hegi et al., 2005). The standard of care for GBM patients has not changed in more than 10 years, the approach is largely ineffective, and responses vary greatly between patients. (Hegi et al., 2005; Stupp et al., 2005). Recently, tumor treating fields (TTFields) have undergone clinical trials for treatment of newly diagnosed GBM patients (Stupp et al., 2015). These alternating, intermediate frequency, low-intensity electric fields, disrupt tumor growth by promoting cell cycle arrest and apoptosis. TTFields in combinations with TMZ prolong progression-free survival and overall survival (Hottinger et al., 2016).

2. Neuroblastoma

Neuroblastoma arises from precursor cells of the sympathetic nervous system derived from the neural crest (Maris et al., 2007). The majority of neuroblastoma tumors will develop on the adrenal glands, but it can also develop in the abdomen, chest and neck (Maris et al., 2007). Primary CNS neuroblastoma is a rare type of intracranial tumor that usually presents during the first five years of life (Bianchi et al., 2018). CNS neuroblastomas are mostly located in the supratentorial region of the brain and characteristically show poorly differentiated neuroepithelial cells, groups of neurocytic cells, variable neuropil-rich stroma. Clinical presentation varies widely, with seizures and focal neurological deficits being the most common symptoms (Bianchi et al., 2018).

2.1 Statistics

According to the American Cancer Society (ACS), neuroblastoma is the most common type of cancer in children younger than one year old, approximately 90% of the cases are diagnosed before five years of age and it is rarely observed in people over ten years old (E. Ward et al., 2014). In the United States, according to the National Cancer Institute (NCI) 650 new cases are diagnosed every year, it represents 5% of all pediatric cancer diagnoses but it is responsible for up to 12% of childhood cancer mortality (Bosse and Maris, 2016). The overall five-year survival rate is 80.2% (1975-2015) (Noone et al., 2018). The age of diagnosis plays a significant role in survival rates, where the relative survival rate for children diagnosed before one year old is 91.1%, decreasing to 54.1% for diagnoses between 15-19 years of age (Noone et al., 2018). Primary CNS neuroblastoma are

relative rare cases and statistics for this kind of tumor are limited (Bianchi et al., 2018). Great advances have been made in recent years for treatment of lower risk cases, however survival rates for children with high risk neuroblastoma remains under 40% (Bosse and Maris, 2016). These statistics illustrate the need for better treatment options for children with high risk neuroblastoma.

2.2 Neuroblastoma Stages and Classification

Neuroblastoma is a heterogeneous disease exhibiting considerable variability in clinical presentation, prognosis and pathogenesis. In order to facilitate diagnosis the International Neuroblastoma Staging System (INSS), was created to classify tumors according to disease stage (Brodeur et al., 1993). The INSS tumor stages are defined as follows (Brodeur et al., 1993):

a. Stage 1: tumor is localized, gross excision is complete, lymph nodes are microscopically clear of tumor.
b. Stage 2A: tumor is localized, gross excision is incomplete, lymph nodes are microscopically clear of tumor.
c. Stage 2B: tumor is localized, gross excision is either complete or incomplete, lymph nodes are positive for tumor.
d. Stage 3: tumor is unilateral, infiltrating the midline (vertebral column) and unresectable, with or without positive lymph nodes.
e. Stage 4: any primary tumor that has dissemination to other organs, including but not exclusive to bone, bone marrow, liver and distant lymph nodes.

f. Stage 4s: localized tumor as previously described for stages 1, 2 and 2A, that have disseminated to skin, liver and/or bone marrow, in infants less than 1 year old.

Additional stratification of patients can be achieved using the guidelines provided by the International Neuroblastoma Risk Group (INRG) system, which classifies patients according to their pretreatment risk based on image-defined risk factors (IDRFs) (Table 2). There are four different groups according to the INRG classification (Monclair et al., 2009):

a. L1: tumor is localized and confined to one body compartment, vital structures are not involved.
b. L2: tumors may be present in continuous body compartments and presents one or more IDRFs.
c. M: tumor presents distant metastases (except as defined for MS).
d. MS: metastatic disease confined to skin, liver, and/or bone marrow. Patient is greater than18 months.

Furthermore, patient's prognosis of 5 year event-free survival can be classified into four different risk groups very low risk (>85%), low (75%-85%), intermediate (<75%) and high risk (<50%) by combining the INRG classification system with tumor stage, age of diagnosis, tumor differentiation, histologic category, MYCN oncogene amplification, chromosome p11 status and DNA ploidy, (Cohn et al., 2009). The differences in these events culminate in distinct physiological features of neuroblastoma that ultimately lead to disease heterogeneity.

Table 2. Image-Defined Risk Factors in Neuroblastoma tumors.
(Adapted from (Monclair et al., 2009)

IDRFs	Tumor Location
Ipsilateral extension (2 body compartments)	Neck-Chest Chest-Abdomen Abdomen-Pelvis
Neck	Encases carotid, vertebral artery and/or jugular vein Extends to base of the skull Compresses the trachea
Cervico-Thoracic	Encases brachial plexus roots Encases carotid, vertebral artery and/or subclavian vessels Compresses the trachea
Thorax	Encases aorta and/or major branches Compresses the trachea or principal bronchi Infiltrates costo-vertebral junction between T9-T12
Thoraco-abdominal	Encases aorta and/or vena cava
Abdomen/pelvis	Infiltrates of the porta hepatis and/or hepatoduodenal ligament Encases superior mesenteric artery Encases origin of the coeliac axis and/or superior mesenteric artery Encases aorta and/or vena cava Encases iliac vessels Crosses the sciatic notch
Intraspinal extension	Invades more than one third of the spinal canal, perimedullary leptomeningeal spaces are not visible and/or spinal cord signal is abnormal
Adjacent organs/structures	Invades pericardium, diaphragm, kidney, liver, duodeno-pancreatic block, mesentery

2.3 Neuroblastoma features

Specific genetic and biological changes in neuroblastoma tumors transforming cells to maintain continuous cell proliferation, bypass growth suppressors signals, attain replicative immortality, promote angiogenesis, evade cell death, avoid immune destruction and alter cellular metabolism (Hanahan and R. A. Weinberg, 2011).

The most common genetic alteration observed in neuroblastoma is the amplification of the proto-oncogene MYCN, usually observed in high-risk neuroblastoma tumors and correlates with advance stages of the disease and less favorable prognosis (Olsen et al., 2017). Part of the Myc family of transcription factors, N-Myc (MYCN) is involved in several cellular proposes such as proliferation, growth, differentiation apoptosis, metabolism, and it plays an important role in brain development (Beltran, 2014). Several studies have shown that deregulation of MYCN, either by amplification or overexpression, promotes tumorigenesis both in neural crest progenitor cells and in mice (Althoff et al., 2015; Montavon et al., 2014; Schulte et al., 2013; Weiss et al., 1997). Other common segmental chromosomal aberrations that correlate with prognosis are deletions in chromosomes 1p, 1q, 3p, 4p or 11q, and gain of chromosome 17q, however the specific candidates responsible for changes in tumor biology are not known (Bosse and Maris, 2016).

Familial cases of neuroblastoma are extremely rare accounting for 1-2% of all neuroblastoma cases, 80% of these cases can be attributed to either a gain of function mutation on anaplastic lymphoma kinase (ALK) or a loss of function

mutation on paired-like homeobox 2B (PHOX2B) (Bosse and Maris, 2016). Constitutive activation of ALK disrupts the balance between differentiation and proliferation. One of the proposed mechanisms involves the activation of RAS-mitogen activated protein kinases (MAPK) signaling pathways leading to increased proliferation. Also, recent evidence suggests that PHOX2B regulates ALK expression (Cheung and Dyer, 2013). Furthermore, mutations that promote constitutive activation of the RAS-MAPK signaling pathway are associated with neuroblastoma relapse (Eleveld et al., 2015).

Telomere lengthening has been observed in high risk neuroblastomas, where rearrangements in the chromosome region 5p15.33 upregulate transcription of TERT, and 10% of neuroblastoma cases show loss of function mutations in alpha thalassemia/mental retardation syndrome X-linked (ATRX), these tumors undergo alternate lengthening of telomeres which is independent of telomerase activity (Bosse and Maris, 2016; Peifer et al., 2015).

2.4 Standard of care and current therapies

The standard of care for neuroblastoma patients varies according to the tumors risk classification. Treatment for patients with low risk tumors is either observation or surgical resection (Strother et al., 2012). Patients with intermediate risk tumors receive several chemotherapy cycles with carboplatin, etoposide, doxorubicin and cyclophosphamide, followed by surgical removal of the primary tumor (Baker et al., 2010). High risk neuroblastoma requires aggressive treatment that combines chemotherapy with cisplatin, etoposide, vincristine, cyclophosphamide, doxorubicin and topotecan, followed by surgery (Kushner et al., 1994; Park et al.,

2011). A round of myeloablative chemotherapy aims to eliminate any residual disease and it is followed by stem cell transplantation (SCT) to replenish the bone marrow, common drug combinations used are carboplatin, etoposide and melphalan, or busulfan and melphalan (Matthay et al., 1999) (Elborai et al., 2016). Patients in remission after SCT are treated with dinutuximab, granolucyte-macrophage colony stimulating factor (GM-CSF), interleukin-2 (IL-2) and isotretinoin (Cheung et al., 2012; Yu et al., 2010).

3. Cancer metabolism

All cancers share a common set of features known as the “hallmarks of cancer”, unrestricted proliferation, evasion of growth suppressors signals and cell death, induction of angiogenesis, activation of invasion and metastasis, and metabolic reprogramming, genomic instability introduces genetic diversity that promotes and sustain the changes necessary for cancer cells to survive. (Hanahan and R. A. Weinberg, 2011). Mutations in distinct metabolic enzymes change the capacity of tumor cells to use alternative substrates in comparison to normal tissue. Collectively, these alterations enhance the survival of tumor cells in a stressful, oxygen deprived, nutrient restricted environment.

3.1 General

The most widely studied metabolic change in cancer cells is aerobic glycolysis, also knowns as the “Warburg effect”, where glucose is converted to lactate even in the presence of oxygen (Bensinger and Christofk, 2012). Even though aerobic glycolysis seems inefficient in terms of ATP production in comparison to oxidative phosphorylation, it provides proliferating cancer cells with precursors for

biosynthesis of macromolecules such as fatty acids, nucleotides, ribose and non-essential amino acids (Vander Heiden et al., 2009). Different mechanisms orchestrate the transcription upregulation of glycolytic enzymes frequently observed in cancer cells. PI3K signaling increases glucose uptake via AKT upregulation of glucose transporter expression (GLUT1), stimulation of hexokinase (HK) activity and posttranslational stabilization of phosphofructokinase 1 (PFK1) (Plas et al., 2001; Rathmell et al., 2003). The transcription factor HIF1-α, also regulated by the PI3K/AKT/mTOR pathway, promotes expression of hexokinase II (HK-II), pyruvate dehydrogenase kinase (PDK) and lactate dehydrogenase (LDH) (Courtnay et al., 2015; Roberts and Miyamoto, 2015). The oncogene MYC can also promote upregulation of glycolytic enzymes and PDK1, while loss of the tumor suppressor p53 decreases expression of TP53-induced glycolysis and apoptosis regulator (TIGAR), which in turn decreases oxidative phosphorylation and increases flux through glycolysis (Bensinger and Christofk, 2012). Furthermore, some metabolic enzymes switch between isoforms further supporting the cell's preference for aerobic glycolysis, for example the splice variant PKM2, normally expressed embryonically, when expressed in tumor tissues is sufficient to promote aerobic glycolysis, however knockdown of this isoform and switch to adult PKM1 results in a decrease in glycolytic rate and cell proliferation (Christofk et al., 2008). Development of cancer cells occurs within an environment where resources are limited, cancer cells use a wide variety of nutrients in order to fulfill their requirements (Vander Heiden and DeBerardinis, 2017). In order to synthesize macromolecules, such as lipids, nucleotides and aminoacids, cancer cells rely on

intermediates from the tricarboxylic acid (TCA) cycle. For lipid biosynthesis, citrate is shuttled outside the mitochondria to be converted into oxaloacetate (OAA) and acetyl-CoA, changes in protein expression and activity of ATP citrate lyase and fatty acid synthase are frequently observed in tumors. Furthermore, OAA and α-KG supply nonessential aminoacids for protein and nucleotide synthesis (DeBerardinis et al., 2008). Glutamine oxidation, also known as glutaminolysis, provides support for bioenergetics and replenishes TCA intermediates (Daye and Wellen, 2012). Glutamine is readily available in circulation, providing cancer cells with a source of carbon and nitrogen for bioenergetics, macromolecule synthesis and cellular homeostasis. Glutaminase (GLS) mediates the conversion of glutamine to glutamate and an ammonium ion, several cancer types show preferential expression of the more active splice variant glutaminase C (GAC); glutamate is further process to α-KG by glutamate dehydrogenase (GLUD) that also produces NADH and NAPDH supporting the TCA cycle, or alanine aminotransferase and aspartate aminotransferase, which provide other aminoacids that can support different biosynthetic processes (Altman et al., 2016).

3.2 Glioblastoma

Specific genetic modifications that occur in GBMs sustain tumor biology and alter metabolism, where mutations in distinct metabolic enzymes change the capacity of tumor cells to use substrates in comparison to normal tissue. Understanding the metabolically-relevant genetic alterations promoting GBM tumor biology will provide unique insights that may improve diagnostic and therapeutic approaches.

3.2.1 Substrate Utilization

Tumor cells utilize substrates distinctly from their normal counterparts to maximize growth and proliferation. A recent study using carbon-13 NMR spectroscopy in rat C6 glioma cells, an *in vitro* model of GBM, revealed the production of lactate from glucose, consistent with aerobic glycolysis, and consumption of glutamine for anaplerosis of the tricarboxylic acid (TCA) cycle; in this system both substrates complement each other to support the high proliferation rates (Portais et al., 1996). An additional study confirmed that GBM cells use aerobic glycolysis and showed that exogenous lactate was the main substrate used for oxidative phosphorylation. The ability of the cells to utilize two distinct sources of lactate could provide a potential growth advantage (Bouzier et al., 1998).

The human GBM cell line U87 is characterized by low respiration, elevated glycolytic rates, and increased stability of hypoxia inducible factors HIF-1α and HIF-2α (Zhou et al., 2011). Studies in U87 cells demonstrated that inhibition of glycolysis reduced cellular ATP production and resulted in cell death (Blum et al., 2005; Zhou et al., 2011). Metabolic trace experiments using ^{13}C-NMR demonstrated that the GBM cell line SF188 uses glucose for aerobic glycolysis, produces abundant levels of labeled lactate and alanine, with glucose carbons entering the TCA cycle as pyruvate through pyruvate dehydrogenase (PDH), which later contributes to fatty acid synthesis (DeBerardinis et al., 2007). This study also revealed that SF188 cells use glutamine as anaplerotic nutrient for the TCA cycle and as a source of NADPH (DeBerardinis et al., 2007). Addiction to glutamine has been shown in SF188 cells, where glutaminolysis preserves mitochondrial activity,

replenishes the TCA cycle and contributes to bioenergetics (Wise et al., 2008). Under hypoxic conditions, the GBM cell line SF188 uses glutamine as a source of α-ketoglutarate, which generates citrate by isocitrate dehydrogenase 2 (IDH2), an event required for fatty acid and cholesterol synthesis, protein acetylation and NADPH production (Wise et al., 2011).

Orthotopic mouse models for primary GBM and ^{13}C-NMR have demonstrated that glucose is used for glycolysis rather than increased flux through the pentose phosphate pathway (PPP) as previously suggested by cell-based studies. Detection of labeled glutamate and γ-aminobutiric acid (GABA) indicated that glucose was converted to acetyl-CoA and then oxidized in the TCA cycle, showing that both aerobic glycolysis and oxidative metabolism occur *in vivo* (Marin-Valencia et al., 2012a). Furthermore, the presence of labeled lactate, glutamate and glutamine provided evidence that glucose serves as an anaplerotic nutrient entering the TCA cycle through pyruvate carboxylase. Labeling of glutamate and glutamine has been demonstrated to be due to normal turnover of the TCA cycle and PDH activity in the tumor, however, these tumors do not oxidize glutamine or require an extracellular supply, since they can synthesize glutamine *de novo* from glucose (Marin-Valencia et al., 2012b). Metabolic analysis of human brain tumors *in vivo* showed similar results to the orthotopic mouse models, where labeled glucose supplied to tumors during surgical resection is engaged in glycolysis as well as oxidation in the TCA cycle, and along with glycine and glutamine synthesis. In this way, glucose is used for energy supply and for macromolecule precursors (Maher et al., 2012). A recent study found that orthotopic mouse brain tumors, as

well as patient GBM tumors, highly expressed acetyl-CoA synthetase enzyme 2 (ACSS2) that catalyzes the conversion of acetate into acetyl-CoA, thus permitting oxidation of acetate in the TCA cycle (Mashimo et al., 2014).

Multiple GBM model systems are available that display distinct preferences for metabolic substrates (Table 3). Metabolic differences may be observed in each of these systems, however, these should be interpreted with caution since they may not apply to all systems and thus may not translate to what happens in GBM patients. Thus, it is imperative to develop more precise model systems and techniques to better understand metabolic differences in GBM tumors that more accurately represent what happens in patients.

Table 3. GBM model systems and substrate utilization.

MODEL SYSTEM	SUBSTRATE	END PRODUCT
C6 RAT GLIOMA	Glucose	Lactate
	Glutamine	TCA cycle anaplerosis
	External Lactate	TCA cycle anaplerosis
U87 CELL LINE	Glucose	Lactate
		Alanine
		TCA cycle – Fatty acid synthesis
	Glutamine	TCA cycle anaplerosis
		Fatty acid synthesis
		Cholesterol synthesis
		Protein acetylation
MOUSE ORTHOTOPIC TUMORS PATIENT GBM TUMORS	Glucose	Lactate
		TCA cycle
		Glutamate, GABA
		Glutamine
	Acetate	Acetyl-CoA

3.2.2 Isocitrate Dehydrogenase

Isocitrate dehydrogenases (IDH1, IDH2) produce α-KG from isocitrate and reduce $NADP^+$ to NADPH (Krell et al., 2011). IDH1 and IDH2 are homodimeric, can either be mitochondrial or cytosolic and can protect the cell against oxidative stress damage (Jo et al., 2001; S. Y. Kim et al., 2007; Krell et al., 2011; X. Xu et al., 2004). Interestingly, the IDH1 gene is commonly mutated in patients with secondary GBMs. Genomic analysis of human GBM tumor samples revealed that all patients had the same mutation in the IDH1 active site where arginine 132 was often replaced by a histidine (R132H). $IDH1^{R132H}$ tends to occur in younger patients, and individuals with this mutation have an improved prognosis, increasing their median survival to 3.8 years in comparison to 1.1 years for IDH1 wild-type patients (Parsons et al., 2008). Other glioma patients have the $IDH1^{R100}$ mutation, while pediatric glioblastoma patients have the $IDH1^{G97}$ mutation. Furthermore, tumors without any IDH1 mutations frequently displayed mutations in the IDH2 gene (P. S. Ward et al., 2011; Yan et al., 2009). IDH2 mutations occurred on the analogous aminoacid R172 in the active site which was replaced by either a glycine (R172G), a lysine (R172K) or a methionine (R172M) (Yan et al., 2009).

In vitro studies showed that GBM derived mutations in IDH1 and IDH2 have greater than 80% reduction of their enzymatic activity when compared to their wild-type counterparts due to decreased affinity for isocitrate, which results in very limited enzymatic activity under physiological conditions. Expression of mutant $IDH1^{R132H}$ in the human GBM cell line U87-MG resulted in decreased levels α-KG in a dose-dependent manner. This may be attributed to the fact that IDH1 works as a

homodimer, expression of $IDH1^{R132H}$ results in dominant inhibition of the wild-type enzyme by forming heterodimers $IDH1^{wt}$:$IDH1^{R132H}$ that are unable to catalyze the production of α-KG (Zhao et al., 2009). However, analysis of patient tumor samples carrying different IDH1 mutations showed that there were no significant differences in α-KG levels between mutant samples and tumor samples carrying wild type IDH1 (Dang et al., 2009). This IDH1 mutation also results in a gain of function activity for the enzyme, where IDH1 heterodimers reduce α-KG in an NADP-dependent manner and produce 2-hydroxyglutarate (2-HG), specifically the R-isomer (R)-2-HG (Figure 1). Elevated levels of 2-HG have also been observed both in GBM cell lines expressing the mutant enzyme as well as in GBM patient samples harboring the $IDH1^{R132H}$ mutation (Dang et al., 2009). The combination of these changes may contribute to malignant progression due to several events since α-KG is required by prolyl-hydroxylases (PHD) enzymes to promote HIF1-α degradation, while decreased levels of α-KG result in stabilization and increased levels of HIF1-α (Zhao et al., 2009). U87 cells stably transfected with $IDH1^{R132H}$, result in inhibition of ATP synthase by 2-HG, having decreased ATP levels and ATP/ADP ratio and decreased mammalian target of rapamycin (mTOR) signaling (Fu et al., 2015). Furthermore, working as an oncometabolite, 2-HG competitively inhibits α-KG dependent histone demethylases due to its structural similarity with α-KG. Expression of $IDH1^{R132H}$ in U87-MG resulted in a decrease of α-KG levels, an increase in 2-HG levels and an increase in histone methylation. Comparable results were observed in patients, where tumor samples carrying the IDH1 mutation had significantly higher levels of histone methylation in comparison to

IDH1-wild type tumor samples (W. Xu et al., 2011). Expression of mutant IDH1 caused hypermethylation of a series of genes in immortalized primary human astrocytes, as well as in low-grade gliomas and secondary GBMs carrying the endogenous IDH1 mutation (Turcan et al., 2012). Some genes involved in glycolysis, including lactate dehydrogenase A (LDHA), are under-expressed in gliomas, brain tumor stem cells (BTSC) and orthotopic xenografts derived from BTSC carrying the mutant IDH, due to methylation of the promoter (Chesnelong et al., 2014).

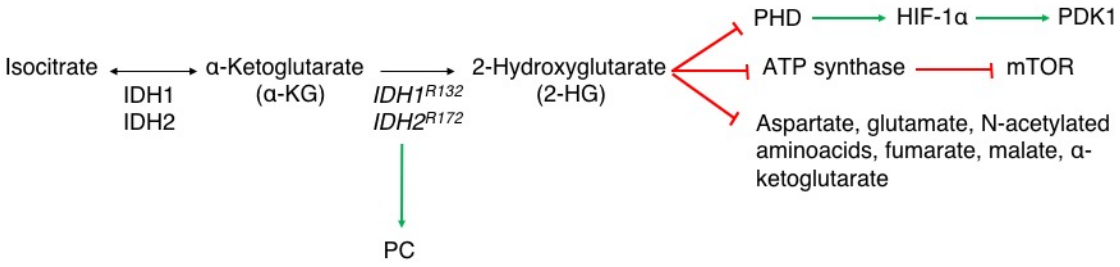

Figure 1. Metabolic changes resulting from IDH mutations.
IDH heterodimers reduce α-ketoglutarate (α-KG) to 2-hydroxyglutarate (2-HG) altering GBM metabolism through a series of reactions. Inhibition prolyl-hydroxylases (PHD) stabilizes HIF1-α and increases PDK1 expression, inhibition of ATP synthase reduces ATP/ADP ratio inhibiting mTOR signaling, decrease levels of α-KG results in reduced levels of several aminoacids and TCA cycle intermediates and increased expression of PC promotes reprogramming of pyruvate metabolism.

Metabolomics analysis of human oligodendroglioma (HOG) cells expressing either wild-type IDH1, IDH2 or $IDH1^{R132H}$, $IDH2^{R172K}$ revealed that cells expressing the mutant proteins have significant differences in their metabolic profile. Mutations in IDH caused changes in aminoacid levels, where a significant decrease was observed in levels of aspartate, glutamate, N-acetylated aminoacids, both reduced and oxidized glutathione, and TCA cycle intermediates including fumarate, malate,

and α-KG. These changes were shown to be due to production of 2-HG since treatment of cells with shRNA against IDH1/2 did not reproduce these altered metabolic profiles, however, similar changes were observed when cells were treated with 2-HG (Reitman et al., 2011). Decreased levels of glutamate were not only observed due to mutant IDH mediated increase flux of α-KG to 2-HG but also as a result of pyruvate metabolism reprogramming. Accumulation of 2-HG raises levels of HIF-1α and causes downregulation of pyruvate dehydrogenase (PDH) activity, which results in decreased decarboxylation of pyruvate into acetyl-CoA before entering the TCA cycle as well as a generally diminished flux of glucose to glutamate, as shown using ^{13}C-MRS in U87 cells carrying mutant IDH (Izquierdo-Garcia et al., 2015). To support TCA cycle anaplerosis, IDH mutant cells exhibit increased expression of pyruvate carboxylase (PC), which catalyzes the conversion of pyruvate into oxaloacetate. Higher expression levels of PC have been observed both in immortalized human astrocytes as well as in TCGA patient samples carrying the IDH1^{R132H} mutation (Izquierdo-Garcia et al., 2014). Understanding the metabolic changes and compensatory mechanisms adopted by tumors expressing mutant IDH will potentially identify novel therapeutic targets that will help improve treatment of patients that present these mutations.

3.2.3 HIF1α

The transcription factor Hypoxia-inducible factor 1 (HIF1) orchestrates the response of mammalian cells under hypoxic conditions inducing the expression of genes involved in angiogenesis and glucose metabolism (Semenza, 1999). HIF1 activity is regulated by stabilization of the HIF1-α subunit. Under normal oxygen

conditions, hydroxylation of certain prolines in the oxygen-dependent degradation (ODD) domain by PHDs results in recruitment of the E3 ubiquitin ligase von Hippel-Lindau tumor suppressor (pVHL) which promotes HIF1-α degradation via the ubiquitin-proteasome pathway (Huang et al., 1998; Jaakkola et al., 2001). Activation of HIF1-α leads to increased angiogenesis and promotes invasion and migration by controlling the expression of several proteins involved in these processes (Kaur et al., 2005).

During hypoxia, it is well known that PTEN inhibits the accumulation of HIF1-α, as U87-MG cells conditionally expressing WT or mutant PTEN showed that loss or mutation of PTEN caused accumulation and stabilization of HIF1-α. Furthermore, chemical inhibition of phosphatidylinositide-3 kinase (PI3K) or knockdown of AKT using small interference RNA (siRNA) blocked both accumulation of HIF1-α and reduced gene expression. Also, knockdown of PTEN in the glioblastoma cell line LN229 resulted in increased expression of the HIF1-α target genes hexokinase1 (HK1) and the glucose transporter 1 (GLUT1) Hypoxia also mediates epithelial to mesenchymal transition (EMT) in GBM cell lines U87 and SNB75 via HIF1-α, which induces the transcription factor zinc finger E-box binding homeobox 1 (ZEB1) that promotes EMT, prompts the expression of mesenchymal markers fibronectin and COL5A (collagen, type V, alpha 1) and promotes migration and a more invasive phenotype. In patient samples, expression of ZEB1 co-localizes with GLUT1, a marker for hypoxia, and chitinase 3 like-1 (CHI3L-1), a mesenchymal marker, in the pseudopalisading area surrounding the necrotic foci (Joseph et al., 2015).

In U87-MG cells, HIF1-α acts as part of an autocrine loop involving insulin-like growth factor receptor 1 (IGFR1), STAT3 (signal transducers and activators of transcription) and IGF-II, which together work to induce release of vascular endothelial growth factor (VEGF) and thus regulate tumor survival. Activation of IGFR1 promotes activation of STAT3 that leads to stabilization of HIF1-α and IGF-II as well as release of VEGF, thus further activating this circuit. Inhibition of IGFR1 activation disrupts the autocrine loop and reduces cell growth (Gariboldi et al., 2010). Moreover, a recent study using T98G cells demonstrated that STAT3 can be repressed by GRIM-19 (gene associated with retinoid-interferon-induced mortality-19) which reduces the levels of HIF1-α. In these cells knockdown of GRIM-19, increases cell proliferation, and facilitates the switch from mitochondrial respiration to glycolysis by increasing GLUT-1 levels at the membrane, enzymatic activity of hexokinase 2 (HK2), pyruvate kinase M2 (PKM2) and phosphofructokinase (PFK), and phosphorylation levels and subsequent inactivation of pyruvate dehydrogenase (PDH) (Liu et al., 2013).

In patient-derived glioma-initiating cells (GICs), HIF1-α induces the microRNA miR-215 by incorporating pri-miRNA-215 into the DROSHA complex for processing under hypoxic conditions. MiR-215 promotes tumor growth by allowing GSCs to adapt to hypoxia by targeting KDM1B, a FAD-dependent histone demethylase of H3K4me1/2. Low expression of KDM1B results in increased expression of genes involved in hypoxia response, glucose metabolism and angiogenesis. It should be noted that in patients, reduced levels of KDM1B correlates with a poor clinical prognosis (Hu et al., 2016).

U87 spheroids show induction of the fatty acid-binding protein 3 (FABP3) and FABP7, which are involved in fatty acid uptake, and accumulation of lipid droplets (LD) in the hypoxic core domain in HIF1-α dependent manner. Inhibition of FABP3/7 impairs tumor growth in a murine xenograft model, which was associated with the decreased levels of LDs. This, in turn, leads to increased reactive oxygen species (ROS) toxicity and decreased cell survival by reducing the amount of ATP production from fatty acid β-oxidation or glycogen degradation (Bensaad et al., 2014).

Since HIF1-α orchestrates the response and adaption to a low O_2 environment, which is characteristic of solid tumors and provides a survival advantage by promoting angiogenesis, migration and invasion, targeting HIF1-α and the pathways regulated by it, would provide new therapies that may contribute to increased survival of GBM patients.

3.2.4 EGFR

The epidermal growth factor receptor (EGFR), a receptor tyrosine kinase (RTK), is responsible for initiating various signal transduction pathways, including RAS/mitogen-activated protein kinase and PI3K/AKT, which are particularly relevant to GBM biology. Abnormal activation of EGFR is common in numerous forms of cancer and usually occurs due to one of the following alterations: increased levels of EGFR ligands, amplification of EGFR genes, overexpression of EGFR members (wild-type or mutants), or EGFR-independent activation of downstream signaling pathways (Nicholas et al., 2006). In GBMs, amplification of EGFR genes is common and frequently accompanied by gene rearrangement; the

most common being a deletion of exons 2 to 7. This results in a mutant receptor with a truncated extracellular domain called EGFRvIII, which is unable to bind to its ligands and it is constitutively phosphorylated and thus continuously activates downstream signaling pathways (Gan et al., 2009; Nagane et al., 2001).

The type of activation of EGFR will determine the downstream signaling, where ligand-dependent activation engages the canonical networks involving ERK and AKT, while overexpression and constitutive activation of the wild-type receptor lead to phosphorylation and activation of the transcription factor IRF3 (interferon regulatory factor 3), which activates a series of survival signals. Importantly, overexpression of $EGFR^{WT}$ in GBM cell lines U251 and U87, reduces sensitivity to chemotherapy, however, exposure to EGF sensitizes cells to temozolomide (Chakraborty et al., 2014).

EGF-mediated stimulation of EGFR induces the expression cyclooxygenase-2 (COX-2) through activation of the p38-MAPK pathway. COX enzymes are crucial for prostaglandins biosynthesis. COX-2 is inducible as a rapid response to various stimuli and may play an important role in tumor biology, where in malignant gliomas increased expression levels correlate with shorter patient survival. In the glioma cell line SF767, EGF binding to EGFR promotes activation of p38-MAPK, which then phosphorylates protein kinase C-delta (PKC-δ) resulting in Sp1 phosphorylation, nuclear translocation and enhanced binding to the COX-2 promoter, followed by increased levels of COX-2 (mRNA and protein). Inhibition of EGFR kinase activity, p38-MAPK, PKC-δ or the transcription factors Sp1/Sp3, blocks the EGF-dependent induction of COX-2 (K. Xu et al., 2009; K. Xu and Shu,

2007). COX-2 expression may also be mediated by the nuclear translocation of EGFR and STAT3, which also controls transcriptional activation of genes like iNOS (inducible nitric oxide synthase) and c-MYC. In glioma patients, activation of STAT3 correlates with expression of insulin-like growth factor binding protein 2 (IGFBP2). In GBM cell lines, SNB19 and U87, it was demonstrated that IGFBP2 activates STAT3 and subsequent transcription of STAT3 target genes by activating and promoting the nuclear accumulation of EGFR (Chua et al., 2016).

Interestingly, EGF activation of EGFR also leads to increased expression of PKM2 but not PKM1. U87 cells overexpressing EGFRvIII exhibit higher levels of PKM2 in comparison to cells U87 overexpressing $EGFR^{WT}$ without EGF stimulation, while inhibition of EGFR activation by treating cells with AG1478 blocked PKM2 upregulation. PKM2 expression by EGFR activation depends on activation of both PKCε and nuclear factor kappa enhancer binding protein, correlates with increased glycolysis and tumorigenesis, and in patients, with the grade of glioma malignancy (W. Yang et al., 2012a).

In mice with inactive p16Ink4/p19ARF and PTEN, expression of EGFRvIII resulted in formation of highly aggressive tumors, while expression of $EGFR^{WT}$ was not as efficient for tumor development. After tumor formation, cells isolated and stimulated with EGF, resulted in phosphorylation of $EGFR^{WT}$ on residues 920, 992, 1045, 1068, 1148 and 1173, whereas, EGFRvIII only showed autophosphorylation on residue 992. These differences also resulted in differences between signaling cascades activated by these two receptors. For example, phosphorylation of STAT3 in tyrosine 705, or MEK/ERK activation was only observed in $EGFR^{WT}$

cells. EGFRvIII showed constitutive phosphorylation of AKT on Ser-473 while $EGFR^{WT}$ showed phosphorylation on Thr-308 upon EGF-stimulation. Similarly, stimulation of $EGFR^{WT}$ cells resulted in activation of mTOR complex 1 (mTORC1) which was not observed in EGFRvIII expressing cells (Zhu et al., 2009). EGFRvIII cells show elevated levels of mTORC2 signaling, where activation is sensitive to changes in metabolite availability, increasing in response to both glucose and acetate in a dose- and time-dependent manner. Regulation of mTORC2 signaling depends on acetyl-CoA levels, which provides the acetyl group for Rictor acetylation and then further increases mTORC2 activity. mTORC2 forms an autoactivation loop by promoting the phosphorylation and subsequent inactivation of histone deacetylase (HDAC) class IIa by PKCα, which then maintains Rictor in its acetylated state. Rictor acetylation in the presence of glucose results in GBM cells that are resistant to therapies that involve inhibition of EGFR, PI3K or AKT, since it allows tumor cells to maintain mTORC2 signaling active independent of upstream stimulation (Masui et al., 2015). Since differential activation of EGFR will dictate the downstream signaling events and affect the aggressiveness and adaptability of the tumor, it is critical to understand the potential outcomes linked to a specific activation event so that we better diagnose patients, since determining the kind of EGFR perturbation will allow the design of more efficacious treatment plans.

3.2.5 PKM2

Pyruvate kinase (PK) catalyzes the last and rate-limiting step in glycolysis, the conversion of phosphoenolpyruvate (PEP) to pyruvate while transferring a high-

energy phosphate to form ATP. There are two genes and four PK isoforms, the PKLR gene encodes for the PKL and PKR isoforms and the PKM gene encodes for PKM1 and PKM2 (Wong et al., 2013). PKM2, the primary isoform expressed in cancer cells, results from the alternative splicing of exons 9 and 10 from the PKM gene. Unlike the M1 isoform that forms stable tetramers and is constitutively active, PKM2 is found both as a dimer or a tetramer and has a lower enzymatic activity. (Christofk et al., 2008; Dombrauckas et al., 2005). PKM2 requires allosteric activation, by fructose-1,6-biphosphate (FBP) which promotes the formation of the more active tetramer form. Tyrosine kinase signaling inhibits the enzyme by facilitating the release of FBP and switching to the less active dimer conformation (Wong et al., 2013). Under nutrient-limited conditions, PKM2's activation depends on levels of the *de novo* purine nucleotide synthesis intermediate succinyl-5-aminoimidazole-4-carboxamide-1-ribose-5'-phosphate (SAICAR) (K. E. Keller et al., 2012). In this manner PKM2 regulates glucose metabolism favoring entrance of pyruvate to the TCA cycle when the enzyme is in the active tetramer form or aerobic glycolysis when present in the less active dimer form, providing cancer cells a metabolic advantage that facilitates cell proliferation (Figure 2) (Christofk et al., 2008; Wong et al., 2013).

PKM1 and PKM2 are differentially expressed, where PKM1 Is expressed in heart, skeletal muscle, and brain, while PKM2 is expressed in most cells except in adult liver, muscle and brain (Wong et al., 2013). Analysis of TCGA exon array data showed that GBM tumors have very low or negative levels of the PKM1-specific exon 9 in comparison to normal tissue, indicating that a switch occurs between

expression of PKM1 to PKM2. Moreover, the degree of switching varied depending on the type of tumor, where the ratio between PKM2/PKM1 is higher in more undifferentiated mesenchymal

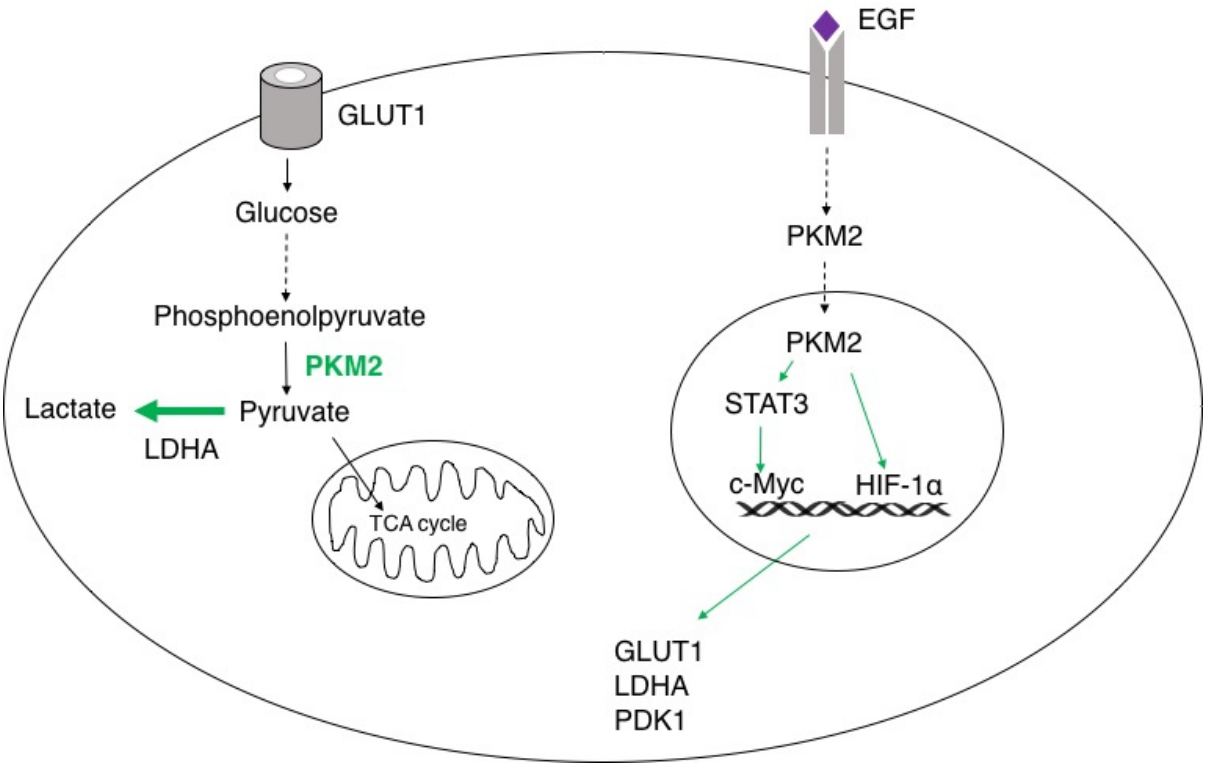

Figure 2. PKM2 promotes aerobic glycolysis through two distinct mechanisms.

PKM2 reduced enzymatic activity decreases entrance of pyruvate into the TCA cycle and increases aerobic glycolysis, while EGF activation promotes nuclear translocation of PKM2 where it can transactivate c-Myc and HIF1-α, therefore upregulating the expression of glycolytic genes like GLUT1, LDHA, and PDK1.

GBMs than in more differentiated proneural GBMs (Desai et al., 2014).

EGF stimulation in U251 and U87/EGFR cells, or in cancer cells carrying the EGFRvIII mutant, promotes the ERK activation dependent translocation of PKM2 to the nucleus. PKM2 interacts directly with ERK2 which phosphorylates S37,

promoting the interaction with peptidyl-prolyl Cis/Trans Isomerase, NIMA-Interacting 1 (PIN1) which facilitates PKM2 binding to importin α5 allowing it to be translocated (W. Yang et al., 2012c). After translocation, PKM2 binds to poly-ADP-ribose (PAR) and this interaction is required for PKM2 nuclear retention and activity. On the other hand, inhibition of the PKM2/PAR interaction by blocking poly-ADP-ribose polymerase-1 (PARP1) prevents PKM2 nuclear localization and diminishes its nuclear functions (Li et al., 2016). PKM2 interacts with c-Src phosphorylated β-catenin (Y333) and phosphorylates histone H3 at T11, which is required for disassociation of histone deacetylase 3 (HDAC3) from the cyclin D1 (CCND1) promoter and histone H3 acetylation and expression of cyclin D1 and c-Myc, both of which are important for cell proliferation (W. Yang et al., 2012b; 2011). PKM2 EGF-induced transactivation of β-catenin also upregulates the c-Myc-dependent expression of glycolytic genes GLUT1 and lactate dehydrogenase A (LDHA) (Figure 2). Depletion of PKM2 using shRNA showed reduced β-catenin transactivation and reduced EGF-induced expression of cyclin D1, c-Myc, its downstream genes and the capacity of these cells to perform aerobic glycolysis, thus showing a reduction in glucose consumption and lactate production (W. Yang et al., 2012c; 2011). Moreover, intracranial injection of either U87 or U87/EGFRvIII cells into mice, showed that U87/EGFRvIII produced tumors faster, while depletion of β-catenin or PKM2, as well as inhibition of c-Src, significantly decreased tumor growth. Furthermore, treatment of tumors with PARP inhibitor olaparib was effective at reducing growth in U87/EGFRvIII tumors, but lost efficacy in PKM2-depleted tumors (Li et al., 2016; W. Yang et al., 2011). Nuclear PKM2 also

functions as a coactivator of HIF1-α, this interaction promotes transactivation of HIF1-α target genes such as GLUT1, LDHA, and pyruvate dehydrogenase kinase 1 (PDK1) (Figure 2); interaction with PHD3 enhances HIF1-α binding by prolyl-hydroxylating PKM2. HIF1-α also promotes the transcription of PKM2 and PHD3, creating a feedforward loop that amplifies the HIF1-α metabolic reprogramming (Luo et al., 2011).

PKM2 activity also influences the oxygen consumption rates and carbon flux into the TCA cycle in the GBM cell line LN229 when cells are placed in a hypoxic or nutrient deficient environment. The mitochondrial serine hydroxymethyltransferase (SHMT2), which is highly expressed in GBM pseudopalisading cells, plays a key role limiting the activity of PKM2. It is thought to do so by reducing the levels of PKM2 activators like serine, FBP, and SAICAR, facilitating survival of cells under hypoxic conditions by limiting flux into the TCA cycle and decreasing oxygen consumption. In a rapid xenograft model, where tumors from subcutaneously injected cells are collected before angiogenesis, high expression levels of SHMT2 provide LN229 cells a survival advantage where the central area of the tumor contains both viable and dying cells, however, suppression of SHMT2 or overexpression of PKM2 reduced the survival of these cells (D. Kim et al., 2015).

3.2.6 PDK1

Pyruvate dehydrogenase kinase (PDK) is one of the enzymes that regulates the activity of the pyruvate dehydrogenase complex (PDC). It functions by phosphorylating one of its components (PDH), causing its inactivation and preventing the entrance of pyruvate into the TCA cycle to be oxidized as well as

promoting its conversion to lactate in the cytosol (Jha and Suk, 2013). As mentioned before, transactivation of HIF1-α by PKM2 promotes increased expression of PDK1 which supports metabolic reprogramming in GBM (Luo et al., 2011).

In mice, with patient-derived GBM tumors, treatment with the VEGF inhibitor bevacizumab induces hypoxia, promoting HIF1-α upregulation and increased expression of PDK1 and other key glycolytic enzymes. Metabolic flux analysis done using $^{13}C_6$-glucose injections in these animals show an increased glucose flux into the tumors, higher levels of lactate and LDHA expression and a significant reduction in many TCA metabolites like succinate, fumarate, malate, and α-KG, indicating an uncoupling of glycolysis from oxidative phosphorylation (Fack et al., 2015). Furthermore, transcriptomic analysis of patient-derived GSCs and GBM cell lines U87 and U251, under short (12h) and long (7d) term severe hypoxia (0.1% O_2) showed strong upregulation of the glycolytic genes HK2, PFKP, and PDK1. Knockdown of PFKP or PDK1 resulted in increased cell death under hypoxic conditions but did not affect cell growth under aerobic conditions. Knockdown of PFKP or PDK1 in GBM xenografts showed an increase in mouse survival of +21.8% and +20,9% respectively. *In vitro,* GBM cells are sensitive to inhibition of PDK1 with dichloroacetate (DCA) and this sensitivity is increased under hypoxic conditions (Sanzey et al., 2015).

PDK1 expression is increased in GBM patient samples and correlates with EGFR expression levels. Crosstalk between PDK1 and EGFR was observed in U251 cells and the xenograft cell line 5310, where inhibition of PDK1 with DCA reduced

expression levels of both PDK1 and EGFR; similarly, treatment with siRNA against PDK1 reduced levels of both total and phosphorylated EGFR. Overexpression of EGFR in these cells showed increased cell proliferation and lactate release, which indicates and induction of aerobic glycolysis. It should be noted, however, that while treatment with DCA or si-PDK1 reduced cell proliferation, lactate production and EGFR phosphorylation, it also induced apoptosis. Intracerebral injections in mice of these cells formed tumors 60% smaller after intravenous treatment with DCA, which resulted in reduced tumor growth and extended survival of these mice (Velpula et al., 2013).

3.2.7 Others

Glucose-6-phosphatase complex (G6PC)

G6PC is highly expressed in GBM tumors in comparison to normal brain tissue. It is a key regulator of the glycogenolytic pathway and glucose homeostasis, where it provides brain tumor initiating cells (BITCs) with a growth advantage by promoting glycogen mobilization and degradation. This is especially true under hypoxic conditions when relying exclusively on glycolysis might not be sufficient due to limited nutrient supply. BITCs isolated from GBM intraoperative samples that can escape glycolytic inhibition by 2-deoxy-glucose (2DG) become highly aggressive and more invasive when compared to control BITCs. They also showed increased expression of G6PC, and knockdown of G6PC increased the amount of glycogen inside the cells, and reduced these cells invasiveness and migrating abilities (Abbadi et al., 2014).

Glutamine Synthetase

The astrocytic enzyme glutamine synthetase (GS) catalyzes the production of glutamine from glutamate and ammonia, and together with glutaminase (GLS), it controls glutamine homeostasis within the cell (Rosati et al., 2013). GS is essential to sustain proliferation of GBM cell lines undergoing glutamine starvation, where cells increase GS expression levels upon glutamine deprivation which diminishes their sensitivity to glutamine withdrawal. Inhibition of GS using the irreversible inhibitor L-methionine sulfoximine (MSO) resensitizes these cells to glutamine starvation. Under these conditions, GS maintains levels of precursors for purine nucleotide biosynthesis, aminoimidazole-4-carboxamide ribotide (AICAR), and inosine monophosphate (IMP). Furthermore, GS is highly expressed in GSCs which allows these cells to grow independently of glutamine supplementation. Patients' samples injected with $^{13}C_6$-glucose prior to surgical resection showed that labeled glutamine was enriched in the tumor, indicating *de novo* synthesis in the tumor or the adjacent tissue. These findings were confirmed by co-culturing the GBM cell line LN18, which doesn't express GS and glutamine starvation impairs its proliferation, and astrocytes, which enabled proliferation of LN18 under glutamine deprivation conditions (Tardito et al., 2015). Mice with GBM orthotopic tumors expressing GS were infused with U^{13}-C-glutamine, showed that tumors uptake glutamine but do not metabolize it significantly. Cells isolated from these tumors and grown as neurospheres did not require glutamine for survival and analysis of different metabolites after treatment with U^{13}-C-glucose indicated that

glutamine was produced from glucose which allows cells to avoid the requirement for extracellular glutamine (Marin-Valencia et al., 2012b)

3.2.8 Integration of GBM metabolism

Several enzymes and signaling pathways are mutated or dysregulated in GBM, causing changes in metabolism by altering glucose flux into the cell, promoting aerobic glycolysis and changing pyruvate metabolism (Figure 3). Mutations in IDH1/IDH2 have been shown to produce the oncometabolite 2-HG which is linked to the hypermethylation phenotype of some tumors, also reduced levels of 2-KG decrease PHD activity and HIF1-α degradation which leads to PDH downregulation. HIF1-α increases expression of VEGF, GLUT1, LDHA, promotes angiogenesis, invasion, and migration and contributes to maintenance and proliferation of GSCs. EGFR overexpression or constitutive activation is a common GBM feature which causes transcriptional activation of STAT3 and c-MYC, increased signaling through mTORC2 and increased expression levels of PKM2, which not only works as control point regulating glucose metabolism but also works at the nuclear level promoting expression of c-MYC and c-MYC-dependent glycolytic genes, and as a HIF1-α coactivator inducing expression of its target genes. One of these genes is PDK1, which is highly expressed in GBM patients, by inactivating PDH it diverts entrance of pyruvate to the TCA cycle promoting glycolysis, this mechanism plays an important role in resistance to the chemotherapeutic bevacizumab. Other enzymes provide advantages to GBM tumors when nutrients are scarce, like G6PC allowing movement and degradation of glycogen and GS providing precursors for *de novo* purine biosynthesis by

producing glutamine from glucose. Combined, all these changes provide GBM tumors with different mechanisms to survive in a stressful environment deprived of oxygen and limited nutrient access and therapies targeted to these adaptations may improve treatment outcome and patient survival.

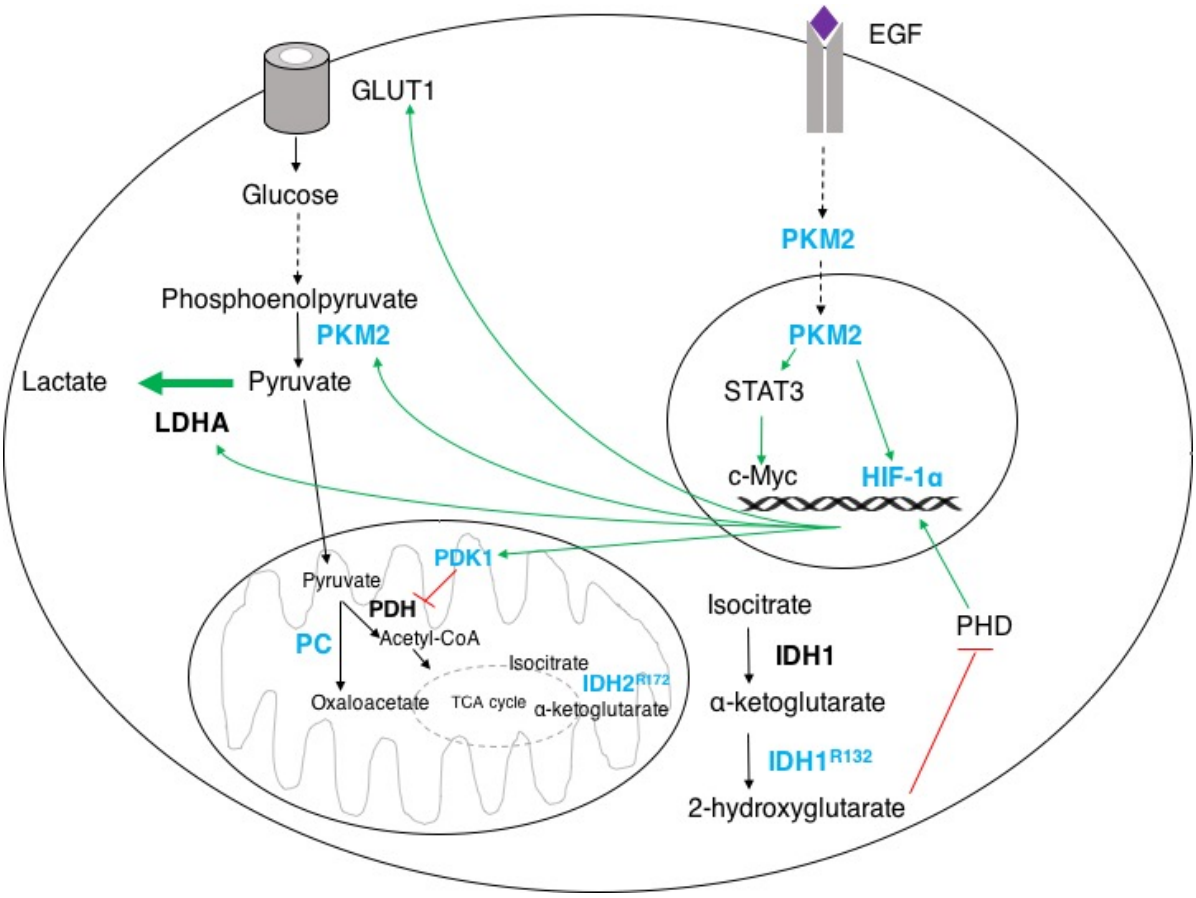

Figure 3. Summary of common metabolic perturbations in GBM.
Changes in expression, activation or mutations in several enzymes allow GBM tumors to adapt and sustain tumor biology. Production of 2-HG by mutant IDH1 decreases certain TCA cycle intermediates, inhibits ATP synthase and stabilizes HIF1-α. PKM2 diverts entrance of pyruvate into the TCA cycle and promotes aerobic glycolysis, after EGF stimulation it translocates to the nucleus where it acts as a coactivator of HIF1-α, thus transactivating genes that will promote glycolysis including GLUT1 and LDHA.

4. Mitochondria and cancer

Mitochondrial dysfunction has been associated with tumor progression of different cancers, including brain cancers (Seoane et al., 2011; Zong et al., 2016). Most studies focus on the role of mitochondria and the ability of a cancer cell to avoid apoptosis, however changes in mitochondrial physiology are essential for metabolic reprogramming (Wallace, 2012). Additionally, limited mitochondrial dysfunction has been shown to drive cell transformation and tumorigenesis (Ichim et al., 2015). Because mitochondria are highly integrated organelles, it is likely that perturbations in nominal organelle function resulting from genetic polymorphisms and a changing environment will have diverse effects within a cell.

4.1 Mitochondrial aberrations in cancer

Many cellular processes are controlled by mitochondria, such as energy production, calcium metabolism, ROS generation, regulation of reduction-oxidation (redox) status, initiation of apoptosis and contribution to different biosynthetic pathways, functional mitochondria that display distinct adaptations to promote sustained proliferation and survival are essential for cancer development (Wallace, 2012).

Mitochondrial DNA (mtDNA) contains 37 genes, of these 13 encode proteins that form part of the oxidative phosphorylation (OXPHOS) complexes, while the rest of required proteins are nuclearly encoded (Schon et al., 2012). Functional mtDNA is essential for cancer cells, depletion of mtDNA reduces tumor growth rates, however, reincorporation of mtDNA is associated with tumor formation and recovery of mitochondrial function and respiration, indicating the importance of

mtDNA in tumor formation and progression (Tan et al., 2015). However, certain germline mutations in the mtDNA have been associated with an increased predisposition to certain cancers. Increased risk of invasive breast cancer or endometrial cancer is associated with two polymorphisms in the NADH:ubiquinone oxidoreductase core subunit 3 (ND3) gene, while mutations of cytochrome C oxidase I (COI) gene have been linked with prostate cancer (Brandon et al., 2006). Additionally, high levels of mtDNA mutations have been described in tumors in comparison with normal tissue from the same patient (Chinnery et al., 2002). Furthermore, various cancers have mutations in the nuclear encoded mitochondrial enzymes succinate dehydrogenase (SDH), fumarate hydratase (FH) and IDH1/IDH2 (Wallace, 2012). Inhibition of SDH leads to stabilization of HIF-1α promoting a metabolic shift to glycolysis and increased production of mitochondrial ROS (Chandel et al., 2000). While high levels of ROS can be toxic for the cell, in cells where apoptosis is compromised, increased mitochondrial ROS can drive oncogenic transformation and promote cell proliferation (F. Weinberg et al., 2010). Mitochondria are essential for execution of apoptosis, however evasion of cell death is a key feature of many cancers, where various cancers show an upregulation of pro-survival B-cell lymphoma-2 (Bcl-2) proteins, which not only promotes tumor progression but has been linked to acquired resistance to chemotherapeutics (Giampazolias and Tait, 2016).

4.2 Bcl-2 proteins

The Bcl-2 family of proteins are master regulators of apoptosis, they are classified into two groups pro-survival and pro-apoptotic (Moldoveanu et al., 2014). The pro-

survival or anti-apoptotic Bcl-2 proteins contain four Bcl-2 Homology (BH) domains (Figure 4) and are found both in the cytosol and integrated within the mitochondrial outer membrane (MOM), the main members of the Bcl-2 anti-apoptotic group are Bcl-2, Bcl-2-related gene, long isoform (Bcl-xL), Bcl-2-related gene A1 (A1) and myeloid cell leukemia (Mcl-1), their main function is to prevent apoptosis by inhibiting pro-apoptotic proteins and preserving MOM integrity (Chipuk et al., 2010). The pro-apoptotic Bcl-2 proteins can be subdivided into two subgroups, effectors and BH3-only proteins (Chipuk et al., 2010). Effector proteins, Bcl-2 associated X protein (BAX) and Bcl-2 antagonist killer 1 (BAK), contain BH1-3 domains (figure 4) and activation of BAK and BAX upon apoptotic stimuli promote conformational changes and oligomerization forming the mitochondrial permeability transition pore (mtPTP) initiating the mitochondrial outer membrane permeabilization (MOMP), which effectively engages the apoptotic program (Giampazolias and Tait, 2016; Moldoveanu et al., 2014). BH3-only proteins, contain only the third BH domain (Figure 4), and are subdivided based on their interactions with other Bcl-2 family proteins by either directly activating pro-apoptotic effector proteins or inhibiting Bcl-2 pro-survival proteins (Moldoveanu et al., 2014). Direct activators BH3-only proteins Bcl-2 interacting domain agonist (BID), Bcl-2 interacting mediator of cell death (BIM) and p53 modulator of apoptosis (PUMA), are able to directly activate BAX and BAK, promoting the conformational changes and oligomerization that will lead to pore formation and subsequent MOMP (Chipuk and Green, 2008). The BH3-only proteins BCL-2 antagonist of cell death (BAD), BCL-2 interacting killer (BIK), BCL-2 modifying

factor (BMF), harakiri (HRK), and Noxa, are known as desensitizers or de-repressors and act by neutralizing Bcl-2 pro-survival proteins which promotes liberation of BAX and BAK, allowing oligomerization and initiation of MOMP (Chipuk and Green, 2008).

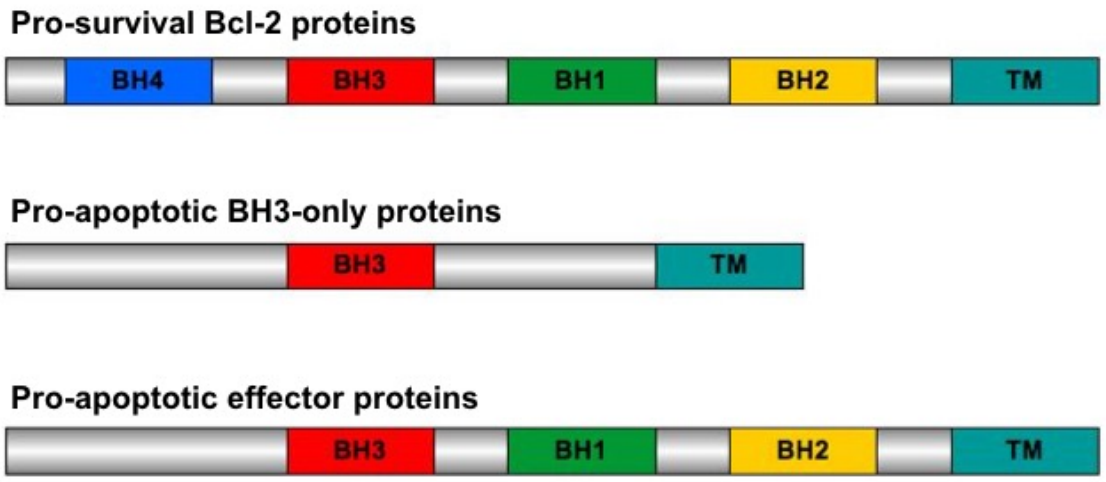

Figure 4. Bcl-2 family of proteins.
Pro-survival proteins have four BH domains (BH1, BH2, BH3 and BH4), pro-apoptotic BH3-only have only the third BH domain, and effector proteins have three domains (BH1, BH2 and BH3).

4.3 Apoptotic priming

For cancer cells to avoid the established pathways for programmed cell death, oncogenic programs make precise changes to the levels of Bcl-2-related family proteins (Letai, 2008). An increase in Bcl-2 pro-survival proteins (Bcl-2, Mcl-1 and Bcl-xL) is commonly associated with apoptotic evasion, while elevated levels of pro-apoptotic BH3-only proteins (Bim, Bid, Puma, Noxa, etc.) may indicate pro-apoptotic mitochondria more susceptible to drug treatment (Letai et al., 2002; Letai, 2008; Ryan et al., 2010; Schellenberg et al., 2013). Apoptotic priming has

been shown to increase sensitivity of certain cancers to chemotherapy thus improving their efficacy (Chonghaile et al., 2011; Montero et al., 2015; Vo et al., 2012). Priming levels are determined by the replacement or sequestration of pro-survival Bcl-2 proteins by BH3-only proteins on the MOM (Chonghaile et al., 2011; Davids et al., 2012; Reed, 2011; Vo et al., 2012). Apoptotic priming can be used to stratify cell lines and tumor samples according to response and resistance to chemotherapeutic drugs (Ryan and Letai, 2013).The levels of Bcl-2 proteins and chemo-responsiveness have been evaluated in neuroblastoma, and BH3-only levels can be used as therapeutic predictor of response and resistance (Goldsmith et al., 2012; 2010), however the relationship between Bcl-2 protein levels and chemo-resistance in GBM has yet to be evaluated.

4.4 Mitochondrial outer membrane permeabilization in oncogenesis and chemosensitivity

Mitochondria plays an essential role in regulating the apoptotic pathway, in cancer cells, evasion of apoptosis is commonly observed (Hanahan and R. A. Weinberg, 2011). Two pathways can initiate apoptosis, the extrinsic pathway which involves activation of cell surface death receptors, and the intrinsic pathway is mediated by mitochondria and involves initiation of MOMP, most chemotherapeutic agents act through the intrinsic pathway (Brahmbhatt et al., 2015). Upon apoptotic stimuli, activation of BAX and BAK by BH3-only proteins promotes oligomerization of BAX and BAK and leads to pore formation and MOMP, mitochondrial proteins, such as cytochrome c, second mitochondria-derived activator of caspase (SMAC) and HtrA serine peptidase 2 (HtrA2), are released from the inter-membrane space (IMS)

which results in caspase activation and apoptosis (Chipuk et al., 2006; Renault and Chipuk, 2014; Tait and Green, 2013). MOMP is considered the “point of no return”, however in some cases cells are able to survive and avoid apoptosis, which becomes relevant in cancer and allows for tumor cell survival. In certain types of cancer, cells can undergo incomplete MOMP leaving some intact mitochondria, which allows them to recover and survive by bypassing caspase activation downstream of MOMP, either due to reduced caspase activity or expression, and it could be a potential mechanism of acquired chemoresistance (Tait et al., 2010). Furthermore, limited MOMP after a sub-lethal stress only sufficient to permeabilize a minority of mitochondria, may lead to caspase activation and the subsequent cleavage of caspase substrates, promoting DNA damage, genomic instability and tumorigenesis (Ichim et al., 2015).

5. Control of Bcl-2 protein levels

The Bcl-2 family of proteins are critical regulators of apoptosis by preserving OMM integrity and preventing MOMP and the subsequent activation of caspases leading to cell death, as such Bcl-2 proteins are tightly controlled both at the transcriptional and the post-translational levels.

5.1 General

Most Bcl-2 proteins regulate their activity by heterodimerization between pro-survival and pro-apoptotic (Tsujimoto and Shimizu, 2000). BAX binds to Bcl-2 and BAK interacts with Mcl-1 and Bcl-xL, thus preventing the conformational changes required for BAX/BAK activation and oligomerization, however, upon apoptotic stimuli BAX and BAK are displaced promoting cell death, when BAD

heterodimerize with Bcl-2 and Bcl-xL and Noxa interacts with Mcl-1 (Oltvai et al., 1993; Willis et al., 2005; E. Yang et al., 1995).

Since apoptotic control depends on the balance between levels of pro-survival and pro-apoptotic proteins, transcriptional regulation and degradation become instrumental in the process. The different Bcl-2 pro-survival proteins are under distinct transcriptional programs according to their tissue specificity and their physiological role. Mcl-1 expression is dependent on growth factors and can be upregulated by different cytokines such as IL-3, IL-5, IL-6 GM-CSF, as well as EGF and VEGF, and transcription is directly repressed by E2F-1 binding to the promoter (Thomas et al., 2010). Bcl-xL transcription is also regulated by growth factors and transcription is induced through the Janus kinase (JAK)/STAT pathway (Grad et al., 2000). Transcription upregulation of BH3-only proteins occurs in response to early apoptotic signals, p53 induces transcription of Noxa and Puma, while upregulation of BIM expression occurs in response to growth factor deprivation via FOXO3A (O forkhead box transcription factor-3A) or endoplasmic reticulum (ER) stress by CEBPα (CCAAT-enhancer binding protein-α) or CHOP (CEBP homologous protein) (Youle and Strasser, 2008).

Control of Bcl-2 proteins is achieved by post-translational modifications and protein degradation, for example polyubiquitination of Mcl-1 and Bcl-2 targets them for proteosomal degradation, while caspase-dependent cleavage of Mcl-1 occurs during apoptosis (Neutzner et al., 2012; Thomas et al., 2010). Furthermore, ubiquitination and subsequent proteosomal degradation has also been observed in the BH3-only proteins BID, BAD, BIM and BIK (Neutzner et al., 2012).

Additionally, phosphorylation of BAD by cAMP-dependent protein kinase (PKA) or by the 70-kDa ribosomal protein S6 kinase (p70S6K) promotes Bad inactivation by sequestration of BAD by 14-3-3 and disrupting the binding to Bcl-2 and Bcl-xL, which has a prosurvival effect (Harada et al., 2001; 1999; Zha et al., 1996).

5.2 MAPK

Post-translational modifications determine the fate of many Bcl-2 family proteins, either by promoting protein stability or by working as a target for protein degradation. The MAPK signaling pathway controls a wide range of cellular processes such as proliferation, differentiation, migration and death, MAPKs can phosphorylate a large number of substrates and the outcome of signaling depends on the magnitude, localization and set of substrates phosphorylated (Ramos, 2008). Similarly, MAPK signaling has been shown to regulate both the induction of apoptosis as well as the inhibition, for example MEK/ERK signaling promotes apoptosis by upregulating the expression of pro-apoptotic proteins Bak, Bax, Puma and down regulating of Bcl-2 and Bcl-xL (Cagnol and Chambard, 2010). However, ERK has also been associated with phosphorylation of Mcl-1 at Thr92/Thr163, which promotes Mcl-1 stability and improves anti-apoptotic function (Domina et al., 2004; Thomas et al., 2010), and phosphorylation of Bim which targets it for ubiquitination and subsequent proteosomal degradation, it also prevents Bim from interacting and activating Bax, which prevents pore formation and has an antiapoptotic effect (Ley et al., 2005).

5.3 JNK and Sab

JNK signaling has been linked to induction of apoptosis and chemosensitization in neuroblastoma cells (Cheng et al., 2014; Fey et al., 2015; Filomeni et al., 2003; Waetzig et al., 2009). Upon different stress stimuli, phosphorylated JNK translocates to the mitochondria where it interacts with the c-terminal part of Sab through a kinase interaction motif (KIM) (Wiltshire et al., 2004; 2002). At the mitochondria, stress-induced JNK signaling promotes mitochondrial dysfunction by amplifying reactive oxygen species (ROS) production, inducing mitochondrial permeability and impairing bioenergetics (J. W. Chambers and LoGrasso, 2011; Hanawa et al., 2008). Mitochondrial JNK signaling also plays a role in cell death, where activated JNK phosphorylates members of the Bcl-2 family of proteins thus promoting apoptosis (J. W. Chambers et al., 2011; Schroeter et al., 2003). JNK phosphorylates Bcl-2 at Ser70 inactivating the protein and facilitating apoptosis, also phosphorylation of Mcl-1 is the first step for Mcl-1 stress-induced degradation (Morel et al., 2009; Yamamoto et al., 1999). Furthermore, JNK-mediated phosphorylation of pro-apoptotic proteins Bim and Bmf, promotes their release from motor complexes where they remain sequestered in the cytosol, once released they are able to induce apoptosis via Bax (Lei and Davis, 2003).

6. Sab

Sab, also known as SH3BP5, is an outer mitochondrial membrane protein that acts as a scaffold for the c-Jun N-Terminal Kinase (JNK) (Wiltshire et al., 2002). Inhibition of the JNK-Sab interaction prevents oxidative stress, mitochondrial dysfunction and cell death. Furthermore amplification of JNK/Sab-mediated

signaling has been shown to sensitize cancer cells and improve chemotherapeutic efficacy (J. W. Chambers et al., 2011; 2013a; 2013b; T. P. Chambers et al., 2015; Wiltshire et al., 2004). However, the impact of Sab-mediated signaling on mitochondrial function and apoptosis has yet to be fully delineated in human glioblastoma or neuroblastoma.

6.1 Structure

Sab was identified using a protein-protein interaction screen by its ability to bind Bruton's tyrosine kinase (BTK) through the SH3 (Src homology 3) domain (Wiltshire et al., 2002). Further inspection of the Sab sequence determine the presence of two KIM motifs, KIM1 and KIM2, in C-terminal portion of the protein, which are required for JNK binding (Wiltshire et al., 2004; 2002). Additionally, bioinformatics studies of the full-length Sab revealed the presence of another two prospective protein-protein interaction motifs (Figure 5). The N-terminal portion of the protein contains two coiled-coiled (CC) motifs, which are generally associated with dimerization and interaction with other proteins (Strauss and S. Keller, 2008), the SH3 motif located within CC2.

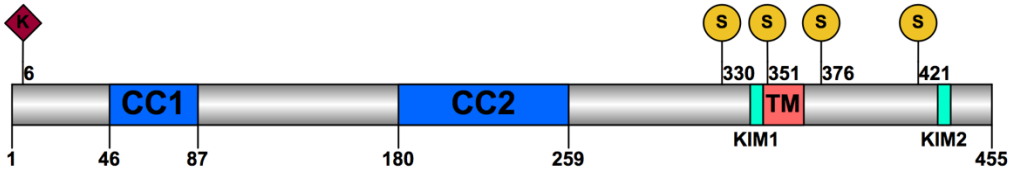

Figure 5. Schematic representation of Sab
CC1: coiled-coiled motif 1, CC2: coiled-coiled motif 2, TM transmembrane domain, KIM1: kinase interaction motif 1, KIM2: kinase interaction motif 2, S: phosphorylation sites.

6.2 Functions

Sab functions as an OMM scaffold for JNK (Wiltshire et al., 2002). Interaction between Sab and JNK is required for the mitochondrial effects of JNK signaling without impairing JNK nuclear signaling, as demonstrated by inhibition of this interaction using Tat-Sab_{KIM1} peptide, which prevented Bcl-2 phosphorylation, loss of mitochondrial membrane potential and cell death but had no effect on c-Jun phosphorylation or transcription of AP-1 (J. W. Chambers et al., 2011). Inhibition of mitochondrial JNK signaling by either silencing Sab or using Tat-Sab_{KIM1} peptide, has a protective effect in sustained liver injury and hepatotoxicity models and in the 6-hydroxydopamine neurotoxicity model (J. W. Chambers et al., 2013a; Win et al., 2011). Moreover, interaction of JNK with Sab has been shown to inhibit mitochondrial respiration, increases production of ROS, which leads to cell death in a model of hepatocyte lipotoxicity (Win et al., 2015) and ER stress induced by tunicamycin or brefeldin A (BFA) (Win et al., 2014). Additionally, Sab mediates oxidative stress and decreases mitochondrial respiration, ATP production and membrane potential in cardiomyocyte-like cells after treatment with imatinib (T. P. Chambers et al., 2017). Sab as also been shown to be expressed throughput the brain, and inhibition of Sab using the Tat-Sab_{KIM1} peptide altered activity of cultured hippocampal neurons by decreasing the firing frequency and the amplitude of spikes, indicating that Sab- mediated signaling plays a role in normal neuronal function (Sodero et al., 2017).

7. References

Abbadi, S., Rodarte, J.J., Abutaleb, A., Lavell, E., Smith, C.L., Ruff, W., Schiller, J., Olivi, A., Levchenko, A., Guerrero-Cazares, H., Quinones-Hinojosa, A., 2014. Glucose-6-phosphatase is a key metabolic regulator of glioblastoma invasion. Mol. Cancer Res. 12, 1547–1559. doi:10.1158/1541-7786.MCR-14-0106-T

Agnihotri, S., Zadeh, G., 2016. Metabolic reprogramming in glioblastoma: the influence of cancer metabolism on epigenetics and unanswered questions. Neuro Oncol 18, 160–172. doi:10.1093/neuonc/nov125

Alcantara Llaguno, S.R., Xie, X., Parada, L.F., 2016. Cell of Origin and Cancer Stem Cells in Tumor Suppressor Mouse Models of Glioblastoma. Cold Spring Harb. Symp. Quant. Biol. 81, 31–36. doi:10.1101/sqb.2016.81.030973

Althoff, K., Beckers, A., Bell, E., Nortmeyer, M., Thor, T., Sprüssel, A., Lindner, S., De Preter, K., Florin, A., Heukamp, L.C., Klein-Hitpass, L., Astrahantseff, K., Kumps, C., Speleman, F., Eggert, A., Westermann, F., Schramm, A., Schulte, J.H., 2015. A Cre-conditional MYCN-driven neuroblastoma mouse model as an improved tool for preclinical studies. Oncogene 34, 3357–3368. doi:10.1038/onc.2014.269

Altman, B.J., Stine, Z.E., Dang, C.V., 2016. From Krebs to clinic: glutamine metabolism to cancer therapy. Nature Publishing Group 16, 619–634. doi:10.1038/nrc.2016.71

Baker, D.L., Schmidt, M.L., Cohn, S.L., Maris, J.M., London, W.B., Buxton, A., Stram, D., Castleberry, R.P., Shimada, H., Sandler, A., Shamberger, R.C., Look, A.T., Reynolds, C.P., Seeger, R.C., Matthay, K.K., Children's Oncology Group, 2010. Outcome after reduced chemotherapy for intermediate-risk neuroblastoma. N Engl J Med 363, 1313–1323. doi:10.1056/NEJMoa1001527

Beltran, H., 2014. The N-myc Oncogene: Maximizing its Targets, Regulation, and Therapeutic Potential. Mol. Cancer Res. 12, 815–822. doi:10.1158/1541-7786.MCR-13-0536

Bensaad, K., Favaro, E., Lewis, C.A., Peck, B., Lord, S., Collins, J.M., Pinnick, K.E., Wigfield, S., Buffa, F.M., Li, J.-L., Zhang, Q., Wakelam, M.J.O., Karpe, F., Schulze, A., Harris, A.L., 2014. Fatty Acid Uptake and Lipid Storage Induced by HIF-1α Contribute to Cell Growth and Survival after Hypoxia-Reoxygenation. CELREP 9, 349–365. doi:10.1016/j.celrep.2014.08.056

Bensinger, S.J., Christofk, H.R., 2012. New aspects of the Warburg effect in cancer cell biology. Semin. Cell Dev. Biol. 23, 352–361. doi:10.1016/j.semcdb.2012.02.003

Bianchi, F., Tamburrini, G., Gessi, M., Frassanito, P., Massimi, L., Caldarelli, M., 2018. Central nervous system (CNS) neuroblastoma. A case-based update. Childs Nerv Syst 34, 817–823. doi:10.1007/s00381-018-3764-3

Blum, R., Jacob-Hirsch, J., Amariglio, N., Rechavi, G., Kloog, Y., 2005. Ras Inhibition in Glioblastoma Down-regulates Hypoxia-Inducible Factor-1α, Causing Glycolysis Shutdown and Cell Death. Cancer Research 65, 999–1006. doi:10.1038/35052535

Bosse, K.R., Maris, J.M., 2016. Advances in the translational genomics of neuroblastoma: From improving risk stratification and revealing novel biology to identifying actionable genomic alterations. Cancer 122, 20–33. doi:10.1002/cncr.29706

Bouzier, A.K., Goodwin, R., de Gannes, F.M., Valeins, H., Voisin, P., Canioni, P., Merle, M., 1998. Compartmentation of lactate and glucose metabolism in C6 glioma cells. A 13c and 1H NMR study. Journal of Biological Chemistry 273, 27162–27169.

Brahmbhatt, H., Oppermann, S., Osterlund, E.J., Leber, B., Andrews, D.W., 2015. Molecular Pathways: Leveraging the BCL-2 Interactome to Kill Cancer Cells--Mitochondrial Outer Membrane Permeabilization and Beyond. Clinical Cancer Research 21, 2671–2676. doi:10.1158/1078-0432.CCR-14-0959

Brandon, M., Baldi, P., Wallace, D.C., 2006. Mitochondrial mutations in cancer. Oncogene 25, 4647–4662. doi:10.1038/sj.onc.1209607

Brennan, C.W., Verhaak, R.G.W., McKenna, A., Campos, B., Noushmehr, H., Salama, S.R., Zheng, S., Chakravarty, D., Sanborn, J.Z., Berman, S.H., Beroukhim, R., Bernard, B., Wu, C.-J., Genovese, G., Shmulevich, I., Barnholtz-Sloan, J., Zou, L., Vegesna, R., Shukla, S.A., Ciriello, G., Yung, W.K., Zhang, W., Sougnez, C., Mikkelsen, T., Aldape, K., Bigner, D.D., Van Meir, E.G., Prados, M., Sloan, A., Black, K.L., Eschbacher, J., Finocchiaro, G., Friedman, W., Andrews, D.W., Guha, A., Iacocca, M., O'Neill, B.P., Foltz, G., Myers, J., Weisenberger, D.J., Penny, R., Kucherlapati, R., Perou, C.M., Hayes, D.N., Gibbs, R., Marra, M., Mills, G.B., Lander, E., Spellman, P., Wilson, R., Sander, C., Weinstein, J., Meyerson, M., Gabriel, S., Laird, P.W., Haussler, D., Getz, G., Chin, L., TCGA Research Network, 2013. The somatic genomic landscape of glioblastoma. Cell 155, 462–477. doi:10.1016/j.cell.2013.09.034

Brodeur, G.M., Pritchard, J., Berthold, F., Carlsen, N.L., Castel, V., Castelberry, R.P., De Bernardi, B., Evans, A.E., Favrot, M., Hedborg, F., 1993. Revisions of the international criteria for neuroblastoma diagnosis, staging, and response to treatment. Journal of Clinical Oncology 11, 1466–1477. doi:10.1200/JCO.1993.11.8.1466

Cagnol, S., Chambard, J.-C., 2010. ERK and cell death: mechanisms of ERK-induced cell death--apoptosis, autophagy and senescence. FEBS J 277, 2–21. doi:10.1111/j.1742-4658.2009.07366.x

Cancer Genome Atlas Research Network, 2008. Comprehensive genomic characterization defines human glioblastoma genes and core pathways. Nature 455, 1061–1068. doi:10.1038/nature07385

Chakraborty, S., Li, L., Puliyappadamba, V.T., Guo, G., Hatanpaa, K.J., Mickey, B., Souza, R.F., Vo, P., Herz, J., Chen, M.-R., Boothman, D.A., Pandita, T.K., Wang, D.H., Sen, G.C., Habib, A.A., 2014. Constitutive and ligand-induced EGFR signalling triggers distinct and mutually exclusive downstream signalling networks. Nat Commun 5, 5811. doi:10.1038/ncomms6811

Chambers, J.W., Cherry, L., Laughlin, J.D., Figuera-Losada, M., LoGrasso, P.V., 2011. Selective inhibition of mitochondrial JNK signaling achieved using peptide mimicry of the Sab kinase interacting motif-1 (KIM1). ACS Chem. Biol. 6, 808–818. doi:10.1021/cb200062a

Chambers, J.W., Howard, S., LoGrasso, P.V., 2013a. Blocking c-Jun N-terminal kinase (JNK) translocation to the mitochondria prevents 6-hydroxydopamine-induced toxicity in vitro and in vivo. J. Biol. Chem. 288, 1079–1087. doi:10.1074/jbc.M112.421354

Chambers, J.W., LoGrasso, P.V., 2011. Mitochondrial c-Jun N-terminal kinase (JNK) signaling initiates physiological changes resulting in amplification of reactive oxygen species generation. J. Biol. Chem. 286, 16052–16062. doi:10.1074/jbc.M111.223602

Chambers, J.W., Pachori, A., Howard, S., Iqbal, S., LoGrasso, P.V., 2013b. Inhibition of JNK mitochondrial localization and signaling is protective against ischemia/reperfusion injury in rats. J. Biol. Chem. 288, 4000–4011. doi:10.1074/jbc.M112.406777

Chambers, T.P., Portalatin, G.M., Paudel, I., Robbins, C.J., Chambers, J.W., 2015. Sub-chronic administration of LY294002 sensitizes cervical cancer cells to chemotherapy by enhancing mitochondrial JNK signaling. Biochemical and Biophysical Research Communications 463, 538–544. doi:10.1016/j.bbrc.2015.05.075

Chambers, T.P., Santiesteban, L., Gomez, D., Chambers, J.W., 2017. Sab mediates mitochondrial dysfunction involved in imatinib mesylate-induced cardiotoxicity. Toxicology 382, 24–35. doi:10.1016/j.tox.2017.03.006

Chandel, N.S., McClintock, D.S., Feliciano, C.E., Wood, T.M., Melendez, J.A., Rodriguez, A.M., Schumacker, P.T., 2000. Reactive oxygen species generated at mitochondrial complex III stabilize hypoxia-inducible factor-1alpha during hypoxia: a mechanism of O2 sensing. Journal of Biological Chemistry 275, 25130–25138. doi:10.1074/jbc.M001914200

Cheng, J., Fan, Y.-H., Xu, X., Zhang, H., Dou, J., Tang, Y., Zhong, X., Rojas, Y., Yu, Y., Zhao, Y., Vasudevan, S.A., Nuchtern, J.G., Kim, E.S., Chen, X., Lu, F., Yang, J., 2014. A small-molecule inhibitor of UBE2N induces neuroblastoma cell death via activation of p53 and JNK pathways. Cell Death and Disease 5, e1079–e1079. doi:10.1038/cddis.2014.54

Chesnelong, C., Chesnelong, C., Chaumeil, M.M., Chaumeil, M.M., Blough, M.D., Blough, M.D., Al-Najjar, M., Al-Najjar, M., Stechishin, O.D., Stechishin, O.D., Chan, J.A., Chan, J.A., Pieper, R.O., Pieper, R.O., Ronen, S.M., Ronen, S.M., Weiss, S., Weiss, S., Luchman, H.A., Luchman, H.A., Cairncross, J.G., Cairncross, J.G., 2014. Lactate dehydrogenase A silencing in IDH mutant gliomas. Neuro Oncol 16, 686–695. doi:10.1093/neuonc/not243

Cheung, N.-K.V., Cheung, I.Y., Kushner, B.H., Ostrovnaya, I., Chamberlain, E., Kramer, K., Modak, S., 2012. Murine anti-GD2 monoclonal antibody 3F8 combined with granulocyte-macrophage colony-stimulating factor and 13-cis-retinoic acid in high-risk patients with stage 4 neuroblastoma in first remission. J. Clin. Oncol. 30, 3264–3270. doi:10.1200/JCO.2011.41.3807

Cheung, N.-K.V., Dyer, M.A., 2013. Neuroblastoma: developmental biology, cancer genomics and immunotherapy. Nature Publishing Group 13, 397–411. doi:10.1038/nrc3526

Chinnery, P.F., Samuels, D.C., Elson, J., Turnbull, D.M., 2002. Accumulation of mitochondrial DNA mutations in ageing, cancer, and mitochondrial disease: is there a common mechanism? Lancet 360, 1323–1325. doi:10.1016/S0140-6736(02)11310-9

Chipuk, J.E., Bouchier-Hayes, L., Green, D.R., 2006. Mitochondrial outer membrane permeabilization during apoptosis: the innocent bystander scenario. Cell Death Differ. 13, 1396–1402. doi:10.1038/sj.cdd.4401963

Chipuk, J.E., Green, D.R., 2008. How do BCL-2 proteins induce mitochondrial outer membrane permeabilization? Trends in Cell Biology 18, 157–164. doi:10.1016/j.tcb.2008.01.007

Chipuk, J.E., Moldoveanu, T., Llambi, F., Parsons, M.J., Green, D.R., 2010. The BCL-2 family reunion. Molecular Cell 37, 299–310. doi:10.1016/j.molcel.2010.01.025

Chonghaile, T.N., Sarosiek, K.A., Vo, T.T., Ryan, J.A., Tammareddi, A., Moore, V.D.G., Deng, J., Anderson, K.C., Richardson, P., Tai, Y.T., Mitsiades, C.S., Matulonis, U.A., Drapkin, R., Stone, R., DeAngelo, D.J., McConkey, D.J., Sallan, S.E., Silverman, L., Hirsch, M.S., Carrasco, D.R., Letai, A., 2011. Pretreatment Mitochondrial Priming Correlates with Clinical Response to Cytotoxic Chemotherapy. Science 334, 1129–1133. doi:10.1126/science.1206727

Christofk, H.R., Vander Heiden, M.G., Harris, M.H., Ramanathan, A., Gerszten, R.E., Wei, R., Fleming, M.D., Schreiber, S.L., Cantley, L.C., 2008. The M2 splice isoform of pyruvate kinase is important for cancer metabolism and tumour growth. Nature 452, 230–233. doi:10.1038/nature06734

Chua, C.Y., Liu, Y., Granberg, K.J., Hu, L., Haapasalo, H., Annala, M.J., Cogdell, D.E., Verploegen, M., Moore, L.M., Fuller, G.N., Nykter, M., Cavenee, W.K., Zhang, W., 2016. IGFBP2 potentiates nuclear EGFR-STAT3 signaling. Oncogene 35, 738–747. doi:10.1038/onc.2015.131

Cohn, S.L., Pearson, A.D.J., London, W.B., Monclair, T., Ambros, P.F., Brodeur, G.M., Faldum, A., Hero, B., Iehara, T., Machin, D., Mosseri, V., Simon, T., Garaventa, A., Castel, V., Matthay, K.K., INRG Task Force, 2009. The International Neuroblastoma Risk Group (INRG) classification system: an INRG Task Force report. J. Clin. Oncol. 27, 289–297. doi:10.1200/JCO.2008.16.6785

Courtnay, R., Ngo, D.C., Malik, N., Ververis, K., Tortorella, S.M., Karagiannis, T.C., 2015. Cancer metabolism and the Warburg effect: the role of HIF-1 and PI3K. Mol Biol Rep 42, 841–851. doi:10.1007/s11033-015-3858-x

Dang, L., White, D.W., Gross, S., Bennett, B.D., Bittinger, M.A., Driggers, E.M., Fantin, V.R., Jang, H.G., Jin, S., Keenan, M.C., Marks, K.M., Prins, R.M., Ward, P.S., Yen, K.E., Liau, L.M., Rabinowitz, J.D., Cantley, L.C., Thompson, C.B., Vander Heiden, M.G., Su, S.M., 2009. Cancer-associated IDH1 mutations produce 2-hydroxyglutarate. Nature 462, 739–744. doi:10.1038/nature08617

Davids, M.S., Deng, J., Wiestner, A., Lannutti, B.J., Wang, L., Wu, C.J., Wilson, W.H., Brown, J.R., Letai, A., 2012. Decreased mitochondrial apoptotic priming underlies stroma-mediated treatment resistance in chronic lymphocytic leukemia. Blood 120, 3501–3509. doi:10.1182/blood-2012-02-414060

Davis, M.E., 2016. Glioblastoma: Overview of Disease and Treatment. Clin J Oncol Nurs 20, S2–8. doi:10.1188/16.CJON.S1.2-8

Daye, D., Wellen, K.E., 2012. Metabolic reprogramming in cancer: unraveling the role of glutamine in tumorigenesis. Semin. Cell Dev. Biol. 23, 362–369. doi:10.1016/j.semcdb.2012.02.002

DeBerardinis, R.J., Lum, J.J., Hatzivassiliou, G., Thompson, C.B., 2008. The biology of cancer: metabolic reprogramming fuels cell growth and proliferation. Cell Metabolism 7, 11–20. doi:10.1016/j.cmet.2007.10.002

DeBerardinis, R.J., Mancuso, A., Daikhin, E., Nissim, I., Yudkoff, M., Wehrli, S., Thompson, C.B., 2007. Beyond aerobic glycolysis: transformed cells can engage in glutamine metabolism that exceeds the requirement for protein and nucleotide synthesis. Proc. Natl. Acad. Sci. U.S.A. 104, 19345–19350. doi:10.1073/pnas.0709747104

Desai, S., Ding, M., Wang, B., Lu, Z., Zhao, Q., Shaw, K., Yung, W.K.A., Weinstein, J.N., Tan, M., Yao, J., 2014. Tissue-specific isoform switch and DNA hypomethylation of the pyruvate kinase PKM gene in human cancers. Oncotarget 5, 8202–8210. doi:10.18632/oncotarget.1159

Dombrauckas, J.D., Santarsiero, B.D., Mesecar, A.D., 2005. Structural basis for tumor pyruvate kinase M2 allosteric regulation and catalysis. Biochemistry 44, 9417–9429. doi:10.1021/bi0474923

Domina, A.M., Vrana, J.A., Gregory, M.A., Hann, S.R., Craig, R.W., 2004. MCL1 is phosphorylated in the PEST region and stabilized upon ERK activation in viable cells, and at additional sites with cytotoxic okadaic acid or taxol. Oncogene 23, 5301–5315. doi:10.1038/sj.onc.1207692

Elborai, Y., Hafez, H., Moussa, E.A., Hammad, M., Hussein, H., Lehmann, L., Elhaddad, A., 2016. Comparison of toxicity following different conditioning regimens (busulfan/melphalan and carboplatin/etoposide/melphalan) for advanced stage neuroblastoma: Experience of two transplant centers. Pediatr Transplant 20, 284–289. doi:10.1111/petr.12638

Eleveld, T.F., Oldridge, D.A., Bernard, V., Koster, J., Daage, L.C., Diskin, S.J., Schild, L., Bentahar, N.B., Bellini, A., Chicard, M., Lapouble, E., Combaret, V., Legoix-Né, P., Michon, J., Pugh, T.J., Hart, L.S., Rader, J., Attiyeh, E.F., Wei, J.S., Zhang, S., Naranjo, A., Gastier-Foster, J.M., Hogarty, M.D., Asgharzadeh, S., Smith, M.A., Guidry Auvil, J.M., Watkins, T.B.K., Zwijnenburg, D.A., Ebus, M.E., van Sluis, P., Hakkert, A., van Wezel, E., van der Schoot, C.E., Westerhout, E.M., Schulte, J.H., Tytgat, G.A., Dolman, M.E.M., Janoueix-Lerosey, I., Gerhard, D.S., Caron, H.N., Delattre, O., Khan, J., Versteeg, R., Schleiermacher, G., Molenaar, J.J., Maris, J.M., 2015.

Relapsed neuroblastomas show frequent RAS-MAPK pathway mutations. Nat Genet 47, 864–871. doi:10.1038/ng.3333

Fack, F., Espedal, H., Keunen, O., Golebiewska, A., Obad, N., Harter, P.N., Mittelbronn, M., Bähr, O., Weyerbrock, A., Stuhr, L., Miletic, H., Sakariassen, P.Ø., Stieber, D., Rygh, C.B., Lund-Johansen, M., Zheng, L., Gottlieb, E., Niclou, S.P., Bjerkvig, R., 2015. Bevacizumab treatment induces metabolic adaptation toward anaerobic metabolism in glioblastomas. Acta Neuropathol. 129, 115–131. doi:10.1007/s00401-014-1352-5

Fey, D., Halasz, M., Dreidax, D., Kennedy, S.P., Hastings, J.F., Rauch, N., Munoz, A.G., Pilkington, R., Fischer, M., Westermann, F., Kolch, W., Kholodenko, B.N., Croucher, D.R., 2015. Signaling pathway models as biomarkers: Patient-specific simulations of JNK activity predict the survival of neuroblastoma patients. Sci Signal 8, ra130–ra130. doi:10.1126/scisignal.aab0990

Filomeni, G., Aquilano, K., Rotilio, G., Ciriolo, M.R., 2003. Reactive oxygen species-dependent c-Jun NH2-terminal kinase/c-Jun signaling cascade mediates neuroblastoma cell death induced by diallyl disulfide. Cancer Research 63, 5940–5949.

Fu, X., Chin, R.M., Vergnes, L., Hwang, H., Deng, G., Xing, Y., Pai, M.Y., Li, S., Ta, L., Fazlollahi, F., Chen, C., Prins, R.M., Teitell, M.A., Nathanson, D.A., Lai, A., Faull, K.F., Jiang, M., Clarke, S.G., Cloughesy, T.F., Graeber, T.G., Braas, D., Christofk, H.R., Jung, M.E., Reue, K., Huang, J., 2015. 2-Hydroxyglutarate Inhibits ATP Synthase and mTOR Signaling. Cell Metabolism 22, 508–515. doi:10.1016/j.cmet.2015.06.009

Furnari, F.B., Furnari, F.B., Fenton, T., Fenton, T., Bachoo, R.M., Bachoo, R.M., Mukasa, A., Mukasa, A., Stommel, J.M., Stommel, J.M., Stegh, A., Stegh, A., Hahn, W.C., Hahn, W.C., Ligon, K.L., Ligon, K.L., Louis, D.N., Louis, D.N., Brennan, C., Brennan, C., Chin, L., Chin, L., DePinho, R.A., DePinho, R.A., Cavenee, W.K., Cavenee, W.K., 2007. Malignant astrocytic glioma: genetics, biology, and paths to treatment. Genes & Development 21, 2683–2710. doi:10.1101/gad.1596707

Gan, H.K., Kaye, A.H., Luwor, R.B., 2009. The EGFRvIII variant in glioblastoma multiforme. J Clin Neurosci 16, 748–754. doi:10.1016/j.jocn.2008.12.005

Gariboldi, M.B., Ravizza, R., Monti, E., 2010. The IGFR1 inhibitor NVP-AEW541 disrupts a pro-survival and pro-angiogenic IGF-STAT3-HIF1 pathway in human glioblastoma cells. Biochemical Pharmacology 80, 455–462. doi:10.1016/j.bcp.2010.05.011

Giampazolias, E., Tait, S.W.G., 2016. Mitochondria and the hallmarks of cancer. FEBS J 283, 803–814. doi:10.1111/febs.13603

Goldsmith, K.C., Gross, M., Peirce, S., Luyindula, D., Liu, X., Vu, A., Sliozberg, M., Guo, R., Zhao, H., Reynolds, C.P., Hogarty, M.D., 2012. Mitochondrial Bcl-2 Family Dynamics Define Therapy Response and Resistance in Neuroblastoma. Cancer Research 72, 2565–2577. doi:10.1158/0008-5472.CAN-11-3603

Goldsmith, K.C., Lestini, B.J., Gross, M., Ip, L., Bhumbla, A., Zhang, X., Zhao, H., Liu, X., Hogarty, M.D., 2010. BH3 response profiles from neuroblastoma mitochondria predict activity of small molecule Bcl-2 family antagonists. Cell Death Differ. 17, 872–882. doi:10.1038/cdd.2009.171

Grad, J.M., Zeng, X.R., Boise, L.H., 2000. Regulation of Bcl-xL: a little bit of this and a little bit of STAT. Curr Opin Oncol 12, 543–549.

Hanahan, D., Weinberg, R.A., 2011. Hallmarks of Cancer: The Next Generation. Cell 144, 646–674. doi:10.1016/j.cell.2011.02.013

Hanawa, N., Shinohara, M., Saberi, B., Gaarde, W.A., Han, D., Kaplowitz, N., 2008. Role of JNK translocation to mitochondria leading to inhibition of mitochondria bioenergetics in acetaminophen-induced liver injury. Journal of Biological Chemistry 283, 13565–13577. doi:10.1074/jbc.M708916200

Harada, H., Andersen, J.S., Mann, M., Terada, N., Korsmeyer, S.J., 2001. p70S6 kinase signals cell survival as well as growth, inactivating the pro-apoptotic molecule BAD. Proc Natl Acad Sci USA 98, 9666–9670. doi:10.1073/pnas.171301998

Harada, H., Becknell, B., Wilm, M., Mann, M., Huang, L.J., Taylor, S.S., Scott, J.D., Korsmeyer, S.J., 1999. Phosphorylation and inactivation of BAD by mitochondria-anchored protein kinase A. Molecular Cell 3, 413–422.

Hegi, M.E., Diserens, A.-C., Gorlia, T., Hamou, M.-F., de Tribolet, N., Weller, M., Kros, J.M., Hainfellner, J.A., Mason, W., Mariani, L., Bromberg, J.E.C., Hau, P., Mirimanoff, R.O., Cairncross, J.G., Janzer, R.C., Stupp, R., 2005. MGMT gene silencing and benefit from temozolomide in glioblastoma. N Engl J Med 352, 997–1003. doi:10.1056/NEJMoa043331

Hottinger, A.F., Pacheco, P., Stupp, R., 2016. Tumor treating fields: a novel treatment modality and its use in brain tumors. Neuro Oncol 18, 1338–1349. doi:10.1093/neuonc/now182

Hu, J., Sun, T., Wang, H., Chen, Z., Wang, S., Yuan, L., Liu, T., Li, H.-R., Wang, P., Feng, Y., Wang, Q., McLendon, R.E., Friedman, A.H., Keir, S.T., Bigner,

D.D., Rathmell, J., Fu, X.-D., Li, Q.-J., Wang, H., Wang, X.-F., 2016. MiR-215 Is Induced Post-transcriptionally via HIF-Drosha Complex and Mediates Glioma-Initiating Cell Adaptation to Hypoxia by Targeting KDM1B. Cancer Cell 29, 49–60. doi:10.1016/j.ccell.2015.12.005

Huang, L.E., Gu, J., Schau, M., Bunn, H.F., 1998. Regulation of hypoxia-inducible factor 1alpha is mediated by an O2-dependent degradation domain via the ubiquitin-proteasome pathway. Proc Natl Acad Sci USA 95, 7987–7992.

Ichim, G., Lopez, J., Ahmed, S.U., Muthalagu, N., Giampazolias, E., Delgado, M.E., Haller, M., Riley, J.S., Mason, S.M., Athineos, D., Parsons, M.J., van de Kooij, B., Bouchier-Hayes, L., Chalmers, A.J., Rooswinkel, R.W., Oberst, A., Blyth, K., Rehm, M., Murphy, D.J., Tait, S.W.G., 2015. Limited Mitochondrial Permeabilization Causes DNA Damage and Genomic Instability in the Absence of Cell Death. Molecular Cell 57, 860–872. doi:10.1016/j.molcel.2015.01.018

Izquierdo-Garcia, J.L., Cai, L.M., Chaumeil, M.M., Eriksson, P., Robinson, A.E., Pieper, R.O., Phillips, J.J., Ronen, S.M., 2014. Glioma Cells with the IDH1 Mutation Modulate Metabolic Fractional Flux through Pyruvate Carboxylase. PLoS ONE 9, e108289. doi:10.1371/journal.pone.0108289

Izquierdo-Garcia, J.L., Viswanath, P., Eriksson, P., Cai, L., Radoul, M., Chaumeil, M.M., Blough, M., Luchman, H.A., Weiss, S., Cairncross, J.G., Phillips, J.J., Pieper, R.O., Ronen, S.M., 2015. IDH1 Mutation Induces Reprogramming of Pyruvate Metabolism. Cancer Research 75, 2999–3009. doi:10.1158/0008-5472.CAN-15-0840

Jaakkola, P., Mole, D.R., Tian, Y.M., Wilson, M.I., Gielbert, J., Gaskell, S.J., Kriegsheim, A.V., Kriegsheim, von, A., Hebestreit, H.F., Mukherji, M., Schofield, C.J., Maxwell, P.H., Pugh, C.W., Ratcliffe, P.J., 2001. Targeting of HIF-alpha to the von Hippel-Lindau Ubiquitylation Complex by O2-Regulated Prolyl Hydroxylation. Science 292, 468–472. doi:10.1126/science.1059796

Jha, M.K., Suk, K., 2013. Pyruvate dehydrogenase kinase as a potential therapeutic target for malignant gliomas. Brain Tumor Res Treat 1, 57–63. doi:10.14791/btrt.2013.1.2.57

Jo, S.H., Son, M.K., Koh, H.J., Lee, S.M., Song, I.H., Kim, Y.O., Lee, Y.S., Jeong, K.S., Kim, W.B., Park, J.W., Song, B.J., Huh, T.L., Huhe, T.L., 2001. Control of Mitochondrial Redox Balance and Cellular Defense against Oxidative Damage by Mitochondrial NADP+-dependent Isocitrate Dehydrogenase. Journal of Biological Chemistry 276, 16168–16176. doi:10.1074/jbc.M010120200

Joseph, J.V., Conroy, S., Pavlov, K., Sontakke, P., Tomar, T., Eggens-Meijer, E., Balasubramaniyan, V., Wagemakers, M., Dunnen, den, W.F.A., Kruyt, F.A.E., 2015. Hypoxia enhances migration and invasion in glioblastoma by promoting a mesenchymal shift mediated by the HIF1α–ZEB1 axis. Cancer Letters 359, 107–116. doi:10.1016/j.canlet.2015.01.010

Kaur, B., Khwaja, F.W., Severson, E.A., Matheny, S.L., Brat, D.J., Van Meir, E.G., 2005. Hypoxia and the hypoxia-inducible-factor pathway in glioma growth and angiogenesis. Neuro Oncol 7, 134–153. doi:10.1215/S1152851704001115

Keller, K.E., Tan, I.S., Lee, Y.-S., 2012. SAICAR stimulates pyruvate kinase isoform M2 and promotes cancer cell survival in glucose-limited conditions. Science 338, 1069–1072. doi:10.1126/science.1224409

Kim, D., Fiske, B.P., Birsoy, K., Freinkman, E., Kami, K., Possemato, R.L., Chudnovsky, Y., Pacold, M.E., Chen, W.W., Cantor, J.R., Shelton, L.M., Gui, D.Y., Kwon, M., Ramkissoon, S.H., Ligon, K.L., Kang, S.W., Snuderl, M., Vander Heiden, M.G., Sabatini, D.M., 2015. SHMT2 drives glioma cell survival in ischaemia but imposes a dependence on glycine clearance. Nature 520, 363–367. doi:10.1038/nature14363

Kim, S.Y., Lee, S.M., Tak, J.K., Choi, K.S., Kwon, T.K., Park, J.-W., 2007. Regulation of singlet oxygen-induced apoptosis by cytosolic NADP+-dependent isocitrate dehydrogenase. Mol Cell Biochem 302, 27–34. doi:10.1007/s11010-007-9421-x

Kleihues, P., Burger, P.C., Scheithauer, B.W., 1993. The New WHO Classification of Brain Tumours. Brain Pathology 3, 255–268. doi:10.1111/j.1750-3639.1993.tb00752.x

Krell, D., Assoku, M., Galloway, M., Mulholland, P., Tomlinson, I., Bardella, C., 2011. Screen for IDH1, IDH2, IDH3, D2HGDH and L2HGDH mutations in glioblastoma. PLoS ONE 6, e19868.

Kushner, B.H., LaQuaglia, M.P., Bonilla, M.A., Lindsley, K., Rosenfield, N., Yeh, S., Eddy, J., Gerald, W.L., Heller, G., Cheung, N.K., 1994. Highly effective induction therapy for stage 4 neuroblastoma in children over 1 year of age. Journal of Clinical Oncology 12, 2607–2613. doi:10.1200/JCO.1994.12.12.2607

Lei, K., Davis, R.J., 2003. JNK phosphorylation of Bim-related members of the Bcl2 family induces Bax-dependent apoptosis. Proc Natl Acad Sci USA 100, 2432–2437. doi:10.1073/pnas.0438011100

Letai, A., Bassik, M.C., Walensky, L.D., Sorcinelli, M.D., Weiler, S., Korsmeyer, S.J., 2002. Distinct BH3 domains either sensitize or activate mitochondrial apoptosis, serving as prototype cancer therapeutics. Cancer Cell 2, 183–192. doi:10.1016/S1535-6108(02)00127-7

Letai, A.G., 2008. Diagnosing and exploiting cancer's addiction to blocks in apoptosis. Nature Publishing Group 8, 121–132. doi:10.1038/nrc2297

Ley, R., Ewings, K.E., Hadfield, K., Cook, S.J., 2005. Regulatory phosphorylation of Bim: sorting out the ERK from the JNK. Cell Death Differ. 12, 1008–1014. doi:10.1038/sj.cdd.4401688

Li, N., Feng, L., Liu, H., Wang, J., Kasembeli, M., Tran, M.K., Tweardy, D.J., Lin, S.H., Chen, J., 2016. PARP Inhibition Suppresses Growth of EGFR-Mutant Cancers by Targeting Nuclear PKM2. CELREP 15, 843–856. doi:10.1016/j.celrep.2016.03.070

Liu, Q., Wang, L., Wang, Z., Yang, Y., Tian, J., Liu, G., Guan, D., Cao, X., Zhang, Y., Hao, A., 2013. GRIM-19 opposes reprogramming of glioblastoma cell metabolism via HIF1α destabilization. Carcinogenesis 34, 1728–1736. doi:10.1093/carcin/bgt125

Louis, D.N., Perry, A., Reifenberger, G., Deimling, von, A., Figarella-Branger, D., Cavenee, W.K., Ohgaki, H., Wiestler, O.D., Kleihues, P., Ellison, D.W., 2016. The 2016 World Health Organization Classification of Tumors of the Central Nervous System: a summary. Acta Neuropathol. 131, 803–820. doi:10.1007/s00401-016-1545-1

Luo, W., Hu, H., Chang, R., Zhong, J., Knabel, M., O'Meally, R., Cole, R.N., Pandey, A., Semenza, G.L., 2011. Pyruvate kinase M2 is a PHD3-stimulated coactivator for hypoxia-inducible factor 1. Cell 145, 732–744. doi:10.1016/j.cell.2011.03.054

Maher, E.A., Marin-Valencia, I., Bachoo, R.M., Mashimo, T., Raisanen, J., Hatanpaa, K.J., Jindal, A., Jeffrey, F.M., Choi, C., Madden, C., Mathews, D., Pascual, J.M., Mickey, B.E., Malloy, C.R., DeBerardinis, R.J., 2012. Metabolism of [U- 13C]glucose in human brain tumors in vivo. NMR Biomed. 25, 1234–1244. doi:10.1002/nbm.2794

Marin-Valencia, I., Cho, S.K., Rakheja, D., Hatanpaa, K.J., Kapur, P., Mashimo, T., Jindal, A., Vemireddy, V., Good, L.B., Raisanen, J., Sun, X., Mickey, B., Choi, C., Takahashi, M., Togao, O., Pascual, J.M., DeBerardinis, R.J., Maher, E.A., Malloy, C.R., Bachoo, R.M., 2012a. Glucose metabolism via the pentose phosphate pathway, glycolysis and Krebs cycle in an orthotopic mouse model of human brain tumors. NMR Biomed. 25, 1177–1186. doi:10.1002/nbm.2787

Marin-Valencia, I., Yang, C., Mashimo, T., Cho, S., Baek, H., Yang, X.-L., Rajagopalan, K.N., Maddie, M., Vemireddy, V., Zhao, Z., Cai, L., Good, L., Tu, B.P., Hatanpaa, K.J., Mickey, B.E., Matés, J.M., Pascual, J.M., Maher, E.A., Malloy, C.R., DeBerardinis, R.J., Bachoo, R.M., 2012b. Analysis of Tumor Metabolism Reveals Mitochondrial Glucose Oxidation in Genetically Diverse Human Glioblastomas in the Mouse Brain In Vivo. Cell Metabolism 15, 827–837. doi:10.1016/j.cmet.2012.05.001

Maris, J.M., Hogarty, M.D., Bagatell, R., Cohn, S.L., 2007. Neuroblastoma. Lancet 369, 2106–2120. doi:10.1016/S0140-6736(07)60983-0

Mashimo, T., Pichumani, K., Vemireddy, V., Hatanpaa, K.J., Singh, D.K., Sirasanagandla, S., Nannepaga, S., Piccirillo, S.G., Kovacs, Z., Foong, C., Huang, Z., Barnett, S., Mickey, B.E., DeBerardinis, R.J., Tu, B.P., Maher, E.A., Bachoo, R.M., 2014. Acetate Is a Bioenergetic Substrate for Human Glioblastoma and Brain Metastases. Cell 159, 1603–1614. doi:10.1016/j.cell.2014.11.025

Masui, K., Tanaka, K., Ikegami, S., Villa, G.R., Yang, H., Yong, W.H., Cloughesy, T.F., Yamagata, K., Arai, N., Cavenee, W.K., Mischel, P.S., 2015. Glucose-dependent acetylation of Rictor promotes targeted cancer therapy resistance. Proc. Natl. Acad. Sci. U.S.A. 112, 9406–9411. doi:10.1073/pnas.1511759112

Matthay, K.K., Villablanca, J.G., Seeger, R.C., Stram, D.O., Harris, R.E., Ramsay, N.K., Swift, P., Shimada, H., Black, C.T., Brodeur, G.M., Gerbing, R.B., Reynolds, C.P., 1999. Treatment of high-risk neuroblastoma with intensive chemotherapy, radiotherapy, autologous bone marrow transplantation, and 13-cis-retinoic acid. Children's Cancer Group. N Engl J Med 341, 1165–1173. doi:10.1056/NEJM199910143411601

Moldoveanu, T., Follis, A.V., Kriwacki, R.W., Green, D.R., 2014. Many players in BCL-2 family affairs. Trends in Biochemical Sciences 39, 101–111. doi:10.1016/j.tibs.2013.12.006

Monclair, T., Brodeur, G.M., Ambros, P.F., Brisse, H.J., Cecchetto, G., Holmes, K., Kaneko, M., London, W.B., Matthay, K.K., Nuchtern, J.G., Schweinitz, von, D., Simon, T., Cohn, S.L., Pearson, A.D.J., INRG Task Force, 2009. The International Neuroblastoma Risk Group (INRG) staging system: an INRG Task Force report. J. Clin. Oncol. 27, 298–303. doi:10.1200/JCO.2008.16.6876

Montavon, G., Jauquier, N., Coulon, A., Peuchmaur, M., Flahaut, M., Bourloud, K.B., Yan, P., Delattre, O., Sommer, L., Joseph, J.-M., Janoueix-Lerosey, I., Gross, N., Mühlethaler-Mottet, A., 2014. Wild-type ALK and activating ALK-R1275Q and ALK-F1174L mutations upregulate Myc and initiate tumor

formation in murine neural crest progenitor cells. Oncotarget 5, 4452–4466. doi:10.18632/oncotarget.2036

Montero, J., Sarosiek, K.A., DeAngelo, J.D., Maertens, O., Ryan, J., Ercan, D., Piao, H., Horowitz, N.S., Berkowitz, R.S., Matulonis, U., Jänne, P.A., Amrein, P.C., Cichowski, K., Drapkin, R., Letai, A., 2015. Drug-Induced Death Signaling Strategy Rapidly Predicts Cancer Response to Chemotherapy. Cell 160, 977–989. doi:10.1016/j.cell.2015.01.042

Morel, C., Carlson, S.M., White, F.M., Davis, R.J., 2009. Mcl-1 integrates the opposing actions of signaling pathways that mediate survival and apoptosis. Molecular and Cellular Biology 29, 3845–3852. doi:10.1128/MCB.00279-09

Nagane, M., Lin, H., Cavenee, W.K., Huang, H.J., 2001. Aberrant receptor signaling in human malignant gliomas: mechanisms and therapeutic implications. Cancer Letters 162 Suppl, S17–S21.

Neutzner, A., Li, S., Xu, S., Karbowski, M., 2012. The ubiquitin/proteasome system-dependent control of mitochondrial steps in apoptosis. Semin. Cell Dev. Biol. 23, 499–508. doi:10.1016/j.semcdb.2012.03.019

Nicholas, M.K., Lukas, R.V., Jafri, N.F., Faoro, L., Salgia, R., 2006. Epidermal growth factor receptor - mediated signal transduction in the development and therapy of gliomas. Clinical Cancer Research 12, 7261–7270. doi:10.1158/1078-0432.CCR-06-0874

Noone, A., Howlader, N., Krapcho, M., Miller, D., Brest, A., Yu, M., Ruhl, J., Tatalovich, Z., Mariotto, A., Lewis, D., Chen, H., Feuer, E., Cronin, K., 2018. SEER Cancer Statistics Review, 1975-2015, National Cancer Institute. Bethesda, MD, https://seer.cancer.gov/csr/1975_2015/, based on November 2017 SEER data submission, posted to the SEER web site, April 2018. httpsseer.cancer.govcsr.

Olsen, R.R., Otero, J.H., García-López, J., Wallace, K., Finkelstein, D., Rehg, J.E., Yin, Z., Wang, Y.-D., Freeman, K.W., 2017. MYCN induces neuroblastoma in primary neural crest cells. Oncogene 36, 5075–5082. doi:10.1038/onc.2017.128

Oltvai, Z.N., Milliman, C.L., Korsmeyer, S.J., 1993. Bcl-2 heterodimerizes in vivo with a conserved homolog, Bax, that accelerates programmed cell death. Cell 74, 609–619.

Ostrom, Q.T., Gittleman, H., Xu, J., Kromer, C., Wolinsky, Y., Kruchko, C., Barnholtz-Sloan, J.S., 2016. CBTRUS Statistical Report: Primary Brain and Other Central Nervous System Tumors Diagnosed in the United States in 2009-2013. Neuro Oncol 18, v1–v75. doi:10.1093/neuonc/now207

Park, J.R., Scott, J.R., Stewart, C.F., London, W.B., Naranjo, A., Santana, V.M., Shaw, P.J., Cohn, S.L., Matthay, K.K., 2011. Pilot induction regimen incorporating pharmacokinetically guided topotecan for treatment of newly diagnosed high-risk neuroblastoma: a Children's Oncology Group study. J. Clin. Oncol. 29, 4351–4357. doi:10.1200/JCO.2010.34.3293

Parsons, D.W., Parsons, D.W., Jones, S., Jones, S., Zhang, X., Zhang, X., Lin, J.C.H., Lin, J.C.-H., Leary, R.J., Leary, R.J., Angenendt, P., Angenendt, P., Mankoo, P., Mankoo, P., Carter, H., Carter, H., Siu, I.-M., Siu, I.-M., Gallia, G.L., Gallia, G.L., Olivi, A., Olivi, A., McLendon, R., McLendon, R., Rasheed, B.A., Rasheed, B.A., Keir, S., Keir, S., Nikolskaya, T., Nikolskaya, T., Nikolsky, Y., Nikolsky, Y., Busam, D.A., Busam, D.A., Tekleab, H., Tekleab, H., Diaz, L.A., Diaz, L.A., Hartigan, J., Hartigan, J., Smith, D.R., Smith, D.R., Strausberg, R.L., Strausberg, R.L., Marie, S.K.N., Marie, S.K.N., Shinjo, S.M.O., Shinjo, S.M.O., Yan, H., Yan, H., Riggins, G.J., Riggins, G.J., Bigner, D.D., Bigner, D.D., Karchin, R., Karchin, R., Papadopoulos, N., Papadopoulos, N., Parmigiani, G., Parmigiani, G., Vogelstein, B., Vogelstein, B., Velculescu, V.E., Velculescu, V.E., Kinzler, K.W., Kinzler, K.W., 2008. An Integrated Genomic Analysis of Human Glioblastoma Multiforme. Science 321, 1807–1812. doi:10.1126/science.1164382

Peifer, M., Hertwig, F., Roels, F., Dreidax, D., Gartlgruber, M., Menon, R., Krämer, A., Roncaioli, J.L., Sand, F., Heuckmann, J.M., Ikram, F., Schmidt, R., Ackermann, S., Engesser, A., Kahlert, Y., Vogel, W., Altmüller, J., Nürnberg, P., Thierry-Mieg, J., Thierry-Mieg, D., Mariappan, A., Heynck, S., Mariotti, E., Henrich, K.-O., Gloeckner, C., Bosco, G., Leuschner, I., Schweiger, M.R., Savelyeva, L., Watkins, S.C., Shao, C., Bell, E., Höfer, T., Achter, V., Lang, U., Theissen, J., Volland, R., Saadati, M., Eggert, A., de Wilde, B., Berthold, F., Peng, Z., Zhao, C., Shi, L., Ortmann, M., Büttner, R., Perner, S., Hero, B., Schramm, A., Schulte, J.H., Herrmann, C., O'Sullivan, R.J., Westermann, F., Thomas, R.K., Fischer, M., 2015. Telomerase activation by genomic rearrangements in high-risk neuroblastoma. Nature 526, 700–704. doi:10.1038/nature14980

Phillips, H.S., Kharbanda, S., Chen, R., Forrest, W.F., Soriano, R.H., Wu, T.D., Misra, A., Nigro, J.M., Colman, H., Soroceanu, L., Williams, P.M., Modrusan, Z., Feuerstein, B.G., Aldape, K., 2006. Molecular subclasses of high-grade glioma predict prognosis, delineate a pattern of disease progression, and resemble stages in neurogenesis. Cancer Cell 9, 157–173. doi:10.1016/j.ccr.2006.02.019

Plas, D.R., Talapatra, S., Edinger, A.L., Rathmell, J.C., Thompson, C.B., 2001. Akt and Bcl-xL promote growth factor-independent survival through distinct effects on mitochondrial physiology. Journal of Biological Chemistry 276, 12041–12048. doi:10.1074/jbc.M010551200

Portais, J.C., Voisin, P., Merle, M., Canioni, P., 1996. Glucose and glutamine metabolism in C6 glioma cells studied by carbon 13 NMR. Biochimie 78, 155–164.

Ramos, J.W., 2008. The regulation of extracellular signal-regulated kinase (ERK) in mammalian cells. International Journal of Biochemistry and Cell Biology 40, 2707–2719. doi:10.1016/j.biocel.2008.04.009

Rathmell, J.C., Fox, C.J., Plas, D.R., Hammerman, P.S., Cinalli, R.M., Thompson, C.B., 2003. Akt-Directed Glucose Metabolism Can Prevent Bax Conformation Change and Promote Growth Factor-Independent Survival. Molecular and Cellular Biology 23, 7315–7328. doi:10.1128/MCB.23.20.7315-7328.2003

Reed, J.C., 2011. Cancer. Priming cancer cells for death. Science 334, 1075–1076. doi:10.1126/science.1215568

Reitman, Z.J., Reitman, Z.J., Jin, G., Jin, G., Karoly, E.D., Karoly, E.D., Spasojevic, I., Spasojevic, I., Yang, J., Yang, J., Kinzler, K.W., Kinzler, K.W., He, Y., He, Y., Bigner, D.D., Bigner, D.D., Vogelstein, B., Vogelstein, B., Yan, H., Yan, H., 2011. Profiling the effects of isocitrate dehydrogenase 1 and 2 mutations on the cellular metabolome. Proc Natl Acad Sci USA 108, 3270–3275. doi:10.1073/pnas.1019393108

Renault, T.T., Chipuk, J.E., 2014. Death upon a kiss: mitochondrial outer membrane composition and organelle communication govern sensitivity to BAK/BAX-dependent apoptosis. Chem. Biol. 21, 114–123. doi:10.1016/j.chembiol.2013.10.009

Roberts, D.J., Miyamoto, S., 2015. Hexokinase II integrates energy metabolism and cellular protection: Akting on mitochondria and TORCing to autophagy. Cell Death Differ. 22, 248–257. doi:10.1038/cdd.2014.173

Rosati, A., Poliani, P.L., Todeschini, A., Cominelli, M., Medicina, D., Cenzato, M., Simoncini, E.L., Magrini, S.M., Buglione, M., Grisanti, S., Padovani, A., 2013. Glutamine synthetase expression as a valuable marker of epilepsy and longer survival in newly diagnosed glioblastoma multiforme. Neuro Oncol 15, 618–625. doi:10.1093/neuonc/nos338

Ryan, J., Letai, A., 2013. BH3 profiling in whole cells by fluorimeter or FACS. Methods 61, 156–164. doi:10.1016/j.ymeth.2013.04.006

Ryan, J.A., Brunelle, J.K., Letai, A., 2010. Heightened mitochondrial priming is the basis for apoptotic hypersensitivity of CD4+ CD8+ thymocytes. Proc. Natl. Acad. Sci. U.S.A. 107, 12895–12900. doi:10.1073/pnas.0914878107

Sanzey, M., Abdul Rahim, S.A., Oudin, A., Dirkse, A., Kaoma, T., Vallar, L., Herold-Mende, C., Bjerkvig, R., Golebiewska, A., Niclou, S.P., 2015. Comprehensive analysis of glycolytic enzymes as therapeutic targets in the treatment of glioblastoma. PLoS ONE 10, e0123544. doi:10.1371/journal.pone.0123544

Schellenberg, B., Wang, P., Keeble, J.A., Rodriguez-Enriquez, R., Walker, S., Owens, T.W., Foster, F., Tanianis-Hughes, J., Brennan, K., Streuli, C.H., Gilmore, A.P., 2013. Bax exists in a dynamic equilibrium between the cytosol and mitochondria to control apoptotic priming. Molecular Cell 49, 959–971. doi:10.1016/j.molcel.2012.12.022

Schon, E.A., DiMauro, S., Hirano, M., 2012. Human mitochondrial DNA: roles of inherited and somatic mutations. Nature Publishing Group 13, 878–890. doi:10.1038/nrg3275

Schroeter, H., Boyd, C.S., Ahmed, R., Spencer, J.P.E., Duncan, R.F., Rice-Evans, C., Cadenas, E., 2003. c-Jun N-terminal kinase (JNK)-mediated modulation of brain mitochondria function: new target proteins for JNK signalling in mitochondrion-dependent apoptosis. Biochem. J. 372, 359–369. doi:10.1042/BJ20030201

Schulte, J.H., Lindner, S., Bohrer, A., Maurer, J., De Preter, K., Lefever, S., Heukamp, L., Schulte, S., Molenaar, J., Versteeg, R., Thor, T., Künkele, A., Vandesompele, J., Speleman, F., Schorle, H., Eggert, A., Schramm, A., 2013. MYCN and ALKF1174L are sufficient to drive neuroblastoma development from neural crest progenitor cells. Oncogene 32, 1059–1065. doi:10.1038/onc.2012.106

Semenza, G.L., 1999. Regulation of mammalian O2 homeostasis by hypoxia-inducible factor 1. Annu. Rev. Cell Dev. Biol. 15, 551–578. doi:10.1146/annurev.cellbio.15.1.551

Seoane, M., Mosquera-Miguel, A., Gonzalez, T., Fraga, M., Salas, A., Costoya, J.A., 2011. The mitochondrial genome is a “genetic sanctuary” during the oncogenic process. PLoS ONE 6, e23327. doi:10.1371/journal.pone.0023327

Sodero, A.O., Rodriguez-Silva, M., Salio, C., Sassoè-Pognetto, M., Chambers, J.W., 2017. Sab is differentially expressed in the brain and affects neuronal activity. Brain Res. 1670, 76–85. doi:10.1016/j.brainres.2017.06.005

Strauss, H.M., Keller, S., 2008. Pharmacological interference with protein-protein interactions mediated by coiled-coil motifs. Handb Exp Pharmacol 186, 461–482. doi:10.1007/978-3-540-72843-6_19

Strother, D.R., London, W.B., Schmidt, M.L., Brodeur, G.M., Shimada, H., Thorner, P., Collins, M.H., Tagge, E., Adkins, S., Reynolds, C.P., Murray, K., Lavey, R.S., Matthay, K.K., Castleberry, R., Maris, J.M., Cohn, S.L., 2012. Outcome after surgery alone or with restricted use of chemotherapy for patients with low-risk neuroblastoma: results of Children's Oncology Group study P9641. J. Clin. Oncol. 30, 1842–1848. doi:10.1200/JCO.2011.37.9990

Stupp, R., Mason, W.P., van den Bent, M.J., Weller, M., Fisher, B., Taphoorn, M.J.B., Belanger, K., Brandes, A.A., Marosi, C., Bogdahn, U., Curschmann, J., Janzer, R.C., Ludwin, S.K., Gorlia, T., Allgeier, A., Lacombe, D., Cairncross, J.G., Eisenhauer, E., Mirimanoff, R.O., European Organisation for Research and Treatment of Cancer Brain Tumor and Radiotherapy Groups, National Cancer Institute of Canada Clinical Trials Group, 2005. Radiotherapy plus concomitant and adjuvant temozolomide for glioblastoma. N Engl J Med 352, 987–996. doi:10.1056/NEJMoa043330

Stupp, R., Taillibert, S., Kanner, A.A., Kesari, S., Steinberg, D.M., Toms, S.A., Taylor, L.P., Lieberman, F., Silvani, A., Fink, K.L., Barnett, G.H., Zhu, J.-J., Henson, J.W., Engelhard, H.H., Chen, T.C., Tran, D.D., Sroubek, J., Tran, N.D., Hottinger, A.F., Landolfi, J., Desai, R., Caroli, M., Kew, Y., Honnorat, J., Idbaih, A., Kirson, E.D., Weinberg, U., Palti, Y., Hegi, M.E., Ram, Z., 2015. Maintenance Therapy With Tumor-Treating Fields Plus Temozolomide vs Temozolomide Alone for Glioblastoma: A Randomized Clinical Trial. JAMA 314, 2535–2543. doi:10.1001/jama.2015.16669

Tait, S.W.G., Green, D.R., 2013. Mitochondrial regulation of cell death. Cold Spring Harb Perspect Biol 5, a008706–a008706. doi:10.1101/cshperspect.a008706

Tait, S.W.G., Parsons, M.J., Llambi, F., Bouchier-Hayes, L., Connell, S., Muñoz-Pinedo, C., Green, D.R., 2010. Resistance to caspase-independent cell death requires persistence of intact mitochondria. Dev. Cell 18, 802–813. doi:10.1016/j.devcel.2010.03.014

Tan, A.S., Baty, J.W., Dong, L.-F., Bezawork-Geleta, A., Endaya, B., Goodwin, J., Bajzikova, M., Kovarova, J., Peterka, M., Yan, B., Pesdar, E.A., Sobol, M., Filimonenko, A., Stuart, S., Vondrusova, M., Kluckova, K., Sachaphibulkij, K., Rohlena, J., Hozak, P., Truksa, J., Eccles, D., Haupt, L.M., Griffiths, L.R., Neuzil, J., Berridge, M.V., 2015. Mitochondrial genome acquisition restores respiratory function and tumorigenic potential of cancer cells without mitochondrial DNA. Cell Metabolism 21, 81–94. doi:10.1016/j.cmet.2014.12.003

Tardito, S., Oudin, A., Ahmed, S.U., Fack, F., Keunen, O., Zheng, L., Miletic, H., Sakariassen, P.Ø., Weinstock, A., Wagner, A., Lindsay, S.L., Hock, A.K., Barnett, S.C., Ruppin, E., Mørkve, S.H., Lund-Johansen, M., Chalmers, A.J.,

Bjerkvig, R., Niclou, S.P., Gottlieb, E., 2015. Glutamine synthetase activity fuels nucleotide biosynthesis and supports growth of glutamine-restricted glioblastoma. Nature Publishing Group 17, 1556–1568. doi:10.1038/ncb3272

Thakkar, J.P., Dolecek, T.A., Horbinski, C., Ostrom, Q.T., Lightner, D.D., Barnholtz-Sloan, J.S., Villano, J.L., 2014. Epidemiologic and molecular prognostic review of glioblastoma. Cancer Epidemiol. Biomarkers Prev. 23, 1985–1996. doi:10.1158/1055-9965.EPI-14-0275

Thomas, L.W., Lam, C., Edwards, S.W., 2010. Mcl-1; the molecular regulation of protein function. FEBS Letters 584, 2981–2989. doi:10.1016/j.febslet.2010.05.061

Tsujimoto, Y., Shimizu, S., 2000. Bcl-2 family: life-or-death switch. FEBS Letters 466, 6–10.

Turcan, S., Rohle, D., Goenka, A., Walsh, L.A., Fang, F., Yilmaz, E., Campos, C., Fabius, A.W.M., Lu, C., Ward, P.S., Thompson, C.B., Kaufman, A., Guryanova, O., Levine, R., Heguy, A., Viale, A., Morris, L.G.T., Huse, J.T., Mellinghoff, I.K., Chan, T.A., 2012. IDH1 mutation is sufficient to establish the glioma hypermethylator phenotype. Nature 483, 479–483. doi:10.1038/nature10866

Vander Heiden, M.G., Cantley, L.C., Thompson, C.B., 2009. Understanding the Warburg Effect: The Metabolic Requirements of Cell Proliferation. Science 324, 1029–1033. doi:10.1126/science.1160809

Vander Heiden, M.G., DeBerardinis, R.J., 2017. Understanding the Intersections between Metabolism and Cancer Biology. Cell 168, 657–669. doi:10.1016/j.cell.2016.12.039

Velpula, K.K., Bhasin, A., Asuthkar, S., Tsung, A.J., 2013. Combined targeting of PDK1 and EGFR triggers regression of glioblastoma by reversing the Warburg effect. Cancer Research 73, 7277–7289. doi:10.1158/0008-5472.CAN-13-1868

Verhaak, R.G.W., Hoadley, K.A., Purdom, E., Wang, V., Qi, Y., Wilkerson, M.D., Miller, C.R., Ding, L., Golub, T., Mesirov, J.P., Alexe, G., Lawrence, M., O'Kelly, M., Tamayo, P., Weir, B.A., Gabriel, S., Winckler, W., Gupta, S., Jakkula, L., Feiler, H.S., Hodgson, J.G., James, C.D., Sarkaria, J.N., Brennan, C., Kahn, A., Spellman, P.T., Wilson, R.K., Speed, T.P., Gray, J.W., Meyerson, M., Getz, G., Perou, C.M., Hayes, D.N., Cancer Genome Atlas Research Network, 2010. Integrated genomic analysis identifies clinically relevant subtypes of glioblastoma characterized by abnormalities in PDGFRA, IDH1, EGFR, and NF1. Cancer Cell 17, 98–110. doi:10.1016/j.ccr.2009.12.020

Vo, T.-T., Ryan, J., Carrasco, R., Neuberg, D., Rossi, D.J., Stone, R.M., Deangelo, D.J., Frattini, M.G., Letai, A., 2012. Relative mitochondrial priming of myeloblasts and normal HSCs determines chemotherapeutic success in AML. Cell 151, 344–355. doi:10.1016/j.cell.2012.08.038

Waetzig, V., Wacker, U., Haeusgen, W., Björkblom, B., Courtney, M.J., Coffey, E.T., Herdegen, T., 2009. Concurrent protective and destructive signaling of JNK2 in neuroblastoma cells. Cell. Signal. 21, 873–880.

Wallace, D.C., 2012. Mitochondria and cancer. Nature Publishing Group 12, 685–698. doi:10.1038/nrc3365

Ward, E., DeSantis, C., Robbins, A., Kohler, B., Jemal, A., 2014. Childhood and adolescent cancer statistics, 2014. CA Cancer J Clin 64, 83–103. doi:10.3322/caac.21219

Ward, P.S., Cross, J.R., Lu, C., Weigert, O., Abel-Wahab, O., Levine, R.L., Weinstock, D.M., Sharp, K.A., Thompson, C.B., 2011. Identification of additional IDH mutations associated with oncometabolite R(−)-2-hydroxyglutarate production. Oncogene 31, 2491–2498. doi:10.1038/onc.2011.416

Weinberg, F., Hamanaka, R., Wheaton, W.W., Weinberg, S., Joseph, J., Lopez, M., Kalyanaraman, B., Mutlu, G.M., Budinger, G.R.S., Chandel, N.S., 2010. Mitochondrial metabolism and ROS generation are essential for Kras-mediated tumorigenicity. Proc. Natl. Acad. Sci. U.S.A. 107, 8788–8793. doi:10.1073/pnas.1003428107

Weiss, W.A., Aldape, K., Mohapatra, G., Feuerstein, B.G., Bishop, J.M., 1997. Targeted expression of MYCN causes neuroblastoma in transgenic mice. EMBO J 16, 2985–2995. doi:10.1093/emboj/16.11.2985

Willis, S.N., Chen, L., Dewson, G., Wei, A., Naik, E., Fletcher, J.I., Adams, J.M., Huang, D.C.S., 2005. Proapoptotic Bak is sequestered by Mcl-1 and Bcl-xL, but not Bcl-2, until displaced by BH3-only proteins. Genes & Development 19, 1294–1305. doi:10.1101/gad.1304105

Wiltshire, C., Gillespie, D.A.F., May, G.H.W., 2004. Sab (SH3BP5), a novel mitochondria-localized JNK-interacting protein. Biochem. Soc. Trans. 32, 1075–1077. doi:10.1042/BST0321075

Wiltshire, C., Matsushita, M., Tsukada, S., Gillespie, D.A.F., May, G.H.W., 2002. A new c-Jun N-terminal kinase (JNK)-interacting protein, Sab (SH3BP5), associates with mitochondria. Biochem. J. 367, 577–585. doi:10.1042/BJ20020553

Win, S., Than, T.A., Fernandez-Checa, J.C., Kaplowitz, N., 2014. JNK interaction with Sab mediates ER stress induced inhibition of mitochondrial respiration and cell death. Cell Death and Disease 5, e989–e989. doi:10.1038/cddis.2013.522

Win, S., Than, T.A., Han, D., Petrovic, L.M., Kaplowitz, N., 2011. c-Jun N-terminal kinase (JNK)-dependent acute liver injury from acetaminophen or tumor necrosis factor (TNF) requires mitochondrial Sab protein expression in mice. J. Biol. Chem. 286, 35071–35078. doi:10.1074/jbc.M111.276089

Win, S., Than, T.A., Le, B.H.A., García-Ruiz, C., Fernandez-Checa, J.C., Kaplowitz, N., 2015. Sab (Sh3bp5) dependence of JNK mediated inhibition of mitochondrial respiration in palmitic acid induced hepatocyte lipotoxicity. J. Hepatol. 62, 1367–1374. doi:10.1016/j.jhep.2015.01.032

Wise, D.R., DeBerardinis, R.J., Mancuso, A., Sayed, N., Zhang, X.-Y., Pfeiffer, H.K., Nissim, I., Daikhin, E., Yudkoff, M., McMahon, S.B., Thompson, C.B., 2008. Myc regulates a transcriptional program that stimulates mitochondrial glutaminolysis and leads to glutamine addiction. Proc. Natl. Acad. Sci. U.S.A. 105, 18782–18787. doi:10.1073/pnas.0810199105

Wise, D.R., Wise, D.R., Ward, P.S., Ward, P.S., Shay, J.E.S., Shay, J.E.S., Cross, J.R., Cross, J.R., Gruber, J.J., Gruber, J.J., Sachdeva, U.M., Sachdeva, U.M., Platt, J.M., Platt, J.M., DeMatteo, R.G., DeMatteo, R.G., Simon, M.C., Simon, M.C., Thompson, C.B., Thompson, C.B., 2011. Hypoxia promotes isocitrate dehydrogenase-dependent carboxylation of -ketoglutarate to citrate to support cell growth and viability. Proc Natl Acad Sci USA 108, 19611–19616. doi:10.1073/pnas.1117773108

Wolf, A., Agnihotri, S., Guha, A., 2010. Targeting metabolic remodeling in glioblastoma multiforme. Oncotarget 1, 552–562. doi:10.18632/oncotarget.101014

Wong, N., De Melo, J., Tang, D., 2013. PKM2, a Central Point of Regulation in Cancer Metabolism. Int J Cell Biol 2013, 242513–11. doi:10.1155/2013/242513

Xu, K., Chang, C.-M., Gao, H., Shu, H.-K.G., 2009. Epidermal growth factor-dependent cyclooxygenase-2 induction in gliomas requires protein kinase C-delta. Oncogene 28, 1410–1420. doi:10.1038/onc.2008.500

Xu, K., Shu, H.-K.G., 2007. EGFR activation results in enhanced cyclooxygenase-2 expression through p38 mitogen-activated protein kinase-dependent activation of the Sp1/Sp3 transcription factors in human gliomas. Cancer Research 67, 6121–6129. doi:10.1158/0008-5472.CAN-07-0141

Xu, W., Yang, H., Liu, Y., Yang, Y., Wang, P., Kim, S.-H., Ito, S., Yang, C., Wang, P., Xiao, M.-T., Liu, L.-X., Jiang, W.-Q., Liu, J., Zhang, J.-Y., Wang, B., Frye, S., Zhang, Y., Xu, Y.-H., Lei, Q.-Y., Guan, K.-L., Zhao, S.-M., Xiong, Y., 2011. Oncometabolite 2-Hydroxyglutarate Is a Competitive Inhibitor of α-Ketoglutarate-Dependent Dioxygenases. Cancer Cell 19, 17–30. doi:10.1016/j.ccr.2010.12.014

Xu, X., Xu, X., Zhao, J., Zhao, J., Xu, Z., Xu, Z., Peng, B., Peng, B., Huang, Q., Huang, Q., Arnold, E., Arnold, E., Ding, J., Ding, J., 2004. Structures of Human Cytosolic NADP-dependent Isocitrate Dehydrogenase Reveal a Novel Self-regulatory Mechanism of Activity. Journal of Biological Chemistry 279, 33946–33957. doi:10.1074/jbc.M404298200

Yamamoto, K., Ichijo, H., Korsmeyer, S.J., 1999. BCL-2 Is Phosphorylated and Inactivated by an ASK1/Jun N-Terminal Protein Kinase Pathway Normally Activated at G 2/M. Molecular and Cellular Biology 19, 8469–8478. doi:10.1128/MCB.19.12.8469

Yan, H., Parsons, D.W., Jin, G., McLendon, R., Rasheed, B.A., Yuan, W., Kos, I., Batinic-Haberle, I., Jones, S., Riggins, G.J., Friedman, H., Friedman, A., Reardon, D., Herndon, J., Kinzler, K.W., Velculescu, V.E., Vogelstein, B., Bigner, D.D., 2009. IDH1and IDH2Mutations in Gliomas. N Engl J Med 360, 765–773. doi:10.1056/NEJMoa0808710

Yang, E., Zha, J., Jockel, J., Boise, L.H., Thompson, C.B., Korsmeyer, S.J., 1995. Bad, a heterodimeric partner for Bcl-XL and Bcl-2, displaces Bax and promotes cell death. Cell 80, 285–291.

Yang, W., Xia, Y., Cao, Y., Zheng, Y., Bu, W., Zhang, L., You, M.J., Koh, M.Y., Cote, G., Aldape, K., Li, Y., Verma, I.M., Chiao, P.J., Lu, Z., 2012a. EGFR-induced and PKCε monoubiquitylation-dependent NF-κB activation upregulates PKM2 expression and promotes tumorigenesis. Molecular Cell 48, 771–784. doi:10.1016/j.molcel.2012.09.028

Yang, W., Xia, Y., Hawke, D., Li, X., Liang, J., Xing, D., Aldape, K., Hunter, T., Alfred Yung, W.K., Lu, Z., 2012b. PKM2 phosphorylates histone H3 and promotes gene transcription and tumorigenesis. Cell 150, 685–696. doi:10.1016/j.cell.2012.07.018

Yang, W., Xia, Y., Ji, H., Zheng, Y., Liang, J., Huang, W., Gao, X., Aldape, K., Lu, Z., 2011. Nuclear PKM2 regulates β-catenin transactivation upon EGFR activation. Nature 480, 118–122. doi:10.1038/nature10598

Yang, W., Zheng, Y., Xia, Y., Ji, H., Chen, X., Guo, F., Lyssiotis, C.A., Aldape, K., Cantley, L.C., Lu, Z., 2012c. ERK1/2-dependent phosphorylation and

nuclear translocation of PKM2 promotes the Warburg effect. Nature Publishing Group 14, 1295–1304. doi:10.1038/ncb2629

Youle, R.J., Strasser, A., 2008. The BCL-2 protein family: opposing activities that mediate cell death. Nature Publishing Group 9, 47–59. doi:10.1038/nrm2308

Yu, A.L., Gilman, A.L., Ozkaynak, M.F., London, W.B., Kreissman, S.G., Chen, H.X., Smith, M., Anderson, B., Villablanca, J.G., Matthay, K.K., Shimada, H., Grupp, S.A., Seeger, R., Reynolds, C.P., Buxton, A., Reisfeld, R.A., Gillies, S.D., Cohn, S.L., Maris, J.M., Sondel, P.M., Children's Oncology Group, 2010. Anti-GD2 antibody with GM-CSF, interleukin-2, and isotretinoin for neuroblastoma. N Engl J Med 363, 1324–1334. doi:10.1056/NEJMoa0911123

Zha, J., Harada, H., Yang, E., Jockel, J., Korsmeyer, S.J., 1996. Serine phosphorylation of death agonist BAD in response to survival factor results in binding to 14-3-3 not BCL-X(L). Cell 87, 619–628.

Zhao, S., Zhao, S., Lin, Y., Lin, Y., Xu, W., Xu, W., Jiang, W., Jiang, W., Zha, Z., Zha, Z., Wang, P., Wang, P., Yu, W., Yu, W., Li, Z., Li, Z., Gong, L., Gong, L., Peng, Y., Peng, Y., Ding, J., Ding, J., Lei, Q., Lei, Q., Guan, K.L., Guan, K.-L., Xiong, Y., Xiong, Y., 2009. Glioma-Derived Mutations in IDH1 Dominantly Inhibit IDH1 Catalytic Activity and Induce HIF-1. Science 324, 261–265. doi:10.1126/science.1170944

Zhou, Y., Zhou, Y., Zhou, Y., Zhou, Y., Shingu, T., Shingu, T., Feng, L., Feng, L., Chen, Z., Chen, Z., Ogasawara, M., Ogasawara, M., Keating, M.J., Keating, M.J., Kondo, S., Kondo, S., Huang, P., Huang, P., 2011. Metabolic Alterations in Highly Tumorigenic Glioblastoma Cells: PREFERENCE FOR HYPOXIA AND HIGH DEPENDENCY ON GLYCOLYSIS. Journal of Biological Chemistry 286, 32843–32853. doi:10.1074/jbc.M111.260935

Zhu, H., Acquaviva, J., Ramachandran, P., Boskovitz, A., Woolfenden, S., Pfannl, R., Bronson, R.T., Chen, J.W., Weissleder, R., Housman, D.E., Charest, A., 2009. Oncogenic EGFR signaling cooperates with loss of tumor suppressor gene functions in gliomagenesis. Proc. Natl. Acad. Sci. U.S.A. 106, 2712–2716. doi:10.1073/pnas.0813314106

Zong, W.-X., Rabinowitz, J.D., White, E., 2016. Mitochondria and Cancer. Molecular Cell 61, 667–676. doi:10.1016/j.molcel.2016.02.011

CHAPTER II

Hypothesis and Rationale

1. Problem Statement

Malignancies of the central nervous system often have poor prognoses due to the rapid recurrence of resistant disease following aggressive treatments. For example, glioblastoma (GBM) patients have a mean life expectancy of 15 months. An examination of the literature revealed that the mechanisms of cell death evasion in CNS tumors has not been rigorously explored. By characterizing the apoptosis machinery and related signal transduction pathways, we will be able to fill this knowledge gap and use the expected outcomes of our research to develop therapeutic approaches to fully enable cell death signaling in CNS tumor cells. Because many of the cell death responses converge on mitochondria, it is necessary to determine how these crucial organelles are altered from the process of oncogenesis. Changes in mitochondrial metabolism and signal transduction in cancer have been shown to aid in tumor proliferation, metastasis, and resistance. Thus, there is an *urgent need* to characterize changes in CNS tumor mitochondria to develop effective treatments to extend the quality of lives for patients.

2. Hypothesis and rationale

Dysregulation of cellular control of mitochondria is an emerging component of oncogenesis in brain tumors (Ichim et al., 2015; Seoane et al., 2011). Restoring proper regulation of mitochondrial physiology may be a useful therapeutic approach to impair tumor progression and sensitize tumor cells to therapies. Diminished apoptosis is a hallmark of numerous cancers, including central nervous system (CNS) tumors like neuroblastoma and glioblastoma (GBM) (Hanahan and Weinberg, 2011). Increased levels of pro-survival Bcl-2 proteins (Bcl-2, Mcl-1, and

Bcl-xL) are associated with decreased apoptosis, while elevated levels of BH3-only proteins (Bim, Bid, Puma, Noxa, etc.) are characteristic of pro-apoptotic mitochondria susceptible to chemotherapy (Brunelle and Letai, 2009; Certo et al., 2006; Chonghaile et al., 2011; Letai et al., 2002). In neuroblastoma, levels of Bcl-2 and BH3-only can be used to predict chemotherapeutic response (Goldsmith et al., 2012). In GBM, the relationship between Bcl-2 protein levels and chemo-resistance has yet to be rigorously evaluated.

The molecular mechanisms responsible for controlling Bcl-2 protein abundance on mitochondria in both neuroblastoma and GBM has yet to be fully delineated. The c-Jun N-terminal kinase (JNK) can induce apoptotic signaling through the manipulation of Bcl-2 proteins. Stress-induced activation of JNK induces translocation of the kinase to mitochondria initiating a signaling cascade that culminates in mitochondrial dysfunction and apoptosis (J. W. Chambers et al., 2011). At mitochondria, JNK interacts with the scaffold protein Sab, and inhibition of the JNK-Sab interaction prevents oxidative stress, mitochondrial dysfunction and cell death (J. W. Chambers and LoGrasso, 2011). Furthermore amplification of JNK/Sab-mediated signaling has been shown to sensitize cancer cells and improve chemotherapeutic efficacy (J. W. Chambers et al., 2011; 2013a; 2013b; T. P. Chambers et al., 2015).

Intriguingly, our preliminary studies investigating the relationship between Sab expression and therapeutic efficacy in ten GBM cell lines revealed the presence of a novel Sab splice variant that lacks the original mitochondrial localization signal. The splice variant of Sab has not been characterized, and thus its impact on GBM

physiology is still unknown. Therefore, there is a critical need to understand the effects of Sab, the Sab variant and JNK signaling in neuroblastoma and GBM physiology. Failure to delineate the impact of Sab-mediated signaling on GBM and neuroblastoma physiology and chemo-responsiveness will obstruct the search for efficacious therapeutic approaches and prevent the proper treatment of patients.

The *long-term goal* of our research is to understand the regulation of mitochondrial JNK signaling in CNS tumor resistance. Our *research objective* is to determine how Sab-mediated JNK signaling influences cell death responses GBM and CNS-based neuroblastoma. Our *central hypothesis* is that Sab-mediated signaling promotes stress-induced mitochondrial dysfunction and apoptosis, whereas the diminished Sab levels may lead to reduced apoptotic potential. This hypothesis was formulated based on our published (J. W. Chambers et al., 2011; T. P. Chambers et al., 2015) and preliminary data demonstrating that Sab levels influence chemoresponsiveness in gynecological cancers. The *rationale* for our proposed research is that understanding the role of mitochondrial JNK signaling in CNS tumor biology will provide insights into oncogenicity and chemo-responsiveness.

3. Project Aims

To investigate our hypothesis and accomplish our research objective, we propose the following specific aims.

1. Examine mitochondrial physiology characteristics of GBM-derived cell lines and determine its impact on apoptosis and chemoresistance. Increased levels of pro-survival Bcl-2 proteins (Bcl-2, Mcl-1, and Bcl-xL) are associated with decreased

apoptosis, while elevated levels of BH3-only proteins (Bim, Bid, Puma, Noxa, etc.) are characteristic of pro-apoptotic mitochondria susceptible to treatment (Brunelle and Letai, 2009; Certo et al., 2006; Chonghaile et al., 2011; Letai et al., 2002). Apoptotic priming, which determines the ratio between Bcl-2 proteins and BH3-only proteins, can be used to predict chemotherapeutic response and resistance in other cancers, however the capability to use as a biomarker in GBM has not been studied. The potential contribution of Sab-mediated signaling in GBM chemo-response is unknown. For this aim, our *working hypothesis* is that Bcl-2/BH3-only protein levels correlate with chemoresponsiveness in GBM, which also correlates with Sab expression levels. We will determine the expression levels of Bcl-2 proteins, BH3-only proteins and Sab, and how they correlate to cell viability and apoptosis after treatment with chemotherapeutic reagents.

2. Define the cellular distribution of the GBM Sab splice variant and determine its impact on JNK-induced mitochondrial dysfunction and apoptosis. Mitochondrial JNK signaling promotes oxidative stress, mitochondrial dysfunction and initiates apoptosis. Peptide mimicry of the Sab-JNK interaction prevents mitochondrial dysfunction (J. W. Chambers et al., 2011). Sab is located in the outer mitochondrial membrane (Wiltshire et al., 2002); however, the localization of the Sab variant is unknown. For this aim, our *working hypothesis* is that the Sab variant has a different cellular localization than Sab, because preliminary data suggest it has lost the original mitochondrial localization signal, and due to its distinct distribution, the Sab variant inhibits apoptotic priming and alters the magnitude of stress-induced mitochondrial dysfunction. We will determine the cellular location of the Sab

variant. Furthermore, we will survey JNK signaling and measure mitochondrial health in order to determine the extent of dysfunction in GBM cells expressing the Sab variant.

3. Determine the impact of Sab-mediated signaling on mitochondrial function and apoptosis in human Neuroblastoma cell lines. Blocking mitochondrial JNK signaling affects Bcl-2 levels and decreases apoptosis in neuroblastoma cells, while amplification of Sab-mediated JNK signaling has been shown to sensitize cancer cells to chemotherapeutic treatment (J. W. Chambers et al., 2013b; 2013a; 2011; T. P. Chambers et al., 2015; Matthay et al., 2009). For this aim, our *working hypothesis* is that expression levels of Sab in neuroblastoma cells correlate with chemo-sensitivity. Preliminary data suggests that Sab expression is reduced in neuroblastoma patients which alters the cells metabolic phenotype and their chemoresponsiveness. We will determine the impact of Sab-mediated signaling on mitochondrial metabolism, and glycolysis, as well as cell proliferation and apoptosis.

4. Abstract of the project

As a result of this project, we have prepared three manuscripts for submission, which will include chapters 3, 4 and 5 of this dissertation. The abstracts of these chapters appear below.

Chapter 3 - Bcl-2 Profiling Defines the Therapeutic Responsiveness in Continuous Glioblastoma Cultures.

Glioblastoma (GBM), is the most common primary brain tumors and have the highest mortality among older adults. The therapeutic standard for managing GBM

remains a combination of surgery, chemotherapy (temozolomide – TMZ), and radiotherapy; however, there is no cure, nor has there been any significant advancement in the clinical approach to GBM since this protocol was established in 2005. This study aims to better understand the molecular characteristics of GBM-derived cell lines to better define treatment groups and potentially identify new avenues for therapy. This study utilized ten continuous GBM cell lines and examined the concentrations of Bcl-2 family proteins on mitochondria for each of the cell lines. The measures were correlated to IC_{50} values for TMZ. We assessed cellular viability in the presence of increasing doses of TMZ (0-10mM) for each cell line. Western blot analysis of pro-survival and pro-apoptotic Bcl-2 proteins revealed that Bcl-2 levels corresponded to chemo-sensitivity, while increased levels of Bim promoted chemo-sensitivity in GBM cell lines. The ratio of Bcl-2 and Bim expression was found to be significantly correlated ($p<0.0001$) to TMZ responsiveness ($r = 0.9755$). Induction of TMZ resistance in U87 cell by exposure to a hypoxic environment increased the Bcl-2/Bim ratio. We found that Bcl-2 protein profiling, specifically the Bcl-2/Bim ratio, was a useful means to determine therapeutic response and resistance to TMZ.

Chapter 4 - A novel splice variant of Sab alters mitochondrial physiology

Mitochondria-cell communication is required for optimal cell function and to monitor mitochondrial health status. Ultimately, mitochondria-cell circuits produce and receive signals that influence biological outcomes. However, the precise molecular mechanisms responsible for mitochondria-cell communication are not very well understood. Scaffold proteins on the mitochondria outer membrane (MOM)

represent crucial hubs for mitochondria-cell communication, where the relative abundance of discrete scaffold proteins will influence the magnitude of a distinct signal transduction event and determine the local biological outcome. Furthermore, variation in scaffold proteins may diversify signaling modules or even polarize mitochondria-cell communication towards specific biological outcomes. The MOM scaffold protein Sab facilitates mitogen-activated protein kinases (MAPKs) signaling on mitochondria which affects organelle function and cell viability. Our previous work demonstrates that Sab levels influence cellular sensitivity to chemotherapy agents in gynecological cancer cell lines. While screening glioma cell lines for Sab protein concentrations, we discovered a unique variant of Sab with an N-terminal truncation that deletes the original mitochondrial localization sequence and a coiled-coil motif. Thus, the goal of our current project is to biochemically characterize the Sab variant, distinguish the function of the truncated Sab variant from that of full-length Sab, and determine the impact of variant-mediated signal transduction on mitochondrial function. We cloned human SF268 cells and found clones that expressed full-length Sab alone and those that expressed both the full length and the variant. We then characterized the cellular morphology, growth rate, respiration and drug responsiveness. We found that the truncated Sab variant localizes to mitochondria, which could be attributed to a new N-terminal stretch of cationic amino acids. Cells that express the variant display an increased growth rate compared to cells with only full-length Sab. Truncated Sab expressing cells have a large, round morphology, while cells that do not express the variant have a fibroblast-like morphology. Expression of the variant

promotes a metabolic shift from respiration to a more glycolysis-dependent phenotype. The truncated Sab variant affects the cellular response to stress, as cells that lack the variant are less sensitive to both genotoxic stress and mitochondrial stress. Our work illustrates that Sab variants may have distinct effects on mitochondrial function. Moreover, altering the structures and concentrations of MOM scaffold proteins represents a unique approach to manipulate organelle function and disease pathophysiology.

Chapter 5 - Sab-mediated signaling influences metabolism and chemosusceptibility in human neuroblastoma cells

Late stage neuroblastomas are commonly resistant to conventional treatments, including chemotherapy, and most patients experience transient effects of chemotherapy followed by a recurrence with a highly malignant treatment-resistant form of neuroblastoma. Thus, new therapeutic options are needed to treat late stage neuroblastomas. Our recent studies in cancer have demonstrated that mitochondrial c-Jun N-terminal kinase (JNK) signaling on the outer mitochondrial scaffold protein Sab is an essential component of cell death responses. Consequently, we found that Sab expression is down-regulated in neuroblastoma patients. In our current study, we examined the impact of Sab-mediated signaling on neuroblastoma physiology. Inhibition Sab-mediated signaling altered cellular metabolism in SH-SY5Y cells as determined by analyses. Treatment of SH-SY5Y cells with the Tat-Sab_{KIM1} peptide, a peptide known to inhibit JNK signaling on Sab, increased oxidation of both glucose and glutamine while decreasing the glycolytic rate. The change in glycolytic rate was not due to a change in glycolytic gene

expression. Furthermore, the SH-SY5Y mitochondria treated with the Tat-Sab$_{KIM1}$ peptide had more Bcl-2 (pro-survival) and less Bim (pro-apoptotic) when compared to controls. SH-SY5Y cells treated with the inhibitory Sab peptide also had reduced proliferation rates and were resistant to chemotherapy agents (carboplatin, cyclophosphamide, doxorubicin, etoposide, and vincristine). Over-expression of Sab in neuroblastoma cells reversed the effects of Sab inhibition. Finally, examination of additional neuroblastoma cell lines revealed that Sab levels correspond to proliferation rate, metabolic phenotype, and chemosensitivity. Consequently, we propose that Sab levels represent a new prognostic for therapeutic efficacy in neuroblastoma patients.

5. References

Brunelle, J.K., Letai, A., 2009. Control of mitochondrial apoptosis by the Bcl-2 family. Journal of Cell Science 122, 437–441. doi:10.1242/jcs.031682

Certo, M., Moore, V.D.G., Nishino, M., Wei, G., Korsmeyer, S., Armstrong, S.A., Letai, A., 2006. Mitochondria primed by death signals determine cellular addiction to antiapoptotic BCL-2 family members. Cancer Cell 9, 351–365. doi:10.1016/j.ccr.2006.03.027

Chambers, J.W., Cherry, L., Laughlin, J.D., Figuera-Losada, M., LoGrasso, P.V., 2011. Selective inhibition of mitochondrial JNK signaling achieved using peptide mimicry of the Sab kinase interacting motif-1 (KIM1). ACS Chem. Biol. 6, 808–818. doi:10.1021/cb200062a

Chambers, J.W., Howard, S., LoGrasso, P.V., 2013a. Blocking c-Jun N-terminal kinase (JNK) translocation to the mitochondria prevents 6-hydroxydopamine-induced toxicity in vitro and in vivo. J. Biol. Chem. 288, 1079–1087. doi:10.1074/jbc.M112.421354

Chambers, J.W., LoGrasso, P.V., 2011. Mitochondrial c-Jun N-terminal kinase (JNK) signaling initiates physiological changes resulting in amplification of reactive oxygen species generation. J. Biol. Chem. 286, 16052–16062. doi:10.1074/jbc.M111.223602

Chambers, J.W., Pachori, A., Howard, S., Iqbal, S., LoGrasso, P.V., 2013b. Inhibition of JNK mitochondrial localization and signaling is protective against ischemia/reperfusion injury in rats. J. Biol. Chem. 288, 4000–4011. doi:10.1074/jbc.M112.406777

Chambers, T.P., Portalatin, G.M., Paudel, I., Robbins, C.J., Chambers, J.W., 2015. Sub-chronic administration of LY294002 sensitizes cervical cancer cells to chemotherapy by enhancing mitochondrial JNK signaling. Biochemical and Biophysical Research Communications 463, 538–544. doi:10.1016/j.bbrc.2015.05.075

Chonghaile, T.N., Sarosiek, K.A., Vo, T.T., Ryan, J.A., Tammareddi, A., Moore, V.D.G., Deng, J., Anderson, K.C., Richardson, P., Tai, Y.T., Mitsiades, C.S., Matulonis, U.A., Drapkin, R., Stone, R., DeAngelo, D.J., McConkey, D.J., Sallan, S.E., Silverman, L., Hirsch, M.S., Carrasco, D.R., Letai, A., 2011. Pretreatment Mitochondrial Priming Correlates with Clinical Response to Cytotoxic Chemotherapy. Science 334, 1129–1133. doi:10.1126/science.1206727

Goldsmith, K.C., Gross, M., Peirce, S., Luyindula, D., Liu, X., Vu, A., Sliozberg, M., Guo, R., Zhao, H., Reynolds, C.P., Hogarty, M.D., 2012. Mitochondrial Bcl-2 Family Dynamics Define Therapy Response and Resistance in Neuroblastoma. Cancer Research 72, 2565–2577. doi:10.1158/0008-5472.CAN-11-3603

Hanahan, D., Weinberg, R.A., 2011. Hallmarks of Cancer: The Next Generation. Cell 144, 646–674. doi:10.1016/j.cell.2011.02.013

Ichim, G., Lopez, J., Ahmed, S.U., Muthalagu, N., Giampazolias, E., Delgado, M.E., Haller, M., Riley, J.S., Mason, S.M., Athineos, D., Parsons, M.J., van de Kooij, B., Bouchier-Hayes, L., Chalmers, A.J., Rooswinkel, R.W., Oberst, A., Blyth, K., Rehm, M., Murphy, D.J., Tait, S.W.G., 2015. Limited Mitochondrial Permeabilization Causes DNA Damage and Genomic Instability in the Absence of Cell Death. Molecular Cell 57, 860–872. doi:10.1016/j.molcel.2015.01.018

Letai, A., Bassik, M.C., Walensky, L.D., Sorcinelli, M.D., Weiler, S., Korsmeyer, S.J., 2002. Distinct BH3 domains either sensitize or activate mitochondrial apoptosis, serving as prototype cancer therapeutics. Cancer Cell 2, 183–192. doi:10.1016/S1535-6108(02)00127-7

Matthay, K.K., Reynolds, C.P., Seeger, R.C., Shimada, H., Adkins, E.S., Haas-Kogan, D., Gerbing, R.B., London, W.B., Villablanca, J.G., 2009. Long-Term Results for Children With High-Risk Neuroblastoma Treated on a Randomized Trial of Myeloablative Therapy Followed by 13- cis-Retinoic

Acid: A Children's Oncology Group Study. Journal of Clinical Oncology 27, 1007–1013. doi:10.1200/JCO.2007.13.8925

Seoane, M., Mosquera-Miguel, A., Gonzalez, T., Fraga, M., Salas, A., Costoya, J.A., 2011. The mitochondrial genome is a “genetic sanctuary” during the oncogenic process. PLoS ONE 6, e23327. doi:10.1371/journal.pone.0023327

Wiltshire, C., Matsushita, M., Tsukada, S., Gillespie, D.A.F., May, G.H.W., 2002. A new c-Jun N-terminal kinase (JNK)-interacting protein, Sab (SH3BP5), associates with mitochondria. Biochem. J. 367, 577–585. doi:10.1042/BJ20020553

CHAPTER III

Bcl-2 Profiling Defines the Therapeutic Responsiveness in Continuous Glioblastoma Cultures.

1. Introduction

Grade IV astrocytoma, also known as *glioblastoma multiforme* (GBM), are the most common and aggressive type of primary brain tumors in adults (Wen and Kesari, 2008). GBM accounts for about 17% of brain cancers in adults between 45 and 70 years of age, affecting more predominantly males than females (Furnari et al., 2007). Patients diagnosed with GBM have a poor prognosis, the median survival is 14.6 month, two-year survival is less than 30% and five-year survival is less than 10% (Furnari et al., 2007; Wen and Kesari, 2008). The standard of care for the disease, a combination of surgery, chemotherapy (temozolomide (TMZ)), and radiation, is ineffective and the response to TMZ varies greatly between patients (Robins et al., 2007; Stupp et al., 2005). New diagnostic strategies are required to better stratify patients in order to define an appropriate and effective treatment plan.

Resistance to cell death is a hallmark of cancers, including GBM (Hanahan and Weinberg, 2011). Circumventing the established circuitry for programmed cell death involves precise manipulation of the Bcl-2 protein family (Letai, 2008). Apoptotic evasion is commonly associated with increasing pro-survival Bcl-2 proteins (Bcl-2, Mcl-1, and Bcl-xL), while elevated pro-apoptotic BH3-only proteins (Bim, Bid, Puma, Noxa, etc.) indicate that cancer cells may be susceptible to treatments (Letai et al., 2002; Letai, 2008; Ryan et al., 2010; Schellenberg et al., 2013). Apoptotic priming, which is dependent on the replacement or sequestration of pro-survival Bcl-2 proteins by BH3-only proteins on the mitochondrial outer membrane, has been shown to increase the sensitivity of certain cancers and solid

tumors to chemotherapy improving its efficacy (Chonghaile et al., 2011; Davids et al., 2012; Reed, 2011; Vo et al., 2012). Moreover, apoptotic priming has been used to stratify cell lines and tumor samples according to chemotherapeutic responses and resistance (Ryan and Letai, 2013). While the levels of Bcl-2 proteins and chemo-responsiveness in solid tumors has been well evaluated in recent studies, the relationship between Bcl-2 protein levels and chemo-resistance in GBM has yet to be evaluated.

In our current study, we examined the mitochondrial characteristics, specifically Bcl-2 profiling, of ten (10) established GBM cell lines in order to address how the concentrations of these proteins correlate to TMZ sensitivity. Our Bcl-2 profiling of 10 GBM cells lines reveal a diverse set of expression profiles for the proteins of the Bcl-2 family. We found expression trends for two proteins Bcl-2 (pro-survival) and Bim (pro-apoptosis). Cells that were resistant to TMZ (U118, SNB19, and U251) had the highest levels of BCl-2 expression and the lowest concentrations of Bim; meanwhile, cells sensitive to TMZ (H4 and SNB75) had the lowest levels of Bcl-2 and the highest levels of Bim. Spearman correlation found that the Bcl-2/Bim ratio in the 10 cell lines were highly related ($r = 0.9755$, $p<0.0001$). These preliminary data suggest that Bcl-2 protein plays a critical role in the effectiveness of chemotherapy in individual cell lines and that mitochondria may be a useful target for complementary therapies for GBM treatment.

2. Materials and Methods

Materials: GBM cell lines, A-172 (CRL-1620), H4 (HTB-148), U-87 MG (HTB-14), and U-118 MG (HTB-15), were purchased from American Type Culture Collection

(Manassas, VA). The remaining GBM cell lines were obtained through the National Institutes of Cancer (NCI) from the NCI-60 cell panel. Cell culture media was purchased from Invitrogen (Grand Island, NY), and serum was purchased from Denville Scientific (South Plainfield, NJ). General chemicals were purchased from Fisher Scientific (Pittsburgh, PA) and Sigma Aldrich (St. Louis, MO) as indicated below. Unless indicated below, antibodies were purchased from Cell Signaling Technology (Danvers, MA).

Cell Culture: GBM cell lines were grown under normal cell culture conditions (37°C and 5% CO_2 with humidity). A-172, H4, U-87 MG, U-118 MG cells and the cells from the NCI-60 panel (SF-268, SF-295, SF-539, SNB-19, SNB-75 and U-251) were grown in Dulbucco's Modified Essential Medium (DMEM) supplemented with 10% fetal bovine serum (FBS), 1,000 U/mL penicillin, 100μg/mL streptomycin, and 5μg/mL plasmocin. Primary fetal human astrocytes (Sciencell Direct) were obtained and grown in astrocyte-specific media (Sciencell Direct) under normal cell culture conditions.

Determining Cell-based IC_{50}s for Temozolomide (TMZ): To determine the relative chemo-sensitivity of the GBM cell lines, cells were treated with increasing concentrations of TMZ (0-10mM). Briefly, GBM cells were plated at $5x10^3$ cells per well in black-walled, clear bottom plates (Perkin Elmer) and grown overnight. The cells were then treated with chemotherapeutic agents for 48 hours. The cells were washed three times in PBS and fixed in 4% paraformaldehyde/PBS. The cells were then stained with 5μM TO-PRO-3 for 45 minutes at RT. The cells were then washed three times in Hank's Buffered Saline Solution (HBSS). The plate was

imaged using the Odyssey CLx scanner (Licor Biosciences) and analyzed using the Image Studio 2.0 software (Licor Biosciences). The IC_{50} for each cell line was calculated using the GraphPad Prism7© software.

Cell Lysis and Western Blot Analysis: To isolate proteins from cells for analysis, cells were plated at $2.5x10^5$ cells/well in a six well plate unless otherwise indicated. Following treatment, cells were lysed, and proteins were harvested as previously described. Briefly, cells were washed twice in phosphate buffered saline (PBS; 137mM NaCl, 2.7mM KCl, 10mM Na_2HPO_4, and 1.8mM KH_2PO_4) and lysed in radioimmunoprecipitation assay buffer (RIPA; 50mM Tris-HCl, pH 8.0, 150mM NaCl, 1% Nonidet P-40, 0.5% deoxycholate, 0.1% SDS) supplemented with 1mM phenylmethanesulfonyl fluoride (PMSF) and Halt Protease and Phosphatase Inhibitor Cocktails (Thermo Scientific). Cells were incubated while gently rocking at 4°C for five minutes, and then transferred to a sterile micro-centrifuge tube. After two minutes on ice, cell disruption was completed using sonication. The lysate was cleared by centrifugation at 14,000 × g for 15 minutes. Protein concentrations of the supernatant were measured using the Pierce BCA Assay kit according to manufacturer's directions. Proteins were then resolved by SDS-PAGE and transferred onto low fluorescence PVDF membranes. Membranes were placed in blocking buffer comprised of PBS supplemented with either 5% non-fat milk (for standard blots) or 5% bovine serum albumin (BSA; for phosphor-specific blots) and incubated for at least one hour at room temperature (RT) or overnight at 4°C. The membranes were incubated in PBS containing 0.1% Tween 20 (PBST) and either 5% non-fat milk or BSA in the presence of primary antibodies for at least 2.5 hours

(RT) or overnight (4°C) while gently rocking. Primary antibodies specific for Bcl-2 (CST, 2870), Bcl-xL (CST, 2764), Mcl-1 (CST, 5453), Bad (CST, 9239), Bik (CST, 4592), Bim (CST, 2933), Bid (CST, 2002), PUMA (CST, 12450), Bax (CST, 5023), Bak (CST, 12105), Actin (CST, 4970),and α-tubulin (CST, 2144) were used at dilutions of 1:1000 for these studies. Membranes were washed three times for five minutes in PBST. Membranes were incubated with secondary antibodies in the appropriate blocking buffer at a ratio of 1:20,000 for one hour at RT gently rocking. The following secondary antibodies were used in the experiments below: IRDye 680RD Goat anti-Rabbit (926-32211) and IRDye 800CW Goat anti-Mouse (926-68070) (Licor Biosciences). Membranes were again washed three times for five minutes in PBST. Membranes were analyzed using fluorescence detection using the Odyssey CLx near infrared scanner (Licor Biosciences). The corresponding bands on the western blots were quantified and normalized using the Image Studio 2.0 software (Licor Biosciences). The fluorescence of specific bands of interest were divided by the fluorescence of the loading control band to equilibrate signal strength and loading. The resulting signal was then normalized by dividing the signals from treated samples by respective untreated or normal tissue control signals for each experiment.

In vitro Hypoxic Cycling of U-87 MG cells: U-87 MG cells were grown as indicated above under normal cell culture conditions. The cells were then placed in a Heracell 150i incubator (Thermo Scientific) and nitrogen gas was used to create a hypoxic environment of 1% O_2. The U-87 MG cells were then placed in the hypoxic environment for one (1) hour, and then returned to a normoxic environment for 30

minutes. This exchange was repeated for two (2) additional cycles. For non-interrupted hypoxia experiments, U-87 MG cells were place in a 1% O2 environment for four (4) hours prior to analysis. Hypoxic adaptation was confirmed by increased hypoxia-inducible factor 1α (HIF-1α) using western blot analysis.

Sensitization the BH3-mimetic ABT-737: ABT-737 is a well-established BH3-mimetic that targets Bcl-2 and Bcl-xL and can induce apoptosis in a Bax/Bak dependent manner.

Inhibition of Mcl-1: S63845 is a Mcl-1 inhibitor known to selectively induce apoptosis in Mcl-1-dependent cancers.

Cytotoxicity Assays: To measure the extent of cell death induced during hypoxic cycling, ABT-737, and S63845 sensitization, we employed three distinct assays. First, we utilized TO-PRO-3 staining for cell viability as described above. Next, we determined caspase activity, cells were grown on 6-well plates. After treatment, cells were lysed with 100μL of PBS supplemented with 1% TritonX-100, for 5 minutes on ice. Cell disruption was completed by sonication, and samples were centrifuged at 15,000 x g for 10 minutes at 4^{o}C. Then, 25μL of the lysate was transferred to a black 96-well plate and incubated with 200μL of the substrate solution comprised of PBS, with or without 25μg/ml of caspase substrate Ac-DEVD-AMC (37μM) in PBS supplemented with 5mM DTT. The assay was incubated at 37^{o}C for 30 minutes, and fluorescence was measured (excitation: 380nm; emission: 440nm).

Biological Replicates and Statistics: A minimum of four biological replicates were used for cell-based studies, with a minimum of six experimental replicates. To evaluate differences between sample groups, the Mann-Whitney test was used. Experiments with more than three comparison groups were subjected analysis of variance (ANOVA) followed by the Tukey Honest Difference test to compare means. Correlation statistics were performed using the Spearman nonparametric test. An asterisk in figures indicated p value is less than 0.05. For correlation between GBM cell lines, standard calculations for the correlation coefficient (r) and r^2 were performed. Data are displayed as means with error bars representing plus and minus one standard deviation of the mean.

3. Results

3.1 GBM cell lines have distinct sensitivities to TMZ. To determine the chemo-responsiveness of the GBM cell lines, the acquired cell panel was grown in 96-well plates and treated with increasing concentrations of TMZ (0-10mM) for 72 hours; afterwards, the cells were fixed and stained with TO-PRO-3 to determine the number of cells remaining (Figure 6A). The IC_{50}s for each cell line were determined by plotting the fluorescence of the remaining cells against the concentration of TMZ (Figure 6B). Using non-parametric analysis of these data, the IC_{50}s were calculated from four biological replicates (Table 4). Based on these experiments, we found that three cell lines (U118, SNB19, and U251) were unresponsive (i.e. resistant) to TMZ at supraphysiological concentrations up to 10mM, while the remaining seven cell lines had varying degrees of responsiveness with H4 and SNB75 cells being the most sensitive of the cell lines. Since MGMT promoter methylation has

been previously used as prognostic marker, we decided to evaluate if MGMT protein expression levels were related to TMZ chemo-responsiveness, but we did not observe any correlation between the two (Figure S1). We further investigated if chemo-responsiveness was related to metabolic differences between the cell lines we first examined expression levels of glycolytic proteins, however there was no discernable trend in the expression of the metabolic enzymes (HKI, HK2, PKM1/2, LDHA, MCT1, MCT4) analyzed (Figure S2). We also examined if the differences observed in response to TMZ was related to a metabolic shift, usually observed in cancer, we measured mitochondrial respiration and glycolysis in the presence or absence of glucose and glutamine, similarly we couldn't determine a consistent trend between metabolic status and chemo-responsiveness (Figure S3).

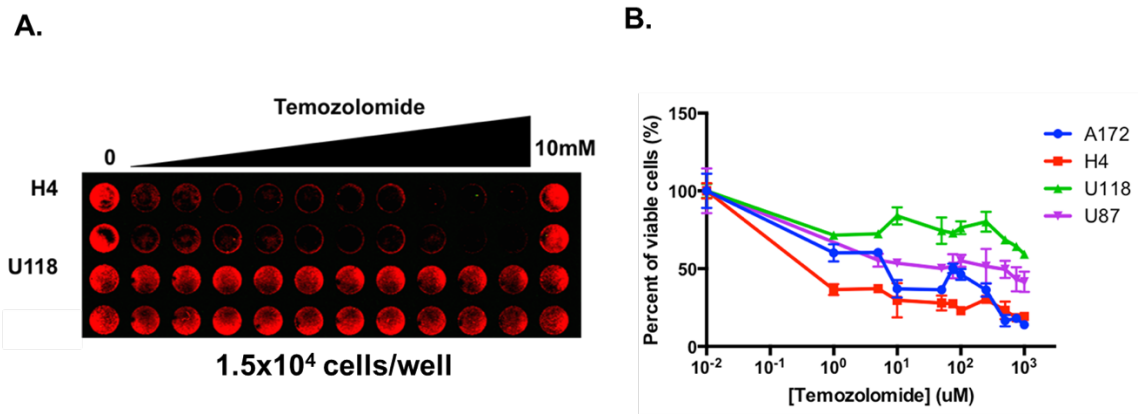

Figure 6. Determining IC_{50} values for TMZ in GBM Cell Lines.
(A) GBM cell lines were incubated for 72 hours in the presence of 0-10mM TMZ. The cells were then fixed and stained with TO-PRO-3 to determine the number of cells. Displayed in this figure are the TMZ-sensitive line (H4) and the TMZ-resistant line (U118). (B) The fluorescence for each TMZ dose was plotted (n=4) and the IC_{50} value was calculated using GraphPad® Prism and displayed in Table 4. Here we display prototypic plots for A172, H4, U118, and U87MG cells.

Table 4: TMZ IC50 Values for Established GBM cell Lines

Cell Line	TMZ IC_{50} (mM)
U118	>10 mM†
SNB19	>10 mM†
U251	>10 mM†
U87	0.75 ± 0.11
SF295	0.64 ± 0.08
SF539	0.37 ± 0.03
SF268	0.21 ± 0.10
A172	0.18 ± 0.05
SNB75	0.07 ± 0.02
H4	0.04 ± 0.01

IC_{50} values for GBM cell lines were determined in a 96-well format on $5x10^3$ cells/well using cell-based fluorescence. †The dose curve for this experiment was from 0-10mM due to the solubility of TMZ

3.2 Bcl-2 protein levels are distinct among GBM cell lines. To evaluate if the chemo-responsiveness of the 10 cell lines was related to the levels of Bcl-2 family proteins, we examined the expression pro-survival and pro-apoptotic proteins across the panel. Examination of the pro-survival Bcl-2 proteins revealed that Bcl-2 levels were highest in U-118 MG, SNB-19, and U-251 cell lines, five cell lines (U-87 MG, SF-295, SF-539, SF-268, and A-172) had some expression of Bcl-2, and two cell lines, H4 and SNB-75, had no detectable Bcl-2 expression (Figure 7). Conversely, no discernable trend could be found for other pro-survival Bcl-2 proteins, Bcl-xL or Mcl-1 (Figure 7, Figure S4). Next, we examined the expression of pro-apoptotic, BH3-only members of the Bcl-2 family. Bim displayed a

complementary expression pattern to Bcl-2 in the cell lines. U-118 MG, SNB-19, and U251 had no or very low expression of Bim, while U-87 MG, SF-295, SF-539, SF-268, and A-172 had higher levels of Bim (Figure 7). H4 and SNB-75 had the highest levels of Bim expression among the cell lines across three biological replicates (Figure 7). There was no discernable trend in the expression of other BH3-only proteins (Bad, Bid, Bik, PUMA) analyzed (Figure S4). Actin served as a loading control for all experiments.

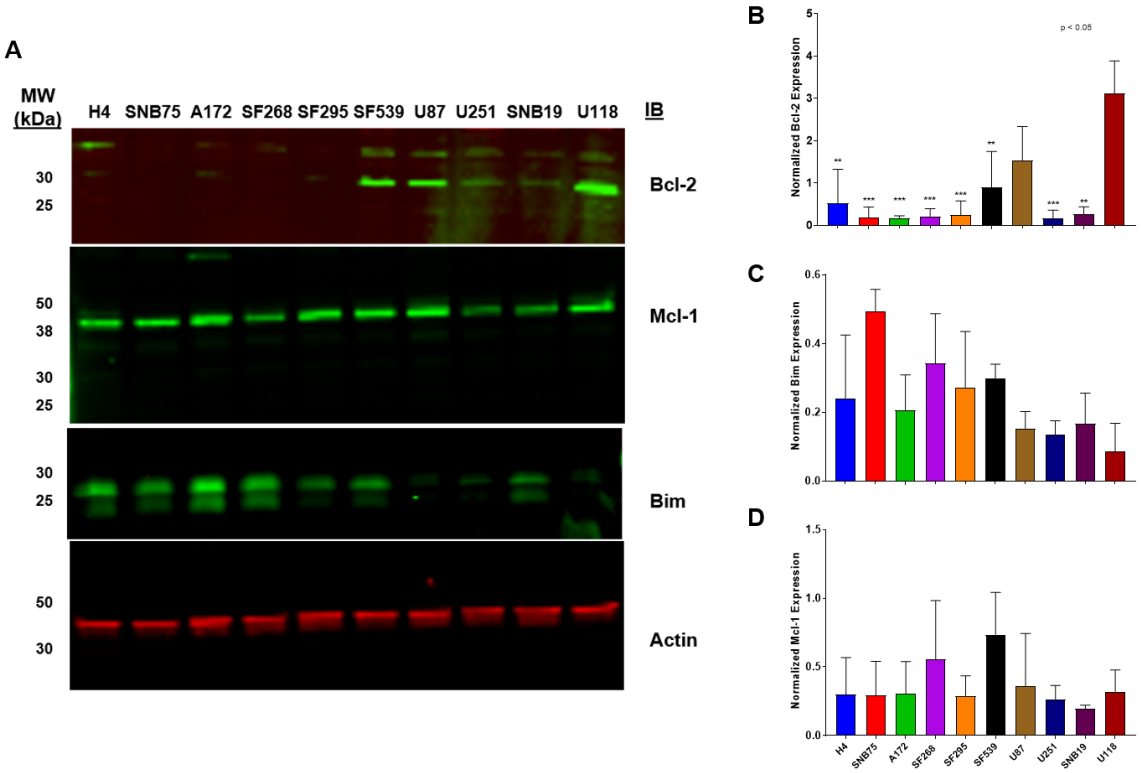

Figure 7. Bcl-2 profiling of GBM Cell Lines.
GBM cell lines were grown, lysed, and protein levels were assessed by western blot analysis for Bcl-2 family proteins. Expression was normalized to the actin loading control. (A) Representative western blot (n=3). Quantification of normalized protein expression of (B) Bcl-2, (C) Mcl-1 and (D) Bim. One-way ANOVA was used to determine differences in protein expression between cell lines, $p<0.05$. Bcl-2 protein level was significantly different in U118 cells, asterisk represent different levels of significance ** $p<0.002$, *** $p<0.0005$

3.3 The Bcl-2/Bim Ratio Correlates to Chemo-responsiveness. To determine if the expression of Bcl-2 and Bim levels corresponded to chemo-resistance in GBM cell lines, we divided the relative expression of Bcl-2 by that of Bim. This ratio provides the amount of pro-survival capacity within mitochondria. A high ratio indicates a great survival capacity (i.e. resistance), while a low value would indicate sensitivity to stress. The ratio was calculated for each cell line and plotted against the previously calculated IC_{50}s for TMZ. We used a non-parametric correlation test (Spearman method) to determine the correlation coefficient (r) (Figure 8). Analysis of the Bcl-2/Bim ratio and TMZ IC_{50}s provided an r value of 0.9755 ($p<0.0001$) suggesting a significant relationship could exist between these two measures (Figure 8). Further, we used these values to stratify the cells by chemo-responsiveness. Cells with a high Bcl-2/Bim were chemo-resistant (U-118 MG, SNB-19, and U-251), those with a moderate Bcl-2/Bim value were responsive at higher concentrations of TMZ (U-87 MG, SF-295, SF539, SF268, and A172), and those cells with a very low Bcl-2/Bim (H4 and SNB75) were found to be sensitive to TMZ.

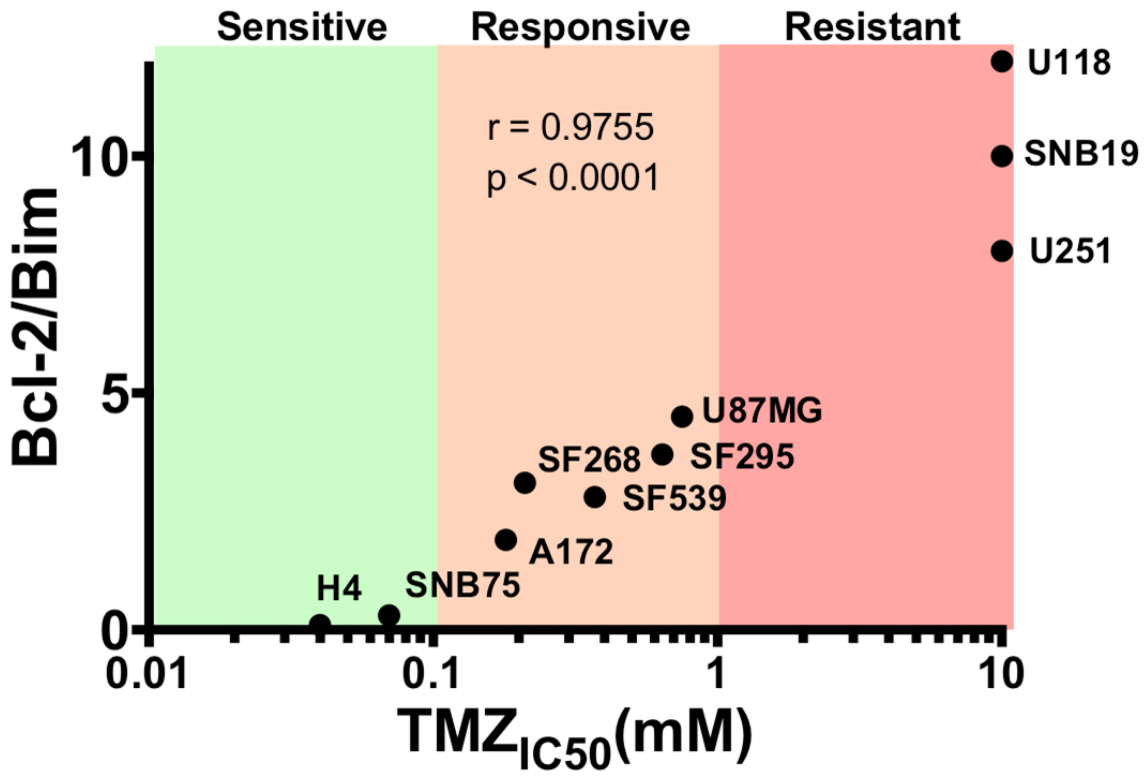

Figure 8. Correlation of Bcl-2/Bim to TMZ Sensitivity.
The Bcl-2/Bim ratio was calculated for each of the GBM cell lines and plotted against the corresponding IC50 for TMZ (n=4). Spearman correlation test was used to determine the correlation coefficient (r).

3.4 Inducing resistance increases the Bcl-2/Bim ratio. It has been previously shown that hypoxic cycling can induce chemo-resistance in U-87 MG cells. To determine if this had an impact on the Bcl-2/Bim ratio, we incubated U-87 MG cells under normoxic and hypoxic conditions for 16 hours. We then tested the cells response to TMZ and found that hypoxic cells had a five-fold increase in the IC_{50} for TMZ (Figure 9A). Analysis of Bcl-2 and Bim levels indicate that Bcl-2 levels increased during the hypoxic treatment of U-87 MG cells, while Bim levels decreased (Figure 9B). Mitochondrial concentration in U-87 MG cells remained the

same as indicated by western blot detection of cyclo-oxygenase IV (COX-1V) and Tubulin was used as a loading control (Figure 9B). This suggests that the Bcl-2/Bim ratio is a useful assessment of TMZ-responsiveness.

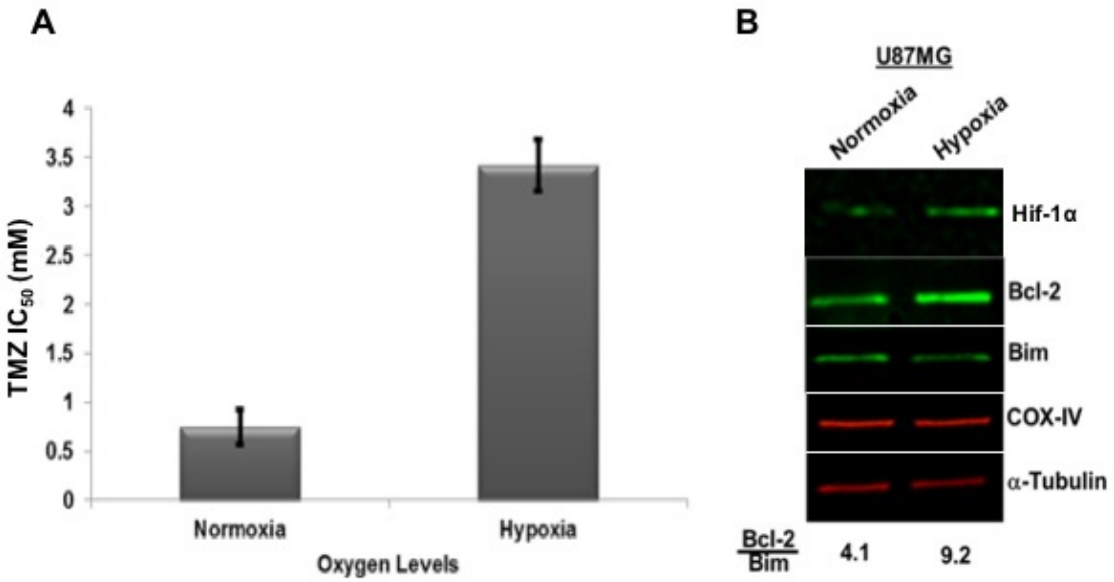

Figure 9: Inducing TMZ Resistance in U87 Cells Increases Bcl-2/Bim Ratio. U87MG cells were plated in 35-mm cell culture dishes and exposed to either normoxia or hypoxia for 16 hours. After 16 hour, cells were either treated with (A) TMZ to determine the IC50 for each condition or (B) lysed in order to measure the levels of HIF-1α, Bcl-2 and Bim. COX-IV was used as a mitochondrial loading control, while Tubulin was used as a cellular loading control. The Bcl-2/Bim ratio was calculated by dividing the normalized expression levels of Bcl-2 and Bim.

3.5 Inhibition of both Bcl-2 and Mcl-1 is necessary to improve chemo-responsiveness. Since the Bcl-2/Bim ratio correlates to chemo-responsiveness, and inducing resistance increases the ratio, we evaluated if inhibition of Bcl-2 by ABT-737, a BH3 mimetic that inhibits Bcl-2 and Bcl-xL enhanced chemoresponsiveness, however concurrent treatment of ABT-737 and TMZ only modestly improved the efficacy of TMZ (Figure S5). We further investigated if

inhibition of Mcl-1 was also required to induce cell death, after 72 hours treatment with increasing concentrations of ABT-737, S63845 (Mcl-1 inhibitor) or a combination of both, we determined the percentage of cell viability (Table 5) and observed that exposure to both ABT-737 and S63A45 resulted in massive cell death at concentrations 10-fold lower (1μM) than the individual exposures (10μM) that produced minimal if any cell death (Figure 10, S6).

Table 5: Percentage of Cell Viability for Established GBM cell Lines

GBM Cell Line	10μM ABT-737	10μM S63845	1μM ABT-737 + 1μM S63845
H4	49.88 ± 5.25	53.08 ± 3.08	1.62 ± 0.72
SNB75	83.65 ± 1.20	71.17 ± 2.23	16.89 ± 0.82
A172	73.43 ± 9.49	93.05 ± 6.72	74.07 ± 21.32
SF268	80.70 ± 2.88	101.26 ± 4.31	44.38 ± 25.67
SF539	85.34 ± 5.62	84.08 ± 5.73	1.79 ± 0.41
SF295	82.63 ± 3.61	74.09 ± 2.25	3.02 ± 1.72
U87	69.67 ± 0.16	87.95 ± 3.25	22.96 ± 3.78
U251	85.21 ± 3.71	93.23 ± 4.22	63.80 ± 2.05
SNB19	87.06 ± 3.98	94.68 ± 3.65	64.75 ± 1.95
U118	48.97 ± 2.96	107.73 ± 6.54	73.29 ± 2.54

Percentage of cell viability for GBM cell lines was determined in a 96-well format on $5x10^3$ cells/well using cell-based fluorescence.

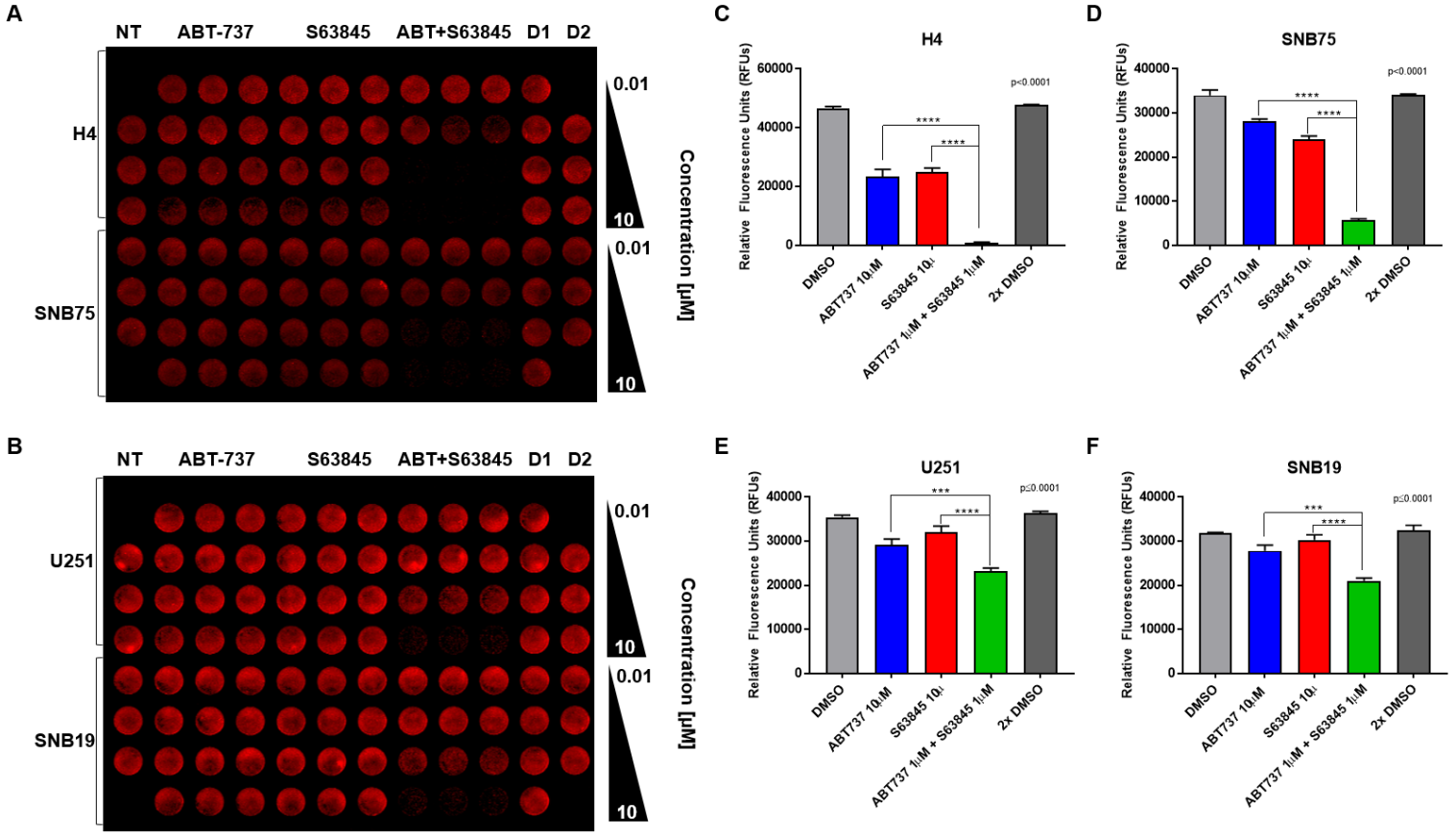

Figure 10: Percentage of Cell Viability after treatment with Bcl-2 and Mcl-1 inhibitors in GBM Cell Lines. (A) GBM cell lines were incubated for 72 hours in the presence of 0-10μM of ABT-737, 0-10μM S63845, or both. The cells were then fixed and stained with CellTag 700 stain to determine the number of cells. Displayed in this figure are the TMZ-sensitive lines (H4, SNB75) and the TMZ-resistant line (U251, SNB19). (B) The fluorescence for each TMZ dose was plotted and comparisons between treatments was performed using ANOVA followed by Tukey's honest test. ***p<0.001, ****p<0.0001

4. Discussion

BH3-only profiling has been proposed as measure to predict the chemosensitivity of solid tumors and certain types of leukemia; however, previous studies in GBM showed that the individual expression levels of different members of the Bcl-2 protein superfamily did not correlate with patient overall survival (Potter and Letai, 2016) (Cartron et al., 2012). Our current study determined that while individual expression of Bcl-2 family proteins is not sufficient to predict prognosis, a collective assessment of anti-apoptotic and pro-apoptotic Bcl-2 proteins may be useful to discern the personalized vulnerability of tumors. In fact, we demonstrate that the ratio between the relative abundance of anti-apoptotic Bcl-2 proteins (Bcl-2, Bcl-xL, and Mcl-1) and the BH3-only protein Bim levels correlate with chemoresponsiveness to TMZ in established GBM cell lines. This was also the case in patient-derived GSCs. Additionally, inducing chemoresistance in U87 cells by hypoxic cycling decreases the anti-apoptotic Bcl-2/Bim ratio. The collective contribution of anti-apoptotic Bcl-2 proteins to cell survival and chemoresistance was verified using a Bim mimetic, ABT-737 (a Bcl-2 and Bcl-xL inhibitor), and a Mcl-1 inhibitor, S63A45 to induce cell death and enhance TMZ potency in established GBM cell lines and GSCs. Based on these findings, we propose that an assessment of apoptotic capacity in GBM cells may be useful to determining personalized treatment options.

Prognostic approaches for GBM currently entail sequencing of commonly mutated genes and histological analysis of tumors, with the problematic hypermethylation of the MGMT promoter losing its previously presumed clinical relevance. The

genomic analyses include genes that are involved in growth and metabolism, and only p53 has any relevance to apoptosis. The histological classification of the tumor is based on the presence of specific cellular markers related to proliferation, and none are reflective of cell death capacity. This is problematic, in our opinion, when assigning therapies because one cannot be certain if a chemotherapy or radiotherapy approach will be effective without insight into the relative potential for GBM tumor cells to undergo apoptosis. Our suggested approach of histological or biochemical assessment of anti-apoptotic Bcl-2 proteins and Bim in GBM specimens would provide an index for the relative chemoresistance based on the collective abundance of Bcl-2, Bcl-xL, and Mcl-1, and give insight into the apoptotic induction threshold by assaying the relative concentrations of Bim. Of course, further studies in healthy patients and GBM patients will be needed to assess what concentrations will correlate to clinical outcomes. This will be a topic of research between the lab and Baptist Health South Florida as part of a collaborative project to improve GBM prognosis and treatment selection.

In our study, we found that only one BH3-only protein concentration, Bim, reflected cell death capacity in GBM cell lines and GSCs. Bim is able to promote apoptosis by either direct activation through Bak and Bax, or by sequestering Bcl-2 anti-apoptotic proteins (Chipuk and Green, 2008). The relative abundance of Bim on mitochondria is controlled in part by increased gene expression and by post-translational modification by stress-induced kinases. In fact, the c-Jun N-terminal kinase (JNK) can phosphorylate Bim in response to chemo- and radiotherapy. JNK phosphorylation of Bim induces mitochondrial translocation where it can impair

anti-apoptotic Bcl-2 proteins and trigger mitochondrial outer membrane permeabilization (MOMP) leading to apoptosis (Lei and Davis, 2003). Based on Bim's actions, we assert that Bim levels are a critical marker for a cell's ability to readily induce apoptosis under basal conditions. In fact, Bim mimetics, such as ABT-737, and related compounds are being explored as chemo-sensitizing agents because of their ability to increase apoptotic thresholds. However, based on the results of our current study, we propose that Bim concentrations should be examined with respect to the abundance of Bim targets such as the anti-apoptotic Bcl-2 proteins. We find that the ratio between anti-apoptotic Bcl-2 proteins and Bim is a more accurate predictor of chemoresponse and could be used to stratify patients (Figure 3) because the ratio reflects the relative capacity of Bim to inhibit anti-apoptotic proteins. For example, in a Bcl-2/Bim ratio greater than 1 in a tumor sample, one may need to employ a sensitizing agent before a treatment approach to lower the apoptotic threshold; where, a ratio below 1 may indicate that a tumor may require less aggressive treatment approaches because of a lower cell death threshold. Additionally, changes in the Bcl-2/Bim ratio can be monitored as mechanism to track acquired resistance in GBM patient samples (Figure 9). It should be noted that the inclusion of Mcl-1 could affect the accuracy of the ratio because Mcl-1 translocation to mitochondria and sequestration to cytosol is related in part to the scaffold 14-3-3 and the actions of another BH3-only protein, Noxa, in other solid tumors (Nakajima et al., 2014). Therefore, the Bcl-2/Bim ratio may need to be supplemented with pharmacological profiling with ABT-737 and S63845 to determine the relative survival capacity of GBM tumor cells.

Our current study as indicated above suggests that chemoresponsiveness and cell survival is influenced by the concerted activities of anti-apoptotic proteins Bcl-2, Bcl-xL, and Mcl-1 on the mitochondrial surface. This was somewhat expected given the common functions of these three proteins. The fact that the concentrations of these proteins alone can be used in conjunction with Bim levels is indeed surprising because of the levels of control in place to coordinate the activities of Bcl-2 proteins to sustain cell viability or to induce apoptosis. For example, the presence of Bcl-2 alone does not always dictate functions. Phosphorylation of Bcl-2 has been shown to affect the balance between survival and cell death. Phosphorylation of residues threonine 56 (Thr56) and serine 87 (Ser87) are necessary for the anti-apoptotic functions of Bcl-2, as mutation of these residues (Thr56Ala and Ser87Ala) failed to prevent glucocorticoid-induced cell death in T-cells (Huang and Cidlowski, 2002). Alternatively, JNK-mediated phosphorylation of Bcl-2 has been shown to induce Bcl-2 migration from the outer mitochondrial membrane and prevent its anti-apoptotic actions. Similar phospho-regulatory mechanisms have been proposed to influence the activities of Bcl-xL, Mcl-1, and BH3-only proteins, such as Bim. Accordingly, if the concentrations of anti-apoptotic Bcl-2 proteins and Bim lose correlation power in patient samples, it may be prudent to consider the phosphorylation state of the proteins when assessing apoptotic capacity and predicting potential therapeutic outcomes.

Finally, treatment of GBM cell lines and GSCs with the BH3 mimetic ABT-737 or the Mcl-1 inhibitor S63845 only modestly affected cell viability. However, exposure to both ABT-737 and S63845 resulted in massive cell death at concentrations 10-

fold lower (1μM) than the individual exposures (10μM) that produced minimal if any cell death. This observation emphasizes the importance of all three anti-apoptotic Bcl-2 proteins to the establishment of the apoptosis threshold. The data also demonstrate the importance of Mcl-1 levels to the anti-apoptotic capacity because ABT-737 has binding affinity for Bcl-2, Bcl-xL and Bcl-w and not Mcl-1 (Oltersdorf et al., 2005). The synergism between ABT-737 and S63845 was apparent when these compounds increased the efficacy of TMZ in the nanomolar range. This benefits patients as the use of ABT-737 and S63845 could lower the dose of the highly toxic TMZ and reduce the risk of potentially debilitating off-target effects in the brain. Unfortunately, Bcl-2 proteins are ubiquitously expressed in the brain, and toxicity studies would need to be performed to assure that the doses used would not adversely affect non-tumor cells in the brain. Without selective targeting to tumor cells, we could render neurons and glial cells vulnerable to the treatments that follow ABT-737 and S63845 by increasing the apoptotic potential in these cells, which may result in permanent neurological damage. Fortunately, similar compounds are in clinical trials or in use and few side effects have been reported. Suggesting that low dose chemosensitization with BH3-mimetics may be a useful approach to improve GBM outcomes.

In our current study, we explore mitochondrial factors that contribute to chemotherapeutic resistance in GBM cell lines and GSCs. We found that the relative abundance of anti-apoptotic proteins (Bcl-2, Bcl-xL, and Mcl-1) and the BH3-only protein Bim could be used to predict chemotherapeutic outcomes; furthermore, inhibition of anti-apoptotic Bcl-2 proteins was found to increase

chemotherapeutic efficacy. Moreover, the inhibition of Bcl-2, Bcl-xL, and Mcl-1 synergistically enhanced the potency of TMZ. Based on our results, we contend that rigorous assessment of Bcl-2 proteins may be a useful approach to determine if specific treatments will be effective in GBM patients. Future studies will focus on determining the relevant concentrations required to predict outcomes in patient tumors and previously-acquired histological samples.

5. References

Cartron, P.F., Loussouarn, D., Campone, M., Martin, S.A., Vallette, F.M., 2012. Prognostic impact of the expression/phosphorylation of the BH3-only proteins of the BCL-2 family in glioblastoma multiforme. Cell Death and Disease 3, e421–9. doi:10.1038/cddis.2012.150

Chipuk, J.E., Green, D.R., 2008. How do BCL-2 proteins induce mitochondrial outer membrane permeabilization? Trends in Cell Biology 18, 157–164. doi:10.1016/j.tcb.2008.01.007

Chonghaile, T.N., Sarosiek, K.A., Vo, T.T., Ryan, J.A., Tammareddi, A., Moore, V.D.G., Deng, J., Anderson, K.C., Richardson, P., Tai, Y.T., Mitsiades, C.S., Matulonis, U.A., Drapkin, R., Stone, R., DeAngelo, D.J., McConkey, D.J., Sallan, S.E., Silverman, L., Hirsch, M.S., Carrasco, D.R., Letai, A., 2011. Pretreatment Mitochondrial Priming Correlates with Clinical Response to Cytotoxic Chemotherapy. Science 334, 1129–1133. doi:10.1126/science.1206727

Davids, M.S., Deng, J., Wiestner, A., Lannutti, B.J., Wang, L., Wu, C.J., Wilson, W.H., Brown, J.R., Letai, A., 2012. Decreased mitochondrial apoptotic priming underlies stroma-mediated treatment resistance in chronic lymphocytic leukemia. Blood 120, 3501–3509. doi:10.1182/blood-2012-02-414060

Furnari, F.B., Furnari, F.B., Fenton, T., Fenton, T., Bachoo, R.M., Bachoo, R.M., Mukasa, A., Mukasa, A., Stommel, J.M., Stommel, J.M., Stegh, A., Stegh, A., Hahn, W.C., Hahn, W.C., Ligon, K.L., Ligon, K.L., Louis, D.N., Louis, D.N., Brennan, C., Brennan, C., Chin, L., Chin, L., DePinho, R.A., DePinho, R.A., Cavenee, W.K., Cavenee, W.K., 2007. Malignant astrocytic glioma: genetics, biology, and paths to treatment. Genes & Development 21, 2683–2710. doi:10.1101/gad.1596707

Hanahan, D., Weinberg, R.A., 2011. Hallmarks of Cancer: The Next Generation. Cell 144, 646–674. doi:10.1016/j.cell.2011.02.013

Huang, S.-T.J., Cidlowski, J.A., 2002. Phosphorylation status modulates Bcl-2 function during glucocorticoid-induced apoptosis in T lymphocytes. FASEB J. 16, 825–832. doi:10.1096/fj.01-0852com

Lei, K., Davis, R.J., 2003. JNK phosphorylation of Bim-related members of the Bcl2 family induces Bax-dependent apoptosis. Proc Natl Acad Sci USA 100, 2432–2437. doi:10.1073/pnas.0438011100

Letai, A., Bassik, M.C., Walensky, L.D., Sorcinelli, M.D., Weiler, S., Korsmeyer, S.J., 2002. Distinct BH3 domains either sensitize or activate mitochondrial apoptosis, serving as prototype cancer therapeutics. Cancer Cell 2, 183–192. doi:10.1016/S1535-6108(02)00127-7

Letai, A.G., 2008. Diagnosing and exploiting cancer's addiction to blocks in apoptosis. Nature Publishing Group 8, 121–132. doi:10.1038/nrc2297

Nakajima, W., Hicks, M.A., Tanaka, N., Krystal, G.W., Harada, H., 2014. Noxa determines localization and stability of MCL-1 and consequently ABT-737 sensitivity in small cell lung cancer. Cell Death and Disease 5, e1052–e1052. doi:10.1038/cddis.2014.6

Oltersdorf, T., Elmore, S.W., Shoemaker, A.R., Armstrong, R.C., Augeri, D.J., Belli, B.A., Bruncko, M., Deckwerth, T.L., Dinges, J., Hajduk, P.J., Joseph, M.K., Kitada, S., Korsmeyer, S.J., Kunzer, A.R., Letai, A., Li, C., Mitten, M.J., Nettesheim, D.G., Ng, S., Nimmer, P.M., O'Connor, J.M., Oleksijew, A., Petros, A.M., Reed, J.C., Shen, W., Tahir, S.K., Thompson, C.B., Tomaselli, K.J., Wang, B., Wendt, M.D., Zhang, H., Fesik, S.W., Rosenberg, S.H., 2005. An inhibitor of Bcl-2 family proteins induces regression of solid tumours. Nature 435, 677–681. doi:10.1038/nature03579

Potter, D.S., Letai, A., 2016. To Prime, or Not to Prime: That Is the Question. Cold Spring Harb. Symp. Quant. Biol. 81, 131–140. doi:10.1101/sqb.2016.81.030841

Reed, J.C., 2011. Cancer. Priming cancer cells for death. Science 334, 1075–1076. doi:10.1126/science.1215568

Robins, H.I., Chang, S., Butowski, N., Mehta, M., 2007. Therapeutic advances for glioblastoma multiforme: current status and future prospects. Curr Oncol Rep 9, 66–70.

Ryan, J., Letai, A., 2013. BH3 profiling in whole cells by fluorimeter or FACS. Methods 61, 156–164. doi:10.1016/j.ymeth.2013.04.006

Ryan, J.A., Brunelle, J.K., Letai, A., 2010. Heightened mitochondrial priming is the basis for apoptotic hypersensitivity of CD4+ CD8+ thymocytes. Proc. Natl. Acad. Sci. U.S.A. 107, 12895–12900. doi:10.1073/pnas.0914878107

Schellenberg, B., Wang, P., Keeble, J.A., Rodriguez-Enriquez, R., Walker, S., Owens, T.W., Foster, F., Tanianis-Hughes, J., Brennan, K., Streuli, C.H., Gilmore, A.P., 2013. Bax exists in a dynamic equilibrium between the cytosol and mitochondria to control apoptotic priming. Molecular Cell 49, 959–971. doi:10.1016/j.molcel.2012.12.022

Stupp, R., Mason, W.P., van den Bent, M.J., Weller, M., Fisher, B., Taphoorn, M.J.B., Belanger, K., Brandes, A.A., Marosi, C., Bogdahn, U., Curschmann, J., Janzer, R.C., Ludwin, S.K., Gorlia, T., Allgeier, A., Lacombe, D., Cairncross, J.G., Eisenhauer, E., Mirimanoff, R.O., European Organisation for Research and Treatment of Cancer Brain Tumor and Radiotherapy Groups, National Cancer Institute of Canada Clinical Trials Group, 2005. Radiotherapy plus concomitant and adjuvant temozolomide for glioblastoma. N Engl J Med 352, 987–996. doi:10.1056/NEJMoa043330

Vo, T.-T., Ryan, J., Carrasco, R., Neuberg, D., Rossi, D.J., Stone, R.M., Deangelo, D.J., Frattini, M.G., Letai, A., 2012. Relative mitochondrial priming of myeloblasts and normal HSCs determines chemotherapeutic success in AML. Cell 151, 344–355. doi:10.1016/j.cell.2012.08.038

Wen, P.Y., Kesari, S., 2008. Malignant gliomas in adults. N Engl J Med 359, 492–507. doi:10.1056/NEJMra0708126

CHAPTER IV

A novel splice variant of Sab alters mitochondrial physiology

1. Introduction

The Bcl-2 superfamily of proteins are critical modulators of cell death responses in human cells, and dysregulation of Bcl-2 proteins can result in human disease. Specifically, the accumulation of anti-apoptotic Bcl-2 proteins, such as Bcl-2, Bcl-xL, and Mcl-1, may enhance the survival of cancer cells by increasing the cells' tolerance to toxic challenges (Brunelle and Letai, 2009). Alternatively, an overabundance of pro-apoptotic Bcl-2 proteins (BH3-only proteins) may lower the apoptotic threshold of cells by inhibiting the actions of anti-apoptotic proteins and promoting mitochondrial outer membrane permeabilization (MOMP) by facilitating the oligomerization of Bax and Bak (Chipuk et al., 2008). Proteins in the Bcl-2 superfamily are tightly regulated by gene expression and by post-translational modification. Phosphorylation of Bcl-2 proteins can differentially influence the anti- and pro-apoptotic functions of these proteins. This phospho-regulation connects apoptotic machinery to cellular growth and stress response pathways.

One of the most prominent stress-responsive regulators of Bcl-2 function is the c-Jun N-terminal kinase (JNK), a serine/threonine protein kinase, that can influence activities of both anti-apoptotic and pro-apoptotic Bcl-2 proteins by phosphorylation. JNK can affect the anti-apoptotic functions of Bcl-2 differently depending on the phosphorylation site. For example, JNK phosphorylation on threonine-56 (Thr56) and serine-87 (Ser87) are required for the anti-apoptotic functions of Bcl-2, and mutation of Thr56 and Ser87 prevents the survival functions of Bcl-2 (Huang and Cidlowski, 2002). Alternatively, JNK phosphorylation of Bcl-2 on Ser70 leads to emigration of Bcl-2 from the outer mitochondrial membrane

(OMM) and promotes apoptosis (Yamamoto et al., 1999). JNK also alters the functions of Bcl-xL and Mcl-1 by phosphorylation. With respect to Bcl-xL, JNK phosphorylation on residues Thr47 and Thr115 prevents apoptosis, while JNK phosphorylation of residue Ser62 on Bcl-xL promotes chemotherapy-induced cell death (Kharbanda et al., 2000). Similarly, JNK phospho-regulation of Mcl-1 influences cell death responses; whereby, JNK phosphorylation of Mcl-1 on Thr163 results in the proteosomal degradation of Mcl-1 in a glycogen synthase kinase-3 (GSK3)-dependent manner (Morel et al., 2009). Also, JNK phosphorylation of Mcl-1 on Ser121 and Thr163 have been linked to a decrease in the pro-apoptotic and anti-apoptotic capacities, respectively (Thomas et al., 2010). Depending on the kinase isoform, stimuli, and cellular context JNK signaling can impact anti-apoptotic Bcl-2 proteins differently and influence cell fate.

However, JNK signaling seems to be more straightforward when it comes to the regulation of pro-apoptotic BH3-only proteins. JNK primarily activates and enhances the apoptotic activities of BH3-only proteins by phosphorylation. JNK phosphorylation of Bim species are perhaps the most well characterized of the JNK-Bcl-2 phospho-regulations. JNK phosphorylation on Ser44, Thr56, and Ser58 are all linked to enhanced apoptotic activities, including Bax-Bak oligomerization, of Bim (Lei and Davis, 2003). Inhibition of JNK in many cell lines has been shown not only to reduce Bim activity, but also resulted in decreased Bim levels. Bad is also another BH3-only protein that can be induced by JNK phosphorylation as well. JNK modification of Bad on Ser128 causes its release from the inhibitory scaffold 14-3-3; meanwhile, JNK phosphorylation on Thr201 of Bad enhances the

interaction of Bad with Bcl-xL, which effectively sequesters and inhibits the anti-apoptotic activities of Bcl-xL. JNK can also promote the gene expression of BH3-only proteins (Wang et al., 2007; Yu et al., 2004). One example is JNK phosphorylation of c-Jun (a component of the transcription factor activator protein-1 (AP-1)) leads to the transcription of death protein-5/harakari (DP5/Hrk) (Ma et al., 2007). Collectively, these results strongly support JNK's role in apoptosis.

Stress-induced activation of JNK causes the translocation of the kinase to the OMM, an event that culminates in mitochondrial dysfunction and apoptosis (J. W. Chambers et al., 2011). The localization of JNK to the OMM places it close to not only the bioenergetic machinery, but also Bcl-2 proteins. At mitochondria, JNK interacts with the OMM scaffold protein Sab through a kinase interaction motif (KIM) located in the C-terminus of Sab (Wiltshire et al., 2004; 2002; Win et al., 2011). Mitochondrial JNK signaling promotes mitochondrial dysfunction by amplifying reactive oxygen species (ROS) production, impairing bioenergetics, and altering mitochondrial membrane potential (J. W. Chambers and LoGrasso, 2011; Hanawa et al., 2008). In addition, mitochondrial JNK signaling also plays a role in cell death as mentioned above (J. W. Chambers et al., 2011; Schroeter et al., 2003). Consequently, inhibition of the JNK-Sab interaction prevents oxidative stress, mitochondrial dysfunction and cell death. Furthermore amplification of JNK/Sab-mediated signaling has been shown to sensitize cancer cells and improve chemotherapeutic efficacy (J. W. Chambers et al., 2011; 2013a; 2013b; T. P. Chambers et al., 2015; Wiltshire et al., 2004). In fact, our recent studies in gynecological cancers, reveal that Sab levels correlated with chemosensitivity;

wherein, low Sab levels are indicative of chemo-resistant cells. Artificial elevation of Sab was shown to increase the levels of BH3-only proteins on mitochondria, while anti-apoptotic Bcl-2 protein concentrations were reduced in cells with elevated Sab levels. However, toxin-induced increases in Sab also sensitized normal cells to apoptosis. Cardiomyocytes exposed to prolonged low doses of imatinib had increased Sab levels and were vulnerable to chemotherapeutic agents and mitochondrial stress. These data suggest that JNK signaling on Sab is a critical event in cell death signaling.

Because of the relevance of JNK-Sab signaling to cell death and the correlation of Sab levels to chemo-responsiveness in gynecological malignancies, we hypothesized that Sab levels would reflect the chemo-vulnerability of GBM cells. We found that the Sab levels did not correlate to the responsiveness of cells to TMZ. Sab levels did not correspond to Bcl-2 or BH3-only profiles as well. However, we observed that a truncated version of Sab was expressed in some of the GBM cell lines. Sequence analysis of the Sab transcripts revealed that the smaller form of Sab was isoform 2, which lacks the first 157 amino acids of the protein. Cellular characterization of the Sab variant reveals that it is localized to mitochondria using a cryptic mitochondrial localization signal. The presence of the truncated Sab does not alter apoptotic signaling or sensitivity to chemotherapeutic challenge. The presence of the Sab variant does enhance glycolysis by way of impaired respiration. Cells with the splice variant have diminished basal respiration and spare respiratory capacity that can be attributed to diminished complex I activity. These data suggest that Sab-mediated signaling may also be important to the

regulation of bioenergetics in brain malignancies with minimal contributions to apoptotic capacity.

2. Materials and Methods

Materials: GBM cell lines, A-172 (CRL-1620), H4 (HTB-148), U-87 MG (HTB-14), and U-118 MG (HTB-15), were purchased from American Type Culture Collection (Manassas, VA). The remaining GBM cell lines were obtained through the National Institutes of Cancer (NCI) from the NCI-60 cell panel. Cell culture media was purchased from Invitrogen (Grand Island, NY), and serum was purchased from Denville Scientific (South Plainfield, NJ). General chemicals were purchased from Fisher Scientific (Pittsburgh, PA) and Sigma Aldrich (St. Louis, MO) as indicated below. Unless indicated below, antibodies were purchased from Cell Signaling Technology (Danvers, MA).

Cell Culture: GBM cell lines were grown under normal cell culture conditions (37^{o}C and 5% CO_2 with humidity). A-172, H4, U-87 MG, U-118 MG cells and the cells from the NCI-60 panel (SF-268, SF-295, SF-539, SNB-19, SNB-75 and U-251) were grown in Dulbecco's Modified Essential Medium (DMEM) supplemented with 10% fetal bovine serum (FBS), 1,000 U/mL penicillin, 100μg/mL streptomycin, and 5μg/mL plasmocin.

SF268 clonal selection: To isolate cells with specific Sab expression patterns, full length versus splice variant, SF268 cells were plated as single cells in a 96-well plate and expanded to obtain a clonal population of cells.

Cell Lysis and Western Blot Analysis: To isolate proteins from cells for analysis, cells were plated at 2.5x10^5 cells/well in a six well plate unless otherwise indicated.

Following treatment, cells were lysed, and proteins were harvested as previously described. Briefly, cells were washed twice in phosphate buffered saline (PBS; 137mM NaCl, 2.7mM KCl, 10mM Na_2HPO_4, and 1.8mM KH_2PO_4) and lysed in radioimmunoprecipitation assay buffer (RIPA; 50mM Tris-HCl, pH 8.0, 150mM NaCl, 1% Nonidet P-40, 0.5% deoxycholate, 0.1% SDS) supplemented with 1mM phenylmethanesulfonyl fluoride (PMSF) and Halt Protease and Phosphatase Inhibitor Cocktails (Thermo Scientific). Cells were incubated while gently rocking at 4°C for five minutes, and then transferred to a sterile micro-centrifuge tube. After two minutes on ice, cell disruption was completed using sonication. The lysate was cleared by centrifugation at 15,000 × g for 15 minutes. Protein concentrations of the supernatant were measured using the Pierce BCA Assay kit according to manufacturer's directions. Proteins were then resolved by SDS-PAGE and transferred onto low fluorescence PVDF membranes. Membranes were placed in blocking buffer comprised of TBS supplemented with 5% bovine serum albumin (BSA) and incubated for at least one hour at room temperature (RT) or overnight at 4°C. The membranes were incubated in TBS containing 0.1% Tween 20 (TBSt) and 5% BSA in the presence of primary antibodies for at least 2.5 hours (RT) or overnight (4^{o}C) while gently rocking. Primary antibodies specific for Sab (Novus, H00009467-M01), Calnexin (CST, 2679), CoxIV (CST, 4850) Actin (CST, 4970), and α-tubulin (CST, 2144) were used at dilutions of 1:1000 for these studies. Membranes were washed three times for five minutes in TBSt. Membranes were incubated with secondary antibodies in the appropriate blocking buffer at a ratio of 1:20,000 for one hour at RT gently rocking. The following secondary antibodies

were used in the experiments below: IRDye 680RD Goat anti-Rabbit (926-32211) and IRDye 800CW Goat anti-Mouse (926-68070) (Licor Biosciences). Membranes were again washed three times for five minutes in TBST. Membranes were analyzed using fluorescence detection using the Odyssey CLx near infrared scanner (Licor Biosciences). The corresponding bands on the western blots were quantified and normalized using the Image Studio 2.0 software (Licor Biosciences). The fluorescence of specific bands of interest were divided by the fluorescence of the loading control band to equilibrate signal strength and loading. The resulting signal was then normalized by dividing the signals from treated samples by respective untreated or normal tissue control signals for each experiment.

Defining the cellular distribution of the Sab splice variant using confocal microscopy: GBM cell lines, SF268 and SF268 clone #6 were plated in 12-well plates containing 18mm glass coverslips in each well bottom at a density of $7x10^4$ cells per well. The cells were incubated with 50nM Mitotracker Deep Red FM (M22426) (ThermoFisher Scientific) for 15 minutes at 37 ^oC protected from light, and then fixed by incubation with 4% paraformaldehyde/PBS. Immunofluorescence was performed to detect Sab (as described in (J. W. Chambers et al., 2013b). Briefly, cells were placed in permeabilization/blocking buffer comprised of PBS with 5%BSA, 0.2% tween and 0.1% triton X-100 for 30 minutes at RT. The coverslips were incubated with PBS containing 0.1% Tween 20 (PBSt) and 5% BSA in the presence of primary antibodies against Sab (H00009467-M01) (Novus Biologicals) overnight at 4^oC. Cells were washed three times for five minutes in PBSt. Coverslips were incubated with secondary antibody

AlexaFluor-488 anti-Mouse (CST-4408) in the appropriate blocking buffer at a ratio of 1:250 for one hour at RT gently rocking. Coverslips were again washed three times for five minutes in PBSt. Coverslips were mounted on microscopy slides using DAPI Fluoromount-G (0100-20) (SouthernBiotech). Cells were imaged using a confocal microscope Fluoview FV1000 (Olympus).

Mitochondrial Isolation: A modified protocol as described in (Magalhães et al., 1998; Yang et al., 1997) was used to obtain mitochondria as described in our previous studies (J. W. Chambers et al., 2013b; 2013a; 2011). Mitochondrial samples with greater than 80% purity were used for experiments.

Metabolic Analysis: Cellular metabolism was assessed by measuring the extracellular acidification rate (ECAR) and the oxygen consumption rate (OCR) of the GBM cell line SF268 and SF268 Clone #6 using the Seahorse Biosciences XF-96 extracellular flux analyzer (Wu et al., 2007). Cells were assayed ($1.0x10^4$ cells/well) using the glycolytic and mitochondrial stress kits. For our studies, 3.0μM oligomycin, 1μM FCCP, 3μM rotenone and 3μM antimycin were used. From these measurements, we derived glycolytic and respiratory parameters, including spare respiratory capacity as previously described (Wu et al., 2007). Data were normalized to cell number.

Cell proliferation by BrDU incorporation: We measured cellular abundance by incorporation of 5-bromo-2'-deoxyuridine (BrdU) cell proliferation assay. We used the BrdU Cell Proliferation assay kit (Cat# 11669915001) (Roche). GBM cells SF268 and SF268 clone #6 were plated at a density of $0.5 x10^4$ cells per well and grown overnight. The cells were then serum starved for 24 hours. After serum

starvation, cells were treated with increasing concentrations of FBS for 24 hours and then monitored BrdU incorporation using the manufacturer's protocol for 24 hours. Light emission was measure using the Synergy H1 Hybrid Reader (BioTek).

Determining Cell-based IC_{50}s for Irinotecan and Rotenone: To determine the relative chemo-sensitivity of the GBM cell line SF268 and SF268 Clone #6, cells were treated with increasing concentrations of either Irinotecan (0-15μM) or Rotenone (0-10μM). Briefly, GBM cells were plated at $5x10^3$ cells per well in black-walled, clear bottom plates (Perkin Elmer) and grown overnight. The cells were then treated with chemotherapeutic agents for 72 hours. The cells were washed three times in PBS and fixed in 4% paraformaldehyde/PBS. The cells were then stained with 0.2μM CellTag 700 Stain (926-41090) (Licor Biosciences) for 1 hour at RT. The cells were then washed three times in Hank's Buffered Saline Solution (HBSS). The plate was imaged using the Odyssey CLx scanner (Licor Biosciences) and analyzed using the Image Studio 2.0 software (Licor Biosciences). The IC_{50} for each cell line was calculated using the GraphPad Prism7© software.

Caspase Activity: To assess caspase 3/7 activity in SF268 and SF268 clone #6 cell lines after treatment with either irinotecan or rotenone, cells were grown on 6-well plates. After treatment, cells were lysed with 100μL of PBS supplemented with 1% TritonX-100, for 5 minutes on ice. Cell disruption was completed by sonication, and samples were centrifuged at 15,000 x g for 10 minutes at 4°C. Then, 25μL of the lysate was transferred to a black 96-well plate and incubated with 200μL of the

substrate solution comprised of PBS, with or without 25μg/ml of caspase substrate Ac-DEVD-AMC (37μM) in PBS supplemented with 5mM DTT. The assay incubated at 37°C for 30 minutes, and fluorescence was measured (excitation: 380nm; emission: 440nm).

Biological Replicates and Statistics: A minimum of four biological replicates were used for cell-based studies, with a minimum of six experimental replicates. To evaluate differences between sample groups, the Mann-Whitney test was used. Experiments with more than three comparison groups were subjected analysis of variance (ANOVA) followed by the Tukey Honest Difference test to compare means. An asterisk in figures indicated p value is less than 0.05. Data are displayed as means with error bars representing plus and minus one standard deviation of the mean.

3. Results

3.1 Sab protein levels are distinct among GBM cell lines. Sab levels have been shown to correlate to chemo-responsiveness in gynecological cancers, we examined if Sab levels would reflect the chemo-responsiveness of GBM cells. We observed no discernable pattern between Sab expression levels and chemo-responsiveness, Sab levels were comparable in the sensitive line H4 and the resistant line U118 (Figure 11). Intriguingly, we observed a second molecular weight species of Sab, suggesting the presence of a novel Sab splice variant in certain GBM cell lines. The transcript for a splice variant of Sab has been identified (Ota et al., 2004), it has a shorter N-terminus (Figure 12), and its predicted molecular weight corresponds to the species observed in SF268 cells.

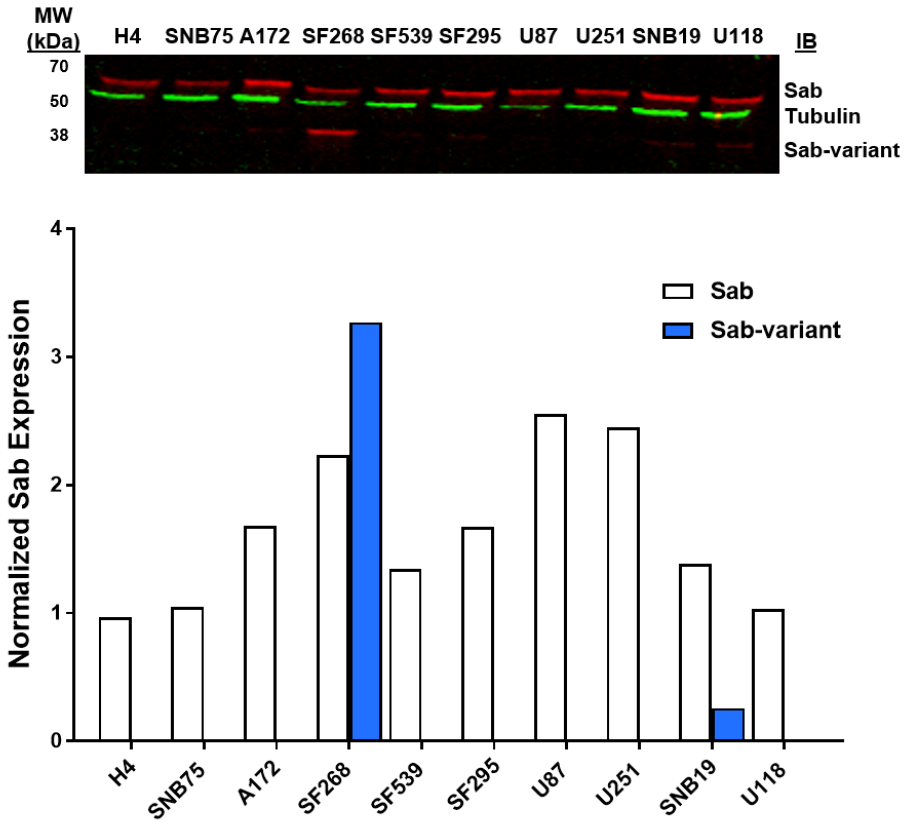

Figure 11. Expression of Sab in different GBM cell lines.

GBM cell lines were grown to 85% confluency and lysed. Proteins (25μg) were quantified and resolved by SDS-PAGE. (A) Western blot analysis was used to detect Sab levels. Tubulin was used as loading control. (B) Quantification of expression levels.

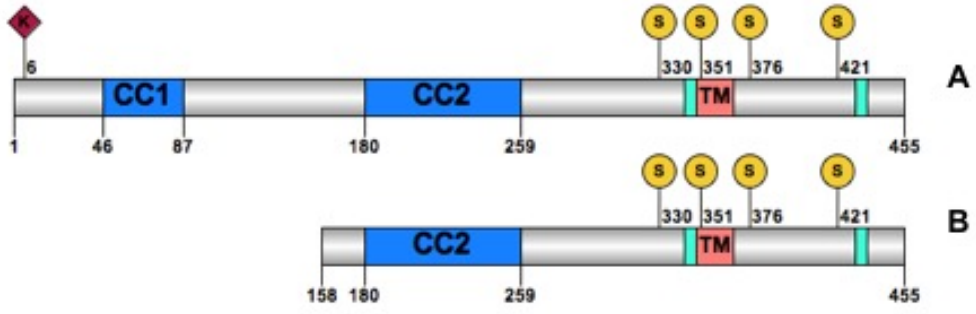

Figure 12. Schematic representation of Sab splice variants.

(A) Sab full-length. (B) Sab splice variant. This representation of the Sab splice variants shows the different regions of each splice variant. CC1: coiled-coiled motif 1, CC2: coiled-coiled motif 2, TM transmembrane domain, KIM1: kinase interaction motif 1, KIM2: kinase interaction motif 2, S: phosphorylation sites.

3.1 Expression of the Sab splice variant is heterogenous in a population of cells. We selected SF268 cells to determine if the Sab variant is homogenously expressed across an entire population of cells. We developed 11 different SF268 clones by expanding a population of cells that originated from a single cell. The expression of the Sab splice variant was heterogenous among clones, showing different levels of expression of the variant and/or ratios between Sab full-length and Sab variant. From the 11 clones developed, SF286 clone #6 was the only clone that didn't express the variant and therefore was selected for our future comparative studies (Figure 13).

3.2 Sab splice variant localizes to mitochondria. Because the mitochondrial localization signal is located in the N-terminus of Sab, a shorter N-terminus for the splice variant suggests that it lacks the canonical mitochondrial localization signal and the Sab variant will have a distinct cellular localization. To determine the cellular localization of the Sab splice variant we performed co-localization studies between immunofluorescence against Sab and the mitochondrial specific dye Mitotracker Deep Red FM. We did not observe any differences in Sab distribution between SF268 cells that express both Sab full-length and the variant (Figure 14A), and SF268 clone #6 that only expresses Sab full-length (Figure 14B). Our immunofluorescence localization findings were validated by subcellular fractionation and mitochondrial isolation that showed the Sab splice variant only in the mitochondrial fraction and not in the cytosolic fraction (Figure 15).

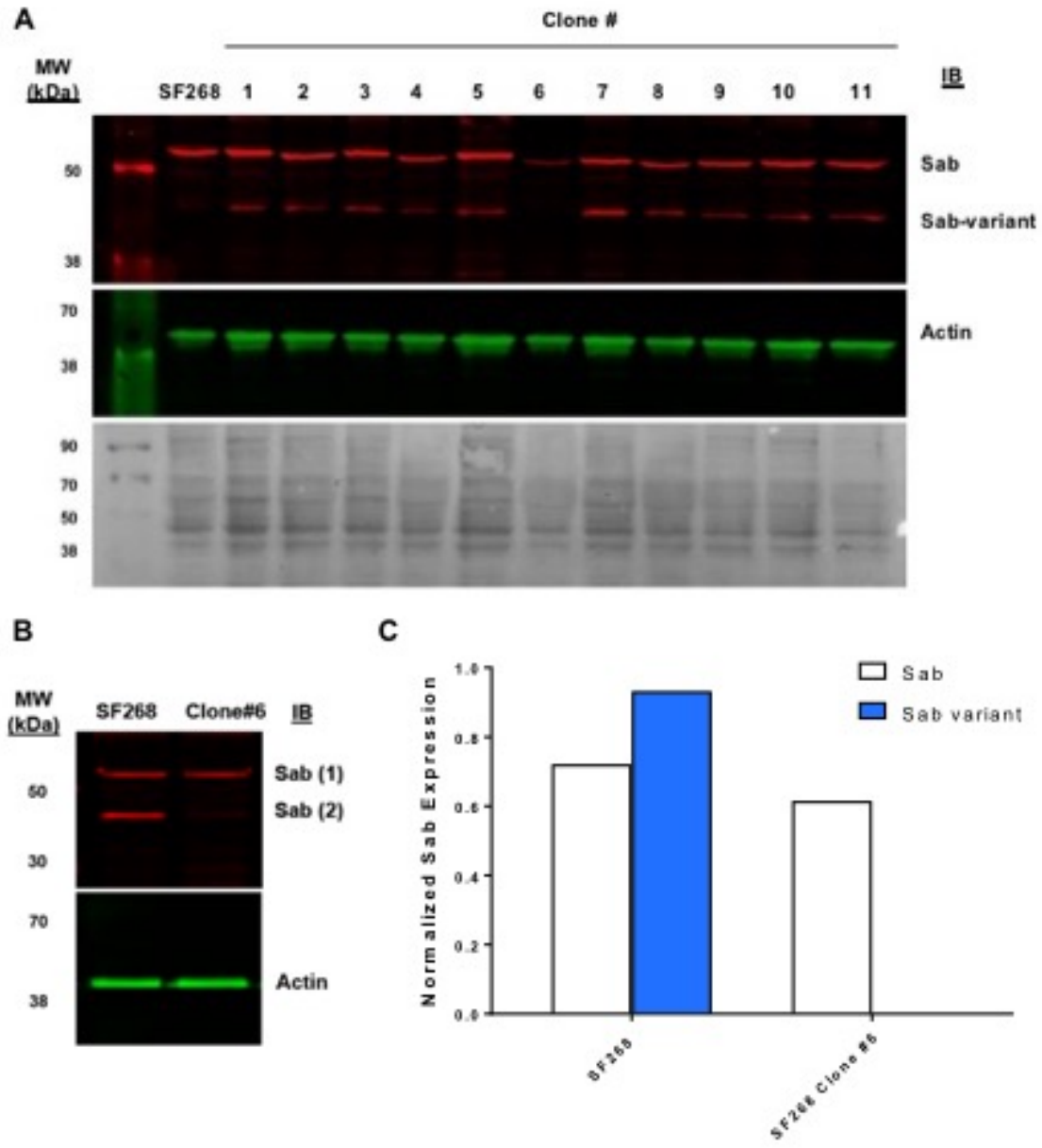

Figure 13. Sab variant expression among a population of SF268 clones. (A) SF268 clones were grown to 85% confluency and lysed. Proteins (25μg) were quantified and resolved by SDS-PAGE. Western blot analysis was used to detect Sab levels. Actin was used as loading control. Sab expression levels were measured using an antibody against the C-terminus (B) and quantified (C)

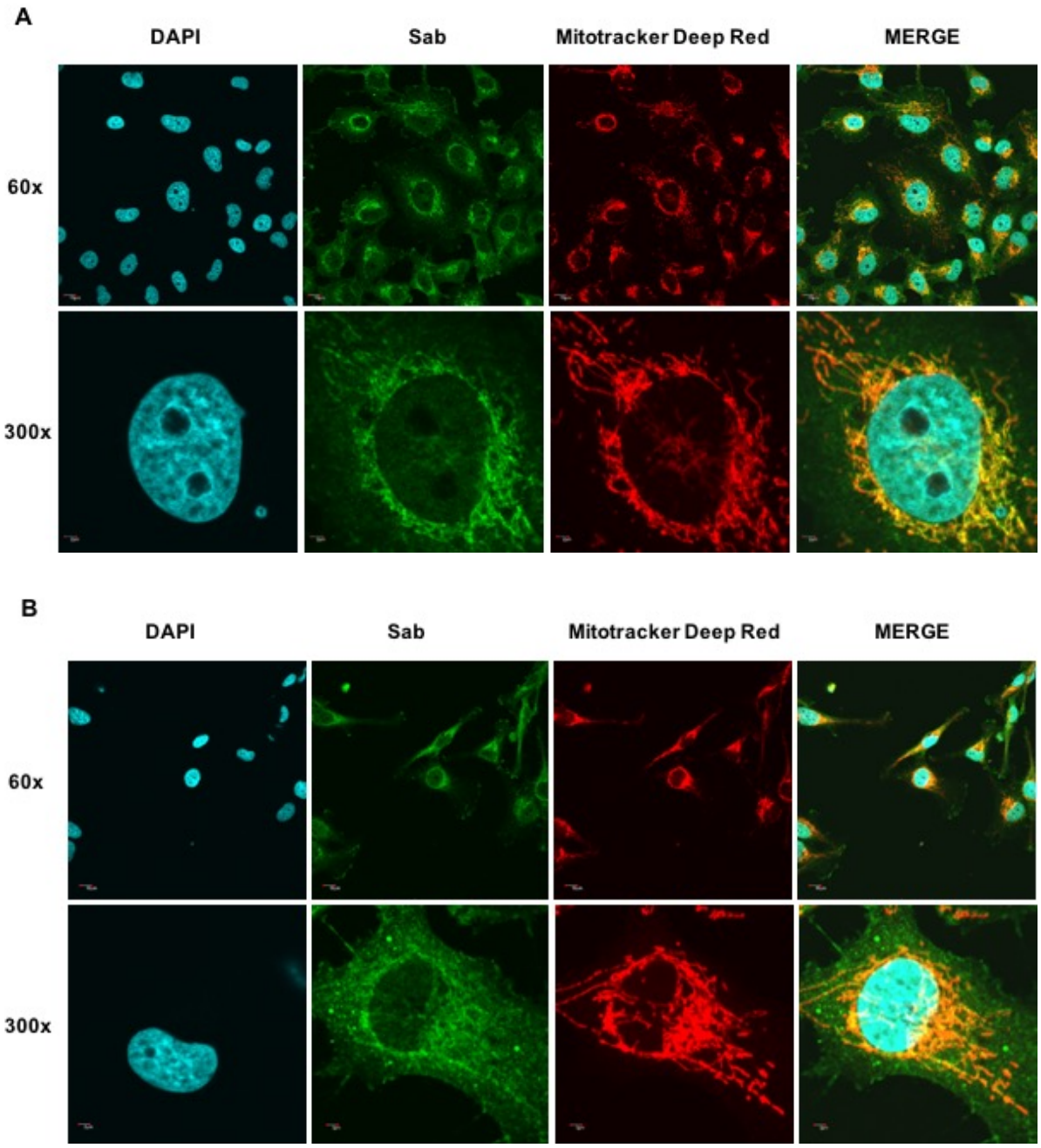

Figure 14. Cellular distribution of Sab in SF268 cells.
Confocal microscopy images were obtain using the GBM cell line SF268 (A) and SF268 clone #6 (B), cells were stained with DAPI (nucleus), Mitrotacker Deep Red FM (mitochondria) and Sab.

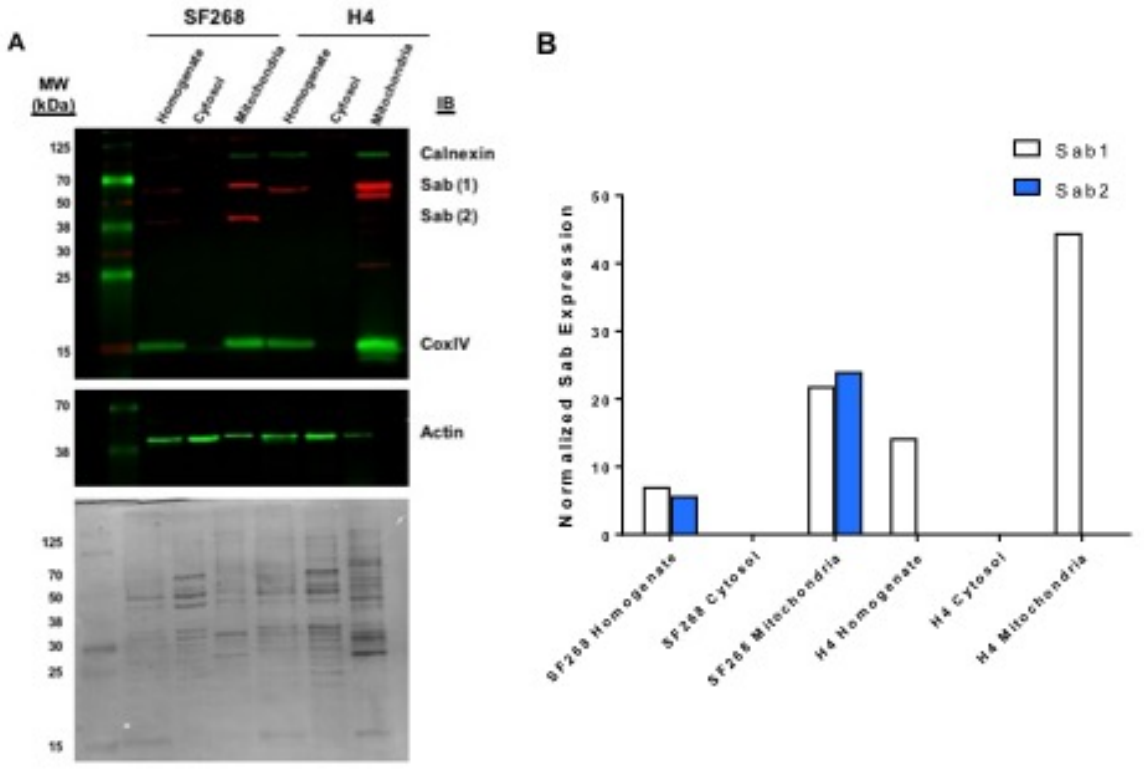

Figure 15. Cellular fractionation and Sab distribution.
Subcellular fractionation was performed from SF268 and H4 cells and analyzed for the presence of Sab. Proteins (25μg) were quantified and resolved by SDS-PAGE. Western blot analysis was used to detect Sab levels. Mitochondrial enrichment was determined by the relative abundance of COX-IV, contamination by other subcellular compartments was determined: cytosol (Actin), ER (Calnexin).

3.4 Sab variant expression reduces oxidative metabolism. To determine if the expression of the Sab variant has an effect on mitochondrial physiology, we measured mitochondrial respiration and glycolysis. We observed a 35% decrease in basal respiration in SF268 cells (Figure 16A), which express the Sab variant, while SF268 clone #6 have 60% more spare respiratory capacity (Figure15B), reduced basal glycolysis (Figure 16C, and increased capacity for pyruvate oxidation (Figure 16E, F). Together these observations suggest that expression of

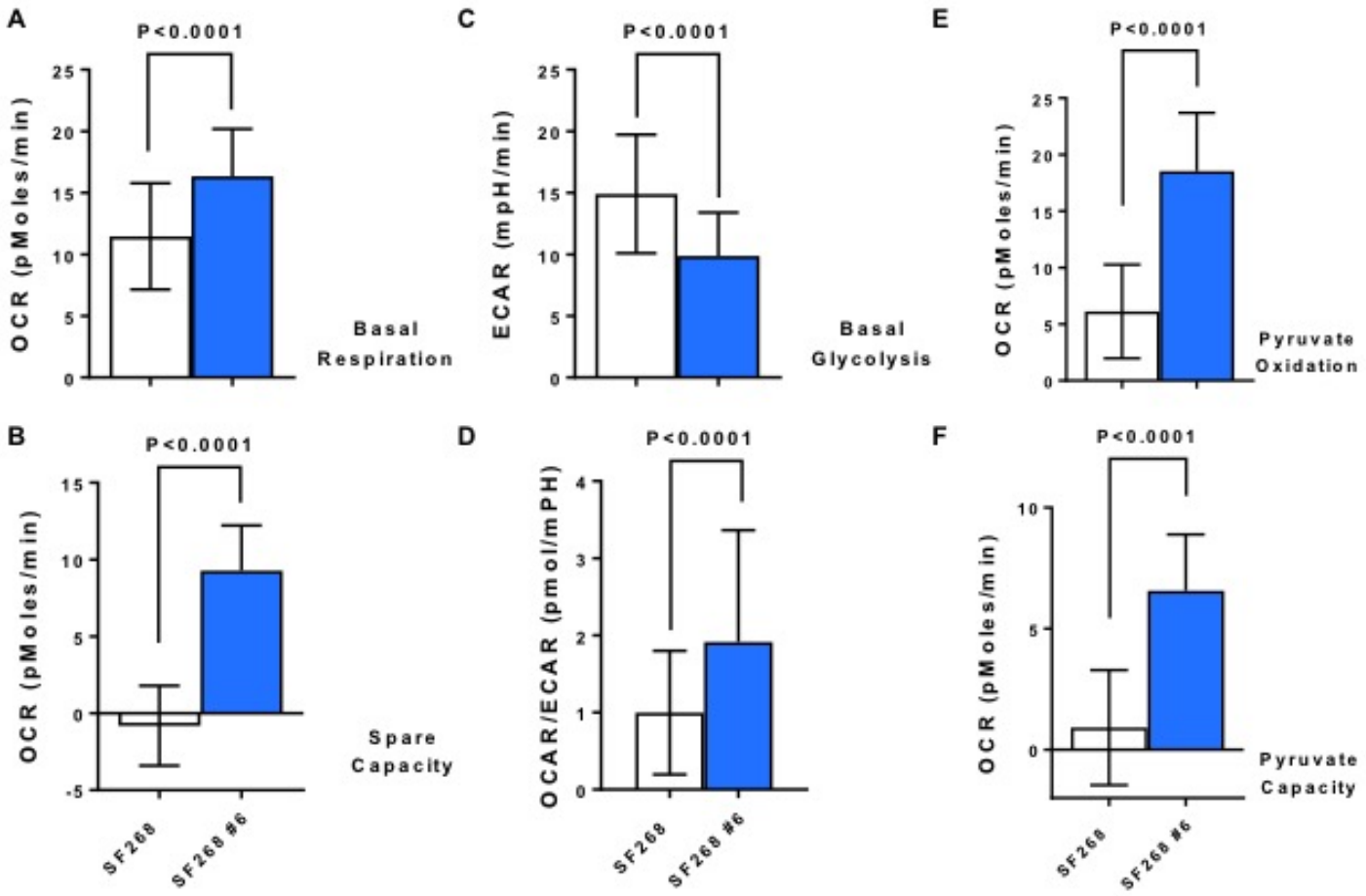

Figure 16. Sab variant expression reduces oxidative metabolism.

The respiratory profile of cells with and without the Sab splice variant was measured using the Seahorse XF-96 extracellular flux analyzer. (A) Basal respiration (B) spare capacity (C) basal glycolysis, (D) OCR/ECAR ratio, (E) Pyruvate oxidation and (F) pyruvate oxidation capacity. Comparisons between groups was performed using the Mann-Whitney test.

the Sab variant affects mitochondrial oxidative metabolism by reducing the cell's respiratory capacity.

3.5 Sab splice variant expression increases cell proliferation. To determine if expression of the Sab splice variant had an effect on cellular physiology, we compared cellular proliferation and viability between cells with and without Sab variant expression. SF268 and SF268 clone # 6 cells were treated with increasing concentrations of FBS (0-10%) for 48 hours. We observed that SF268 cells that expressed the Sab variant had increased cell viability in comparison to SF268 clone #6 cells in a dose dependent manner when treated with increasing concentrations of FBS (Figure 17A). SF268 cells also had increased cellular proliferation, specially at lower serum concentrations, in comparison to SF268 clone #6. At higher serum concentrations there was no significant difference in proliferation rates (Figure 17B).

3.6 Sab variant expression increases chemosensitivity. To determine if Sab variant expression also has an effect on chemoresponse, we measured cell viability in SF268 and SF268 clone #6 cells after treatment with increasing concentrations with either irinotecan or rotenone. We observed a more pronounced decrease in cell viability in SF268 cells (Figure 18), suggesting that the Sab splice variant expression improves chemosensitivity. To determine if decreased viability was due to an increase in apoptosis we measured caspase activity in SF268 and SF268 clone #6 cells treated with either irinotecan (3.5μM) or rotenone (1μM) for 24, 36 and 48 hours, staurosporine (1μM) was used as a positive control. We did not observed differences in response between SF268

cells and SF268 clone #6, irinotecan induced a more robust caspase activation than rotenone and the positive control staurosporine in both cell lines (Figure 18C &17F). These results suggest that changes in drug response and cell viability elicited by the Sab variant are independent of caspase activation.

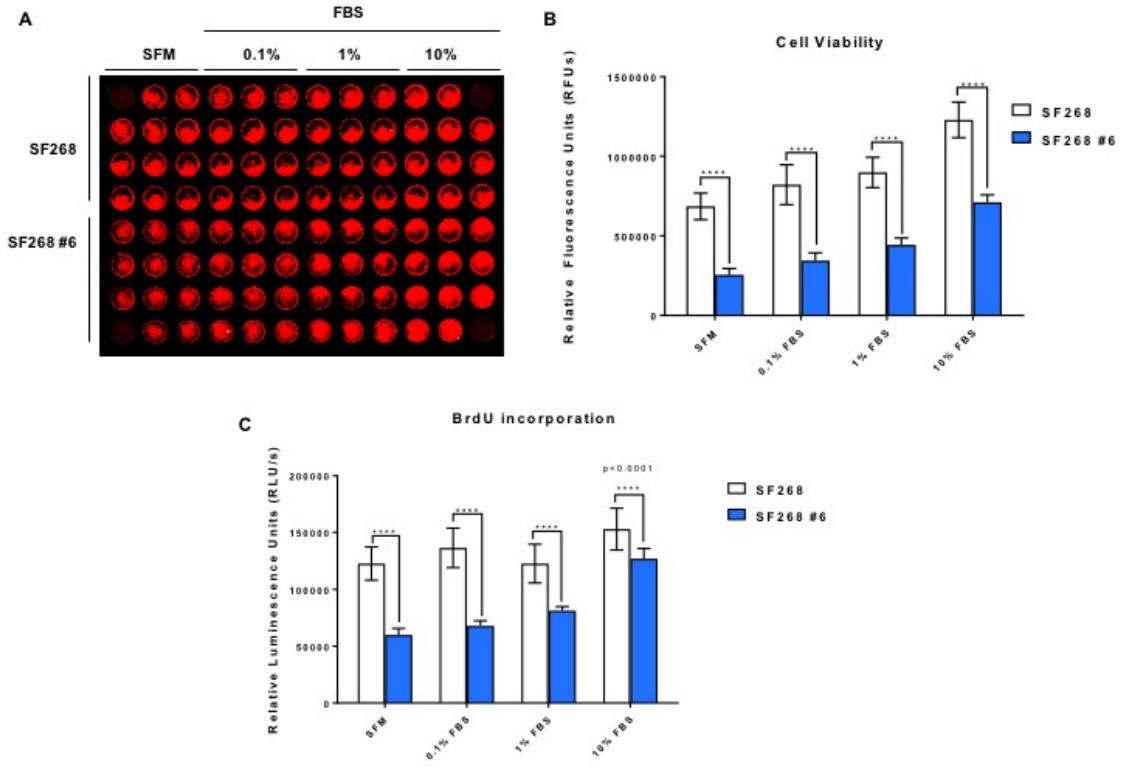

Figure 17. Sab splice variant increases cell viability and proliferation. SF268 and SF268 clone #6 cell lines were incubated for 48 hours with increasing concentrations of FBS (0-10%). (A) The cells were then fixed and stained with CellTag 700 Stain to determine cell viability (B) Fluorescence quantification for each FBS dose. (C) Cell proliferation was measured by BrdU incorporation. Comparisons between groups was performed using the Mann-Whitney test.

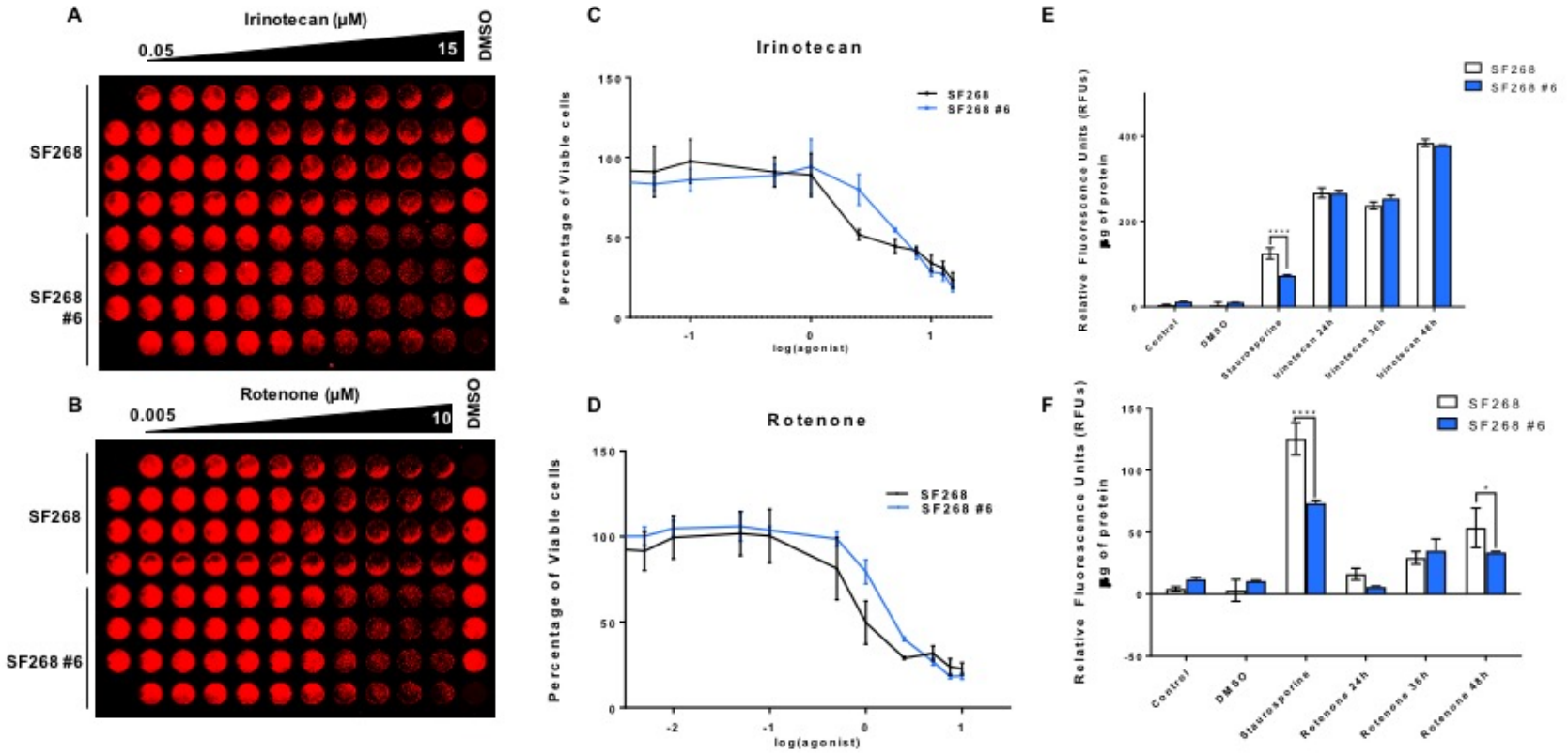

Figure 18. Determining IC_{50} values for Irinotecan and Rotenone in SF268 Cell Lines.

(SF268 and SF268 clone #6 cell lines were incubated for 72 hours in the presence of 0-15μM Irinotecan (A) or 0.005-10μM Rotenone (D). The cells were then fixed and stained with CellTag 700 stain to determine the number of cells. The fluorescence for each of irinotecan (B) or rotenone (E)dose was plotted and the IC_{50} value was calculated using GraphPad® Prism. Induction of apoptosis by 3.5μM Irinotecan (C) or 1μM rotenone (F) was measured by caspase activation, STS was used as a positive control. Comparisons between groups was performed using the Mann-Whitney test.

4. Discussion

The scaffold protein Sab is involved in outer membrane mitochondrial signaling and it plays a role in mitochondrial dysfunction and apoptosis (J. W. Chambers and LoGrasso, 2011; T. P. Chambers et al., 2015). Our current study focused on characterizing a novel Sab splice variant that we recently discover in GBM cell lines. We found that expression of the Sab variant only occurs in some GBM cell lines. In particular, SF268 cells had the highest variant expression levels; however, within a population of these cells expression is heterogenous with some cells expressing both the full-length and the truncated variant, while others only express only full-length Sab. No cells were found to express only the variant. This was an interesting observation that suggests isoform 1 of Sab (full-length) is necessary for cellular function. This is also reflected by our unpublished attempts to make global Sab knockout mice. Mice that are homozygous for the Sab knockout cassette die before day 7 of embryogenesis. These data highlight a yet to be described essential activity for Sab-mediated signaling beyond the induction of apoptosis.

Despite our initial hypothesis that the truncated form may be in the cytosol acting as a JNK inhibitor, we found that the Sab splice variant localizes to mitochondria according to immunolocalization and subcellular fractionation. A closer analysis of the protein sequence reveals that there is a polycationic stretch of lysines and arginines near the N-terminus of the polypeptide that resemble cryptic mitochondrial localization sequences. Consequently, this means that both sab isoforms would have cytosolic KIM2 motifs for JNK (or other MAPK interactions). The transmembrane motif is intact meaning that the KIM1 motif is likely obscured

by the OMM. This means that the variant (isoform 2) still has a functional SH3-motif within the coil-coiled 2 (CC2) domain. However, the CC1 domain is gone. This means that Sab isoform 2 has lost a protein-protein interaction site. With the CC2 motif looking extremely familiar to a dimerization domain (and our preliminary data support that Sab is a dimer) it is probable that CC1 interacts with proteins in the intermembrane space. Perhaps, the protein interacting with CC1 in full-length Sab is an inhibitor of complex I; thus, in Sab isoform 2, the inhibitor is released and would explain the diminished respiration in cells possessing the variant. Previous studies, have shown that stress-induced mitochondrial JNK signaling leads to Sab-mediated inhibition of respiratory complexes, specifically complex I (J. W. Chambers and LoGrasso, 2011). Unlike Sab full length, the truncated N-terminus of the Sab splice variant is missing the first coiled coil motif, as a scaffolding protein Sab interacts with other proteins acting as a signaling hub while providing stability to protein complexes and losing a site for protein-protein interaction likely has profound downstream effects (Strauss and Keller, 2008). Additionally, Win and colleagues showed that when active JNK binds Sab on the outer mitochondrial membrane a conformational change releases the protein phosphatase SHP1 in the inner mitochondrial space, leading to intramitochondrial Src inactivation and electron transport inhibition (Win et al., 2016). We predict this missing coiled coil motif is required for proper regulation of Sab-mediated inner mitochondrial signaling, either because of its interacting partners or due to required conformational changes in Sab structure for proper signal transduction.

The metabolic shift observed in cells expressing the Sab splice variant may confer an advantage that allows cells to show increased proliferation (Figure16). Utilization of glucose for aerobic glycolysis produces a series of precursors for macromolecule synthesis, such as fatty acids, nonessential amino acids and nucleotides (Vander Heiden et al., 2009).

Surprisingly, we also observed that cells expressing the Sab variant are not more susceptible to both genotoxic and mitochondrial stress (Figure 18). Enhanced Sab-mediated signaling has been linked to chemosensitization (T. P. Chambers et al., 2015) However, the lack of difference in caspase activation and the failure to display changes in Bcl-2 proteins may suggest that the OM scaffolding properties of Sab remain intact and mitochondrial JNK signaling on the OMM proceeds as normal.

In summary, we propose that the splice variant of Sab reduces oxidative metabolism by inhibiting complex I activity, promoting a metabolic shift that contributes to increased proliferation.

5. References

Brunelle, J.K., Letai, A., 2009. Control of mitochondrial apoptosis by the Bcl-2 family. Journal of Cell Science 122, 437–441. doi:10.1242/jcs.031682

Chambers, J.W., Cherry, L., Laughlin, J.D., Figuera-Losada, M., LoGrasso, P.V., 2011. Selective inhibition of mitochondrial JNK signaling achieved using peptide mimicry of the Sab kinase interacting motif-1 (KIM1). ACS Chem. Biol. 6, 808–818. doi:10.1021/cb200062a

Chambers, J.W., Howard, S., LoGrasso, P.V., 2013a. Blocking c-Jun N-terminal kinase (JNK) translocation to the mitochondria prevents 6-hydroxydopamine-induced toxicity in vitro and in vivo. J. Biol. Chem. 288, 1079–1087. doi:10.1074/jbc.M112.421354

Chambers, J.W., LoGrasso, P.V., 2011. Mitochondrial c-Jun N-terminal kinase (JNK) signaling initiates physiological changes resulting in amplification of reactive oxygen species generation. J. Biol. Chem. 286, 16052–16062. doi:10.1074/jbc.M111.223602

Chambers, J.W., Pachori, A., Howard, S., Iqbal, S., LoGrasso, P.V., 2013b. Inhibition of JNK mitochondrial localization and signaling is protective against ischemia/reperfusion injury in rats. J. Biol. Chem. 288, 4000–4011. doi:10.1074/jbc.M112.406777

Chambers, T.P., Portalatin, G.M., Paudel, I., Robbins, C.J., Chambers, J.W., 2015. Sub-chronic administration of LY294002 sensitizes cervical cancer cells to chemotherapy by enhancing mitochondrial JNK signaling. Biochemical and Biophysical Research Communications 463, 538–544. doi:10.1016/j.bbrc.2015.05.075

Chipuk, J.E., Fisher, J.C., Dillon, C.P., Kriwacki, R.W., Kuwana, T., Green, D.R., 2008. Mechanism of apoptosis induction by inhibition of the anti-apoptotic BCL-2 proteins. Proc. Natl. Acad. Sci. U.S.A. 105, 20327–20332. doi:10.1073/pnas.0808036105

Hanawa, N., Shinohara, M., Saberi, B., Gaarde, W.A., Han, D., Kaplowitz, N., 2008. Role of JNK translocation to mitochondria leading to inhibition of mitochondria bioenergetics in acetaminophen-induced liver injury. Journal of Biological Chemistry 283, 13565–13577. doi:10.1074/jbc.M708916200

Huang, S.-T.J., Cidlowski, J.A., 2002. Phosphorylation status modulates Bcl-2 function during glucocorticoid-induced apoptosis in T lymphocytes. FASEB J. 16, 825–832. doi:10.1096/fj.01-0852com

Kharbanda, S., Saxena, S., Yoshida, K., Pandey, P., Kaneki, M., Wang, Q., Cheng, K., Chen, Y.N., Campbell, A., Sudha, T., Yuan, Z.M., Narula, J., Weichselbaum, R., Nalin, C., Kufe, D., 2000. Translocation of SAPK/JNK to mitochondria and interaction with Bcl-x(L) in response to DNA damage. Journal of Biological Chemistry 275, 322–327.

Lei, K., Davis, R.J., 2003. JNK phosphorylation of Bim-related members of the Bcl2 family induces Bax-dependent apoptosis. Proc Natl Acad Sci USA 100, 2432–2437. doi:10.1073/pnas.0438011100

Ma, C., Ying, C., Yuan, Z., Song, B., Li, D., Liu, Y., Lai, B., Li, W., Chen, R., Ching, Y.-P., Li, M., 2007. dp5/HRK is a c-Jun target gene and required for apoptosis induced by potassium deprivation in cerebellar granule neurons. Journal of Biological Chemistry 282, 30901–30909. doi:10.1074/jbc.M608694200

Magalhães, P.J., Andreu, A.L., Schon, E.A., 1998. Evidence for the presence of 5S rRNA in mammalian mitochondria. Mol. Biol. Cell 9, 2375–2382.

Morel, C., Carlson, S.M., White, F.M., Davis, R.J., 2009. Mcl-1 integrates the opposing actions of signaling pathways that mediate survival and apoptosis. Molecular and Cellular Biology 29, 3845–3852. doi:10.1128/MCB.00279-09

Ota, T., Suzuki, Y., Nishikawa, T., Otsuki, T., Sugiyama, T., Irie, R., Wakamatsu, A., Hayashi, K., Sato, H., Nagai, K., Kimura, K., Makita, H., Sekine, M., Obayashi, M., Nishi, T., Shibahara, T., Tanaka, T., Ishii, S., Yamamoto, J.-I., Saito, K., Kawai, Y., Isono, Y., Nakamura, Y., Nagahari, K., Murakami, K., Yasuda, T., Iwayanagi, T., Wagatsuma, M., Shiratori, A., Sudo, H., Hosoiri, T., Kaku, Y., Kodaira, H., Kondo, H., Sugawara, M., Takahashi, M., Kanda, K., Yokoi, T., Furuya, T., Kikkawa, E., Omura, Y., Abe, K., Kamihara, K., Katsuta, N., Sato, K., Tanikawa, M., Yamazaki, M., Ninomiya, K., Ishibashi, T., Yamashita, H., Murakawa, K., Fujimori, K., Tanai, H., Kimata, M., Watanabe, M., Hiraoka, S., Chiba, Y., Ishida, S., Ono, Y., Takiguchi, S., Watanabe, S., Yosida, M., Hotuta, T., Kusano, J., Kanehori, K., Takahashi-Fujii, A., Hara, H., Tanase, T.-O., Nomura, Y., Togiya, S., Komai, F., Hara, R., Takeuchi, K., Arita, M., Imose, N., Musashino, K., Yuuki, H., Oshima, A., Sasaki, N., Aotsuka, S., Yoshikawa, Y., Matsunawa, H., Ichihara, T., Shiohata, N., Sano, S., Moriya, S., Momiyama, H., Satoh, N., Takami, S., Terashima, Y., Suzuki, O., Nakagawa, S., Senoh, A., Mizoguchi, H., Goto, Y., Shimizu, F., Wakebe, H., Hishigaki, H., Watanabe, T., Sugiyama, A., Takemoto, M., Kawakami, B., Yamazaki, M., Watanabe, K., Kumagai, A., Itakura, S., Fukuzumi, Y., Fujimori, Y., Komiyama, M., Tashiro, H., Tanigami, A., Fujiwara, T., Ono, T., Yamada, K., Fujii, Y., Ozaki, K., Hirao, M., Ohmori, Y., Kawabata, A., Hikiji, T., Kobatake, N., Inagaki, H., Ikema, Y., Okamoto, S., Okitani, R., Kawakami, T., Noguchi, S., Itoh, T., Shigeta, K., Senba, T., Matsumura, K., Nakajima, Y., Mizuno, T., Morinaga, M., Sasaki, M., Togashi,

T., Oyama, M., Hata, H., Watanabe, M., Komatsu, T., Mizushima-Sugano, J., Satoh, T., Shirai, Y., Takahashi, Y., Nakagawa, K., Okumura, K., Nagase, T., Nomura, N., Kikuchi, H., Masuho, Y., Yamashita, R., Nakai, K., Yada, T., Nakamura, Y., Ohara, O., Isogai, T., Sugano, S., 2004. Complete sequencing and characterization of 21,243 full-length human cDNAs. Nat Genet 36, 40–45. doi:10.1038/ng1285

Schroeter, H., Boyd, C.S., Ahmed, R., Spencer, J.P.E., Duncan, R.F., Rice-Evans, C., Cadenas, E., 2003. c-Jun N-terminal kinase (JNK)-mediated modulation of brain mitochondria function: new target proteins for JNK signalling in mitochondrion-dependent apoptosis. Biochem. J. 372, 359–369. doi:10.1042/BJ20030201

Strauss, H.M., Keller, S., 2008. Pharmacological interference with protein-protein interactions mediated by coiled-coil motifs. Handb Exp Pharmacol 186, 461–482. doi:10.1007/978-3-540-72843-6_19

Thomas, L.W., Lam, C., Edwards, S.W., 2010. Mcl-1; the molecular regulation of protein function. FEBS Letters 584, 2981–2989. doi:10.1016/j.febslet.2010.05.061

Vander Heiden, M.G., Cantley, L.C., Thompson, C.B., 2009. Understanding the Warburg Effect: The Metabolic Requirements of Cell Proliferation. Science 324, 1029–1033. doi:10.1126/science.1160809

Wang, X.-T., Pei, D.-S., Xu, J., Guan, Q.-H., Sun, Y.-F., Liu, X.-M., Zhang, G.-Y., 2007. Opposing effects of Bad phosphorylation at two distinct sites by Akt1 and JNK1/2 on ischemic brain injury. Cell. Signal. 19, 1844–1856. doi:10.1016/j.cellsig.2007.04.005

Wiltshire, C., Gillespie, D.A.F., May, G.H.W., 2004. Sab (SH3BP5), a novel mitochondria-localized JNK-interacting protein. Biochem. Soc. Trans. 32, 1075–1077. doi:10.1042/BST0321075

Wiltshire, C., Matsushita, M., Tsukada, S., Gillespie, D.A.F., May, G.H.W., 2002. A new c-Jun N-terminal kinase (JNK)-interacting protein, Sab (SH3BP5), associates with mitochondria. Biochem. J. 367, 577–585. doi:10.1042/BJ20020553

Win, S., Than, T.A., Han, D., Petrovic, L.M., Kaplowitz, N., 2011. c-Jun N-terminal kinase (JNK)-dependent acute liver injury from acetaminophen or tumor necrosis factor (TNF) requires mitochondrial Sab protein expression in mice. J. Biol. Chem. 286, 35071–35078. doi:10.1074/jbc.M111.276089

Win, S., Than, T.A., Min, R.W.M., Aghajan, M., Kaplowitz, N., 2016. c-Jun N-terminal kinase mediates mouse liver injury through a novel Sab (SH3BP5)-

dependent pathway leading to inactivation of intramitochondrial Src. Hepatology 63, 1987–2003. doi:10.1002/hep.28486

Wu, M., Neilson, A., Swift, A.L., Moran, R., Tamagnine, J., Parslow, D., Armistead, S., Lemire, K., Orrell, J., Teich, J., Chomicz, S., Ferrick, D.A., 2007. Multiparameter metabolic analysis reveals a close link between attenuated mitochondrial bioenergetic function and enhanced glycolysis dependency in human tumor cells. AJP: Cell Physiology 292, C125–36. doi:10.1152/ajpcell.00247.2006

Yamamoto, K., Ichijo, H., Korsmeyer, S.J., 1999. BCL-2 Is Phosphorylated and Inactivated by an ASK1/Jun N-Terminal Protein Kinase Pathway Normally Activated at G 2/M. Molecular and Cellular Biology 19, 8469–8478. doi:10.1128/MCB.19.12.8469

Yang, J., Liu, X., Bhalla, K., Kim, C.N., Ibrado, A.M., Cai, J., Peng, T.I., Jones, D.P., Wang, X., 1997. Prevention of apoptosis by Bcl-2: release of cytochrome c from mitochondria blocked. Science 275, 1129–1132.

Yu, C., Minemoto, Y., Zhang, J., Liu, J., Tang, F., Bui, T.N., Xiang, J., Lin, A., 2004. JNK suppresses apoptosis via phosphorylation of the proapoptotic Bcl-2 family protein BAD. Molecular Cell 13, 329–340.

CHAPTER V

Sab-Mediated Signaling Influences Metabolism and Chemosusceptibility in Human Neuroblastoma Cells.

1. Introduction

Neuroblastoma is a prevalent pediatric cancer accounting for approximately 15% of cancer-related deaths in children (Maris, 2010). Late stage neuroblastomas are resistant to conventional treatments, including chemotherapy (Matthay et al., 2009; Porro et al., 2010; Teitz et al., 2000). New therapeutic options targeting the unique aspects of neuroblastomas are needed to treat late-stage malignancies and improve patient survival.

Neuroblastoma cells undergo specific changes in metabolism to support growth and develop resistance to apoptosis during oncogenesis. Metabolically, cells shift their bioenergetic and biosynthetic processes to sustain proliferation and survival (Vander Heiden et al., 2009). While cancer cells increase glucose utilization for biosynthesis and ATP generation, tumor cells rely on mitochondrial reactions to replenish the tricarboxylic acid (TCA) cycle and maintain reducing equivalents (DeBerardinis et al., 2007). Glutamine utilization can replenish TCA cycle intermediates and maintain mitochondrial integrity, redox homeostasis, and macromolecular biosynthesis (Qing et al., 2012). Consequently, the unique metabolism of tumor cells can be a predictive index for chemosensitivity and the proteins responsible for metabolic changes may be useful neuroblastoma drug targets (Ren et al., 2015; Sandulache et al., 2011; L. Yang et al., 2014).

The attenuation of apoptosis is a hallmark of cancers, including neuroblastomas (Hanahan and Weinberg, 2011). Circumventing the pathways for apoptosis involves manipulation of Bcl-2 protein function. Apoptotic evasion is associated with increasing pro-survival Bcl-2 proteins (Bcl-2, Mcl-1, and Bcl-xL), while

abundant BH3-only proteins (Bim, Bid, Puma, Noxa, etc.) indicate pro-apoptotic mitochondria susceptible to treatments (Brunelle and Letai, 2009; Certo et al., 2006; Chonghaile et al., 2011; Letai et al., 2002). In neuroblastoma, BH3-only protein levels can be used to predict chemotherapeutic responses and resistance (Goldsmith et al., 2012; 2010). The levels of Bcl-2 proteins and chemo-responsiveness has been well evaluated recently; however, the molecular mechanisms responsible for controlling Bcl-2 proteins abundance on mitochondria in neuroblastoma has yet to be fully delineated.

The c-Jun N-terminal kinase (JNK) can induce apoptotic signaling. JNK signaling has been linked to induction of apoptosis and chemosensitization in neuroblastoma cells (Cheng et al., 2014; Fey et al., 2015; Filomeni et al., 2003; Waetzig et al., 2009). Previous research has demonstrated that mitochondrial JNK is required to induce cell death responses (J. W. Chambers et al., 2011a; 2013a; J. W. Chambers and LoGrasso, 2011; J. W. Chambers et al., 2013b; Nijboer et al., 2013; Win et al., 2014). Silencing Sab, an outer mitochondrial scaffold protein, or selectively inhibiting the interaction between JNK and Sab prevents JNK translocation to mitochondria and decreases mitochondrial dysfunction (J. W. Chambers et al., 2011a). Furthermore, blocking mitochondrial JNK translocation impairs Bcl-2 emigration from mitochondria preventing apoptosis (Matthay et al., 2009). Preventing mitochondrial JNK signaling is a useful means to block induction of apoptosis in neuroblastoma cells (J. W. Chambers et al., 2013a; 2011b; Kristiansen et al., 2010; Nijboer et al., 2013; Zhou et al., 2008). These studies

demonstrate the influence of mitochondrial JNK signaling on apoptosis in neuroblastoma.

In this study, we examined the impact of Sab-mediated signaling on mitochondrial function and apoptosis in human neuroblastoma cells. We found that Sab expression was significantly diminished in neuroblastoma patients. Inhibiting Sab-mediated signaling decreased proliferation, reduced glycolysis, and increased oxidative metabolism; meanwhile, over-expression of Sab resulted in decreased pyruvate dehydrogenase and complex I activities. Sab-inhibited neuroblastoma cells had more Bcl-2 proteins and less BH3-only proteins. Cells treated with an inhibitory Sab peptide were less sensitive to chemotherapy agents. Finally, Sab levels correspond to metabolic phenotype and chemo-sensitivity in a small panel of neuroblastoma cells. Thus, Sab levels may be a useful prognostic biomarker for neuroblastoma.

2. Materials and Methods

Gene Expression: The expression of Sab (SH3-binding protein 5; SH3BP5) was examined using the Oncomine database (http://www.oncomine.org) in October 2017 (Rhodes et al., 2007). By querying four neuroblastoma datasets that included Sab as part of past studies (Albino et al., 2008; Asgharzadeh et al., 2006; Janoueix-Lerosey et al., 2008; Wang et al., 2006), we compared experimental data for normal tissue, ganglioneuromas, and neuroblastomas. The data were compiled from a total of 8 normal tissue samples and 286 neuroblastoma samples (Table 6).

Table 6: Summary of Neuroblastoma Expression Studies and Observed Changes in Sab Expression.
*The mean fold changes were generated by averaging the fold changes from the studies.

STUDY	TOTAL SAMPLES	CANCER SAMPLES	NORMAL SAMPLES	NORMAL TISSUE	GENES ANALYZED	HUMAN GENOME ARRAY(S)	LOG_2 FOLD CHANGE	AVG. FOLD CHANGE	P	REFERENCE
ALBINO	19	15	4	Ganglioneuroma	12,624	U113A	-0.804	-1.75	0.002	Albino, D. Cancer. (2008)
ASGHARZADEH	117	117	0	None	12,624	U133A	N/A	N/A	N/A	Asgharzadeh, S. J. Natl. Cancer Inst. (2006)
JANOUEIX-LEROSEY	56	53	3	Ganglioneuroma	19,574	U133 Plus 2.0	-1.22	-1.815	2.59 E-5	Janoueix-Lerosey I. Nature. (2008)
WANG	102	101	1	Fetal Brain	8,603	U95A-Av2	-2.20	-2.437	0.001	Wang, Q. Cancer Res. (2006)
TOTALS/ MEANS	**294**	**286**	**8**				**-1.408**	**-2.001**		

Materials: CHP-212 (CRL-2273), IMR-32 (CCL-127), SK-N-SH (HTB-11), and SH-SY5Y cells (CRL-2266) were purchased from American Type Culture Collection. General reagents were purchased from Fisher Scientific and Sigma Aldrich.

Cell Culture and Treatment with Peptides: Human SH-SY5Y neuroblastoma cells were cultured as described in previously (Biedler et al., 1978). CHP-212, IMR-32, and SK-N-SH lines, cells were grown in DMEM with 10% FBS, 100U/mL penicillin, 100μg/mL streptomycin, and 5μg/mL plasmocin. To inhibit Sab-mediated signaling, cells were treated with either the Tat-Sab_{KIM1} peptide or the Tat-Scrambled peptide as described below and in our prior studies (J. W. Chambers et al., 2013b; 2013a; 2011a).

Cell Proliferation: We employed two assays to measure cellular abundance: 5-bromo-2'-deoxyuridine (BrdU) and 3-(4,5-dimethylthiazol-2-yl)-2,5-diphenyltetrazolium bromide (MTT) cell proliferation assays. First, we used the BrdU Cell Proliferation assay kit (Cell Signaling Technologies). Neuroblastoma cells were plated at a density of 0.8 $x10^4$ cells per well and treated as indicated below. Cell growth was monitored using the manufacturer's protocol over the course of five days. Absorbance was read at 450nm. Similarly, we employed the MTT Proliferation Assay (Cayman Chemical). Neuroblastoma cells were plated as described for the BrdU assay, and the cells were cultured for up to five days. The assay was performed following the manufacturer's instructions. The absorbance was measured at 590nm. The number of cells was calculated based on a standard curve of known cell numbers and averaged between the two assays.

Caspase Activity: To assess caspase 3/7 activity in neuroblastoma cell lines, cells were grown on clear 96-well plates. The plate was centrifuged (400xg) for five minutes, and the supernatant was removed. The cells washed in 150μL of PBS and centrifuged (400xg for 5 minutes). Next, 100μL of PBS supplemented with 1% TritonX-100 was added to lyse the cells. Following a 30-minute incubation on a room temperature orbital shaker, the plate was centrifuged at 800xg for 10 minutes, and 90μL of the lysate was transferred to a black 96-well plate. Then, 10μL of PBS or 10μL of a caspase inhibitor (Ac-DEVD-CHO; 10μM) was added to the well, and 100μL of caspase substrate Ac-DEVD-AMC (100μM) in PBS supplemented with 20mM DTT was added last. The assay incubated at 37^{o}C for 30 minutes, and fluorescence was measured (excitation: 488nm; emission: 535nm).

Metabolic Analysis: Cellular metabolism was assessed by measuring the extracellular acidification rate (ECAR) and the oxygen consumption rate (OCR) of neuroblastoma cells using the Seahorse Biosciences XF-96 extracellular flux analyzer (Wu et al., 2007). Cells were assayed ($1.5x10^4$ cells/well) using the glycolytic and mitochondrial stress kits. For our studies, 1.0μM oligomycin, 100μM 2-DOG, 50μM 5-thioglucose (5-tGlc), and 1μM FCCP were used. From these measurements, we derived glycolytic and respiratory parameters, including spare respiratory capacity as previously described (Wu et al., 2007). Data were normalized to cell number.

Mitochondrial Isolation: A modified protocol as described in (Magalhães et al., 1998; J. Yang et al., 1997) was used to obtain mitochondria as described in our previous studies (J. W. Chambers et al., 2013b; 2013a; 2011a). Mitochondrial samples with greater than 80% purity were used for experiments.

Lactate Measurements: Lactate concentrations were measured in cell culture media using a Lactate Assay Kit (MAK064, Sigma-Aldrich). Samples (10μL) were added to a black-walled clear-bottom 96-well plate and combined with reagents according to manufacturer's instructions. After a 30-minute incubation, the fluorescence was measured (excitation: 535nm; emission: 585nm). Lactate concentrations were determined using a standard curve.

Glucose Uptake: To monitor glucose uptake, we utilized the IRDye® 800CW 2-deoxy-D-glucose (2-DOG) probe from Li-Cor Biosciences (926-08946). Cells were plated in a black-walled, clear bottom 96-well plate. Next, the 800CW 2-DOG probe was added to the culture media to a final concentration of 20μM. After two hours, the media was removed, and the cells were placed in warm Hanks Buffered Saline solution (HBSS). The plate was imaged on a Li-Cor Odyssey CLx Imager and data were analyzed using the ImageStudio software package (Li-Cor).

Enzyme Assays: To verify the metabolic changes, biochemical assays were employed to assess pyruvate dehydrogenase complex and respiratory chain complexes. For pyruvate dehydrogenase (PDH) complex, the PDH activity assay kit was purchased from Sigma-Aldrich and conducted following manufacturer's instructions. Mitochondria [50μg (protein)] were used. Absorbance was measured at 450nm. Enzyme activity was quantified using a standard curve using

recombinant, active PDH and normalized to protein levels. For respiratory chain assays, we used colorimetric analyses for activity in 100μg of mitochondria isolates and normalized the data to mitochondrial protein concentrations. Specifically, Complex I (NADH dehydrogenase) activity was analyzed with the MitoTox™ Complex I OXPHOS Activity Assay kit (Abcam) according to the vendor's instructions.

Cellular Lysis and Western Blot Analysis: Cell lysis and western blotting were performed as previously described (J. W. Chambers et al., 2013a; 2011b). Primary antibodies for our studies were Sab (Novus Biologicals, H00009467-M01), β-actin (Cell Signaling Technology (CST), 4970), α-tubulin (CST 2144), hexokinase-1 (CST #2024), hexokinase-2 (CST #2867), lactate dehydrogenase (CST #3582), pyruvate kinase (CST #3190), pyruvate kinase M2 (CST #4053), pyruvate dehydrogenase (CST #3205), GLUT-1 (CST #12939), GLUT4 (CST #2213), Bcl-2 (CST #2870), Bcl-xL (CST #2764), Mcl-1 (CST #5453), Bim (CST #2933), Bid (CST, #2002), PUMA (CST, #12450), COX-IV (CST, #4850), Pyruvate dehydrogenase E1α-subunit (Abcam, ab110334), MCT-1 (Santa Cruz, sc50324), and MCT-4 (Santa Cruz, sc50329) and secondary antibodies used were IRDye 680RD Goat anti-Rabbit (926-32211) and IRDye 800CW Goat anti-Mouse (926-68070) from Li-Cor. Western blots were developed using the Odyssey CLx (Li-Cor) and quantified using the Image Studio software (Li-Cor).

Chemosensitivity: The IC_{50}s for carboplatin, cyclophosphamide, doxorubicin, etoposide, and vincristine in neuroblastoma cells were determined using the TO-PRO-3 near-infrared dye (Invitrogen) as described in our previous studies (T. P.

Chambers et al., 2015). General cytotoxicity measurements were performed at 2x the IC_{50}s for SH-SY5Y cells for carboplatin and vincristine.

Overexpression of Sab: To increase Sab levels in neuroblastoma cells, we transiently transfected SH-SY5Y with plasmids designed to express Sab (pLOC:Sab) or red fluorescent protein (RFP; pLOC:RFP) (T. P. Chambers et al., 2015; 2017). Plasmid DNA and FugeneHD (Promega) were combined in Optimem (Invitrogen) at a ratio of 1:9 and incubated for 15 minutes at RT before addition to culture. Eight hours after the addition of the transfection complex to media, the media was exchanged. Protein levels were assessed by western blot analysis at 72 hours post-transfection, and only cells that demonstrated a greater than four-fold increase in Sab expression were used.

Mitochondrial ROS Production: To determine if ROS generation was increased in mitochondria, we assessed ROS levels using MitoSOX Red (Invitrogen). We used the approach described in our previous studies (J. W. Chambers et al., 2013a; 2011a; J. W. Chambers and LoGrasso, 2011).

Statistical Analysis and Replicates: Biochemical and other cellular measures were done with a minimum of six experimental replicates. Mitochondrial and protein analysis experiments were performed on a minimum of three biological replicates. To determine statistical significance, Mann-Whitney analysis was employed for significance between treatments. Statistical significance is indicated by an asterisk in figures in which the p-value is less than 0.05. Data are displayed as means with error bars representing plus and minus one standard deviation.

3. Results

3.1 Sab expression is decreased in neuroblastoma tumors. We found four neuroblastoma patient datasets in the Oncomine repository (Rhodes et al., 2007) that evaluated Sab expression (summarized in Table 6). Across 286 neuroblastoma clinical samples, we found that Sab was decreased in all the studies an average of 2-fold in neuroblastoma patients compared to normal tissue and ganglioneuroma controls. However, other pro-apoptotic JNK signaling genes were not altered consistently among the studies (data not shown). Further analysis revealed that Sab expression was decreased in recurrent neuroblastoma (-1.33-fold), increased in tumors with Schwann cell rich stromata (1.62-fold), and Sab expression did not change between neuroblastoma stages. These observations suggest that altered Sab expression may impact neuroblastoma physiology.

3.2 Inhibition of Sab-mediated signaling slows proliferation. JNK signaling on Sab can be inhibited using a peptide (Tat-Sab_{KIM1}) in human SH-SY5Y neuroblastoma cells (J. W. Chambers et al., 2013a). To discern if neuroblastoma cells were affected by diminished Sab-mediated events, we measured cellular proliferation in the presence and absence of the Tat-Sab_{KIM1} inhibitor. SH-SY5Y cells were treated with increasing concentrations of the Tat-Sab_{KIM1} peptide (0-25μM) or scrambled control (Tat-Scramble) for five days. SH-SY5Y cells treated with the Tat-Sab_{KIM1} had diminished proliferation in a dose-dependent manner; wherein, 25μM Tat-Sab_{KIM1} slowed proliferation by nearly 40% (Figure 19A). To determine if decreased proliferation was due to an acute or sustained effect, we measured cell proliferation daily over five days. SH-SY5Y cells treated with Tat-

Sab_{KIM1} peptide had reduced proliferation from the initial dosing of the peptide, and this sustained inhibition was increased dose-dependently (Figure 19B). To assess whether the decrease in proliferation was due to less cell growth rather than increased apoptosis, we measured caspase activity in SHSY5Y cells treated with increasing doses of Tat-Sab_{KIM1}. As compared to the positive control [1μM staurosporine (STS)], Tat-Sab_{KIM1} treatment did not significantly increase caspase activity (Figure 19C). Thus, decreased Sab-mediated signaling slows proliferation of SH-SY5Y cells.

3.3 Impaired Sab-mediated signaling decreases the glycolytic rate. Because proliferation is integrated with cancer metabolism, specifically glycolysis, we examined the impact of diminished Sab-mediated signaling in neuroblastoma cell metabolism. We first assessed the glycolytic rate and found that SH-SY5Y cells treated with 5μM Tat-Sab_{KIM1} for 24 hours had decreased glycolysis (Figure 19D). Specifically, we noticed a decrease in the basal glycolytic rate and the glycolytic capacity (Figure 19D & 18E). To verify the decreased extracellular acidification was due to less lactate production, we measured lactate content in the supernatant of SH-SY5Y cells treated with either 5μM Tat-Scramble or $TatSab_{KIM1}$ for 24 hours. There was a reduction (~25%) in extracellular lactate levels from SH-SY5Y cells treated with 5μM Tat-Sab_{KIM1} (Figure 19F). To address if the change in glycolysis was due to altered glucose import into SH-SY5Y cells, we performed a glucose transport assay (Figure 19G, top panel). We found that treatment with increasing concentrations of the Tat-Sab_{KIM1} peptide impaired glucose import in a dose-dependent manner; however, only a modest change was noted at 5μM Tat-Sab_{KIM1}

(Figure 19G). To determine if the changes in glucose metabolism stemmed from reduced gene expression, we measured the levels of glycolytic proteins following 24 hours of treatment 5μM $TatSab_{KIM1}$ (Figure 19H). We didn't find any discernable change in protein levels among those surveyed. Consequently, Sab-mediated signaling may affect glycolysis by post-translational mechanisms.

3.4 Targeting Sab-mediated signaling relieves PDH inhibition. Pyruvate dehydrogenase (PDH) complex is an important nexus between aerobic glycolysis and oxidative metabolism; recently, the JNK has been shown to phosphorylate the PDH E1α subunit and impair enzymatic activity (Zhou et al., 2008; 2009). To determine if PDH E1α phosphorylation and catalytic activity are altered by diminished Sab levels, we examined the phosphorylation of PDH E1α in the presence and absence of the $Tat\text{-}Sab_{KIM1}$. Following 24 hours of treatment with $TatSab_{KIM1}$, western blotting for PDH E1α revealed two bands in control cells, which the slower migrating form represents phosphorylated E1α subunit (Figure 20A). SH-SY5Y mitochondria from cells treated with 5μM $Tat\text{-}Sab_{KIM1}$ for 24 hours had less phosphorylated PDH E1α (Figure 20A), which when quantified was nearly a 50% decrease (Figure 20B). To assess if the change in phosphorylation status impacted catalysis, we measured PDH activity with increasing concentrations of $Tat\text{-}Sab_{KIM1}$. Inhibition of Sab-mediated signaling enhanced PDH activity in SH-SY5Y in a dose-dependent manner (Figure 20C). To determine if this was an effect exclusive to PDH, we measured the activities of lactate dehydrogenase (Figure 20D) and α-ketoglutarate dehydrogenase (Figure 20E) after 24 hours of treatment

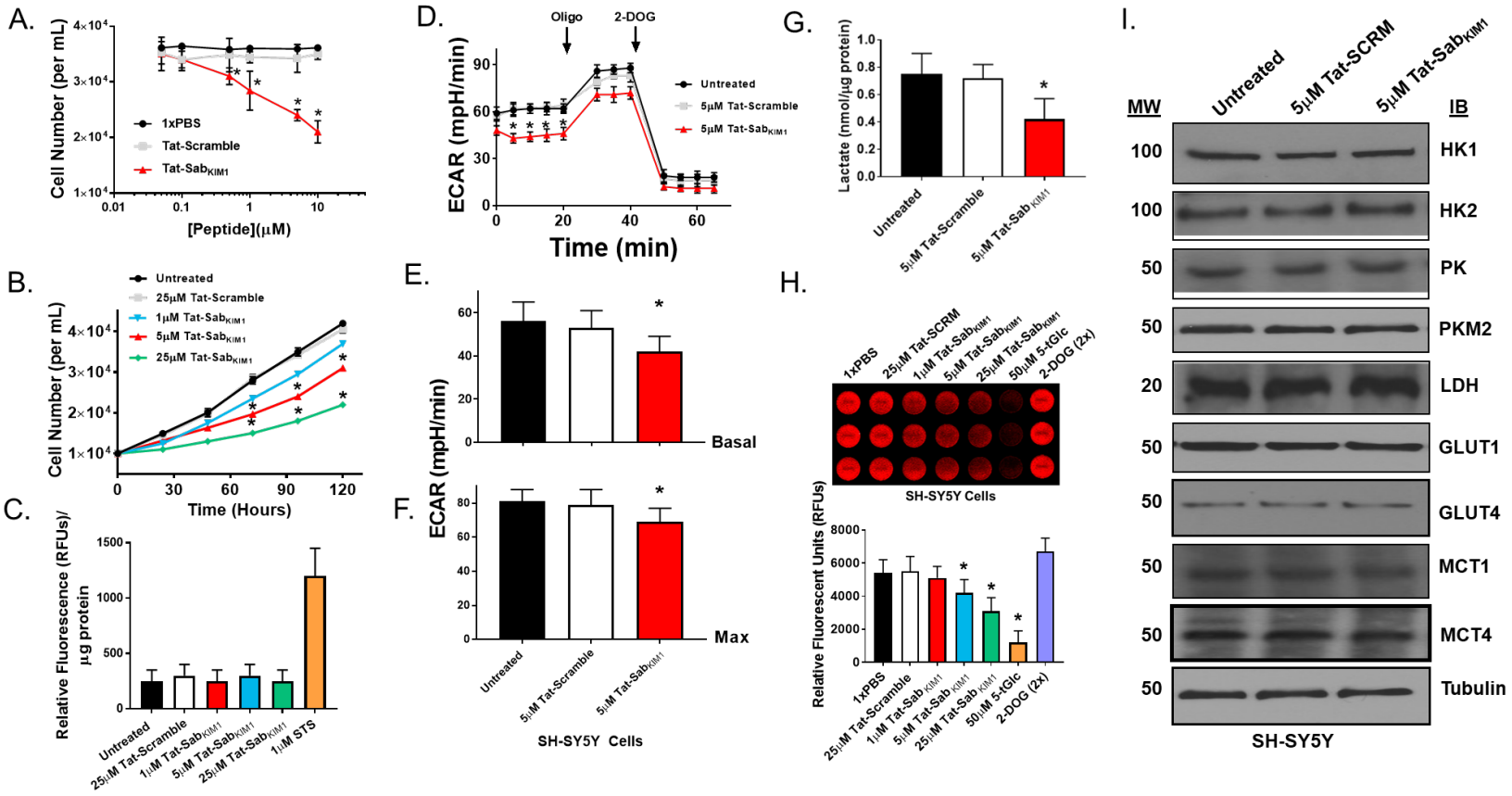

Figure 19. Inhibition of Sab-mediated signaling slows proliferation and decreases glycolysis.

SH-SY5Y cells were grown in the presence of increasing concentrations of Tat-Sab$_{KIM1}$ or scrambled controls and proliferation were assessed at day 5 (A) or daily over the course of 5 days (B). The induction of apoptosis in these cells was measured by caspase assay with STS as a control (C). The glycolytic profile of SH-SY5Y cells treated with 5μM Tat-Sab$_{KIM1}$ for 24 hours and controls was measured (D) and the basal rate (E) and maximum rate (F) were obtained. Extracellular lactate levels were measured (G) along with glucose uptake using a near-fluorescent probe (H). The relative abundance of glycolysis-relevant proteins was measured (I).

with 5μM TatSab$_{KIM1}$ peptide, and there was no change in activities for either enzyme (Figure 20D & 20E). These data imply that impaired Sab-mediated signaling improves PDH activity.

3.5 Inhibition of Sab-mediated signaling increases oxidative metabolism. To determine if oxidative metabolism was altered by changing Sab levels, we measured respiration in the presence and absence of 5μM Tat-Sab$_{KIM1}$ (Figure 20F). Cells treated with the Tat-Sab$_{KIM1}$ had significantly elevated (~20%) basal respiration (Figure 20G, top panel) and increased (~15%) spare respiratory capacity (Figure 20G, bottom panel). In Figure 20H, the oxidation of glucose (Figure 20H, top panel) glutamine (Figure 20H, middle panel) were increased in the absence of Sab-mediated signaling while, no significant change was observed in branched-chain amino acid oxidation (Figure 20H, bottom panel). To discern whether the substrate discrepancies in oxygen consumption were due to changes in respiratory complex activities, we used biochemical assays and found that only complex I activity significantly increased after treatment 5μM Tat-Sab$_{KIM1}$ (data not shown). Further analysis of complex I activity in cells treated with 5μM Tat-Sab$_{KIM1}$ had increased oxygen consumption in the presence of complex I substrates, and the introduction of 500nM rotenone did not inhibit oxygen consumption to the same extent as controls (Figure 20I). This effect was not observed with complexes II and III (Figure 20J). To determine if increased complex I activity was due to elevated protein levels, we measured the abundance of proteins from each complex and, no change was observed (Figure 20K). Therefore, Sab-mediated signaling may suppress oxidative metabolism by inhibiting complex I.

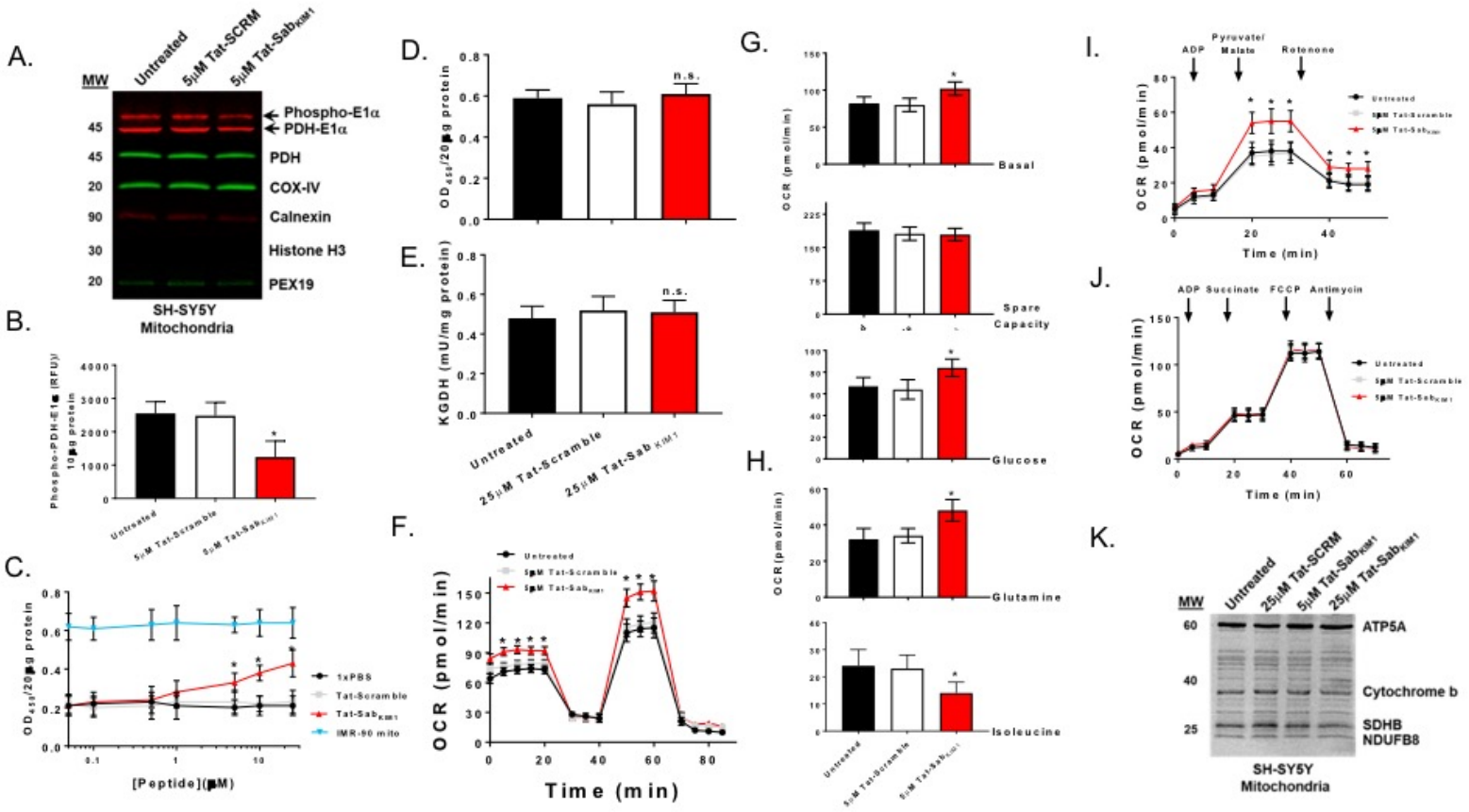

Figure 20. Diminished Sab-mediated signaling increases oxidative metabolism.

PDH phosphorylation was assessed by western blotting (A) and quantified (B) after treatment with peptides for 24 hours. PDH activity was also measured in the presence of increasing concentrations of Tat-Sab$_{KIM1}$ and control peptide (C). LDH and KDH were assayed as well (D). The respiratory profile of cells with and without Sab inhibition was measured using the Seahorse XF-96 extracellular flux analyzer (D). Basal respiration, spare capacity (E), and oxidation of glucose, glutamine and isoleucine (F) were measured. Complex I (I) and Complex II/III (J) functions were also measured along with respiratory protein levels (K) in the presence of Tat-Sab$_{KIM1}$ (24h).

3.6 Inhibiting Sab-based signaling increases chemoresistance in a Bcl-2 dependent manner. Because of the relationship between JNK and Bcl-2 proteins (J. W. Chambers et al., 2011a), we examined whether impaired Sab-mediated signaling altered Bcl-2 family proteins levels. After treatment of SH-SY5Y cells with 5μM Tat-Sab_{KIM1}, mitochondria were found to have increased Bcl-2 levels in cells treated with Tat-Sab_{KIM1} (Figure 21A & 18B). Also, a decrease in Bim levels was observed (Figures 18A & 18B). To determine if impaired Sab-mediated apoptotic signaling, we measured viability after treatment with 750nM cisplatin in SH-SY5Y cells exposed to increasing concentrations of Tat-Sab_{KIM1}. Inhibition of Sab-mediated signaling improved cell viability in cells treated with cisplatin in a dose-dependent manner (Figure 21C). To determine if the cisplatin resistance was specific or applicable to other drugs, we treated SH-SY5Y cells with chemotherapy agents following administration of 5μM Tat-Sab_{KIM1}. We found that for cyclophosphamide, doxorubicin, etoposide, and vincristine, inhibiting Sab-mediated signaling improved viability (Figure 21D), suggesting that limiting Sab-mediated signaling prevents robust induction of apoptosis.

3.7 Increased Sab expression induces glycolysis and enhances chemosensitivity. To determine if the metabolic and apoptotic changes could be specifically attributed to Sab levels, we over-expressed Sab in SH-SY5Y cells (Figure 22A & B), which did not alter mitochondrial density (Figure 22C). We observed that Sab-overexpressing cells had higher cell numbers (~30%) than controls (Figure 22D). SH-SY5Y cells with heightened Sab expression had an increased glycolytic rate (Figure 22E), decreased PDH activity (Figure 22F),

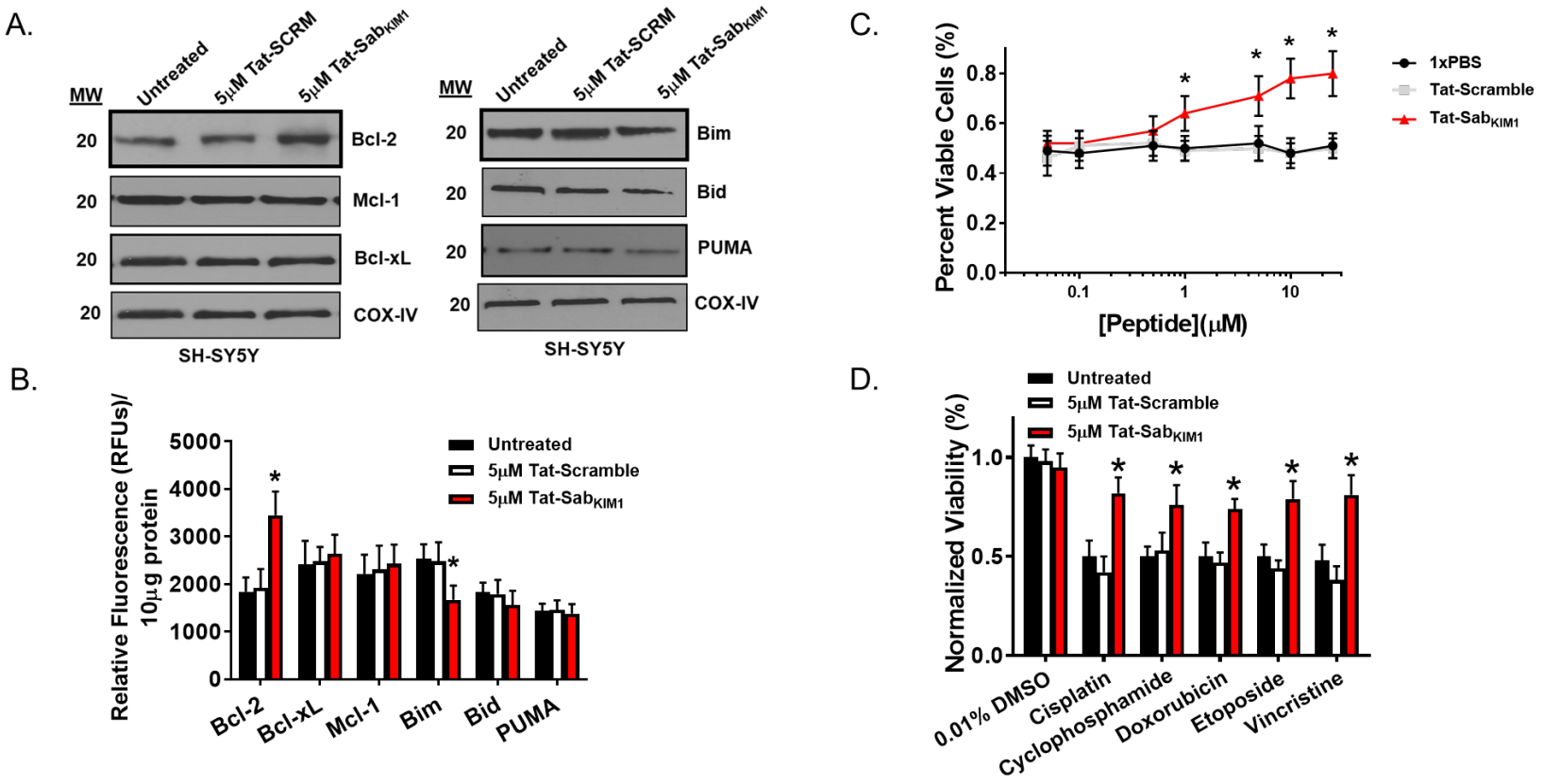

Figure 21. Impaired Sab-mediated signaling leads to chemoresistance.

Pro-survival (A, left) and pro-apoptotic (A, right) Bcl-2 family protein levels were measured and quantified (B) in the presence and absence of Sab-mediated signaling (Tat-Sab$_{KIM1}$, 24h). Cytotoxicity of 750nM cisplatin in the presence and absence of increasing Tat-Sab$_{KIM1}$ was assessed (C). The effect of Sab-inhibition (5μM Tat-Sab$_{KIM1}$ concurrent with drugs) was examined with 750nM cisplatin, 1μM cyclophosphamide, 100nM doxorubicin, 2.5μM etoposide, and 150nM vincristine (D).

reduced basal oxygen consumption (Figure 22G), and less complex I activity (Figure 4H). We also observed increased ROS generation in mitochondria from cells overexpressing Sab (Figure 22I). Increasing Sab resulted in a decrease in Bcl-2 levels and an increase in Bim on mitochondria (Figure 22J), and improved chemoresponsiveness to cisplatin (Figure 22K) and vincristine (Figure 22L). Thus, increasing Sab sensitizes neuroblastoma cells to chemotherapy.

3.8 Metabolic and chemoresponsive phenotypes correlate to Sab levels in neuroblastoma cells. We examined a panel of three neuroblastoma cell lines with different levels of Sab expression and found that CHP-212 had high Sab expression, SK-N-SH has a moderate amount of Sab expressing line, and IMR-32 was a low Sab expressing line (Figure 23A). Metabolic analysis of these cell lines revealed that cells with lower Sab expression had higher OCR/ECAR ratios (Figure 23B) suggesting that the cells were more oxidative. We also examined chemo-responsiveness of the three lines to cisplatin and vincristine, which revealed that CHP-212 (high Sab levels) was the most sensitive, while IMR-32 (low Sab expression) had significantly higher cell viability (Figure 23C). Consequently, the concentration of Sab may be influencing mitochondrial function and apoptosis in neuroblastoma cells.

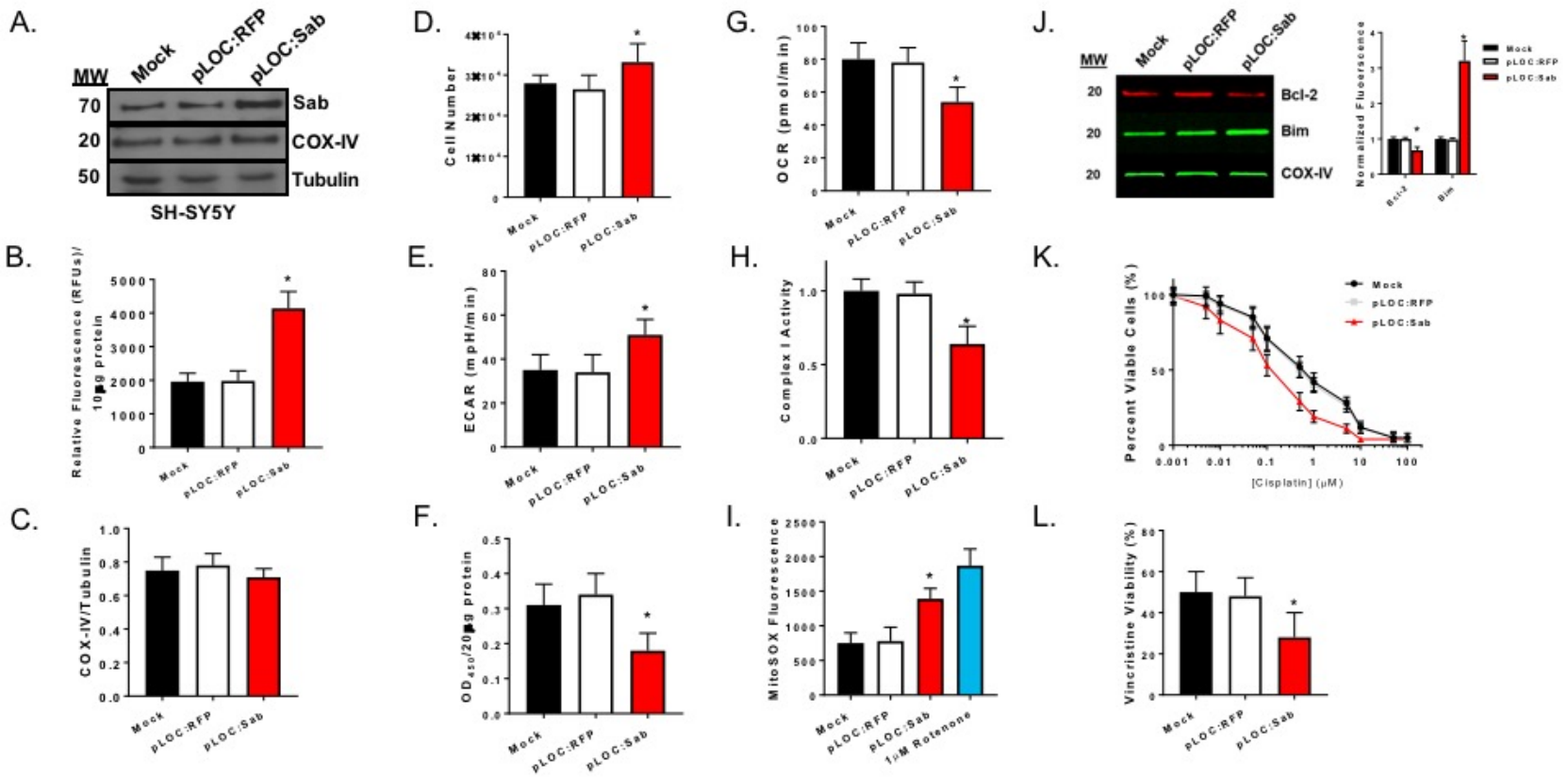

Figure 22. Overexpression of Sab enhances glycolysis and chemoresponsiveness.

Sab was overexpressed in SH-SY5Y cells as confirmed by western blotting (A) and quantitation (B) in regards to mitochondrial density (C). Proliferation (D), glycolytic rate (E), PDH activity (F), basal respiration (G), complex I activity (H), and mitochondrial ROS production (I) were measured following 72 hours of transfection. Bcl-2 and Bim levels were measured (J) in addition to chemosensitivity to cisplatin (K) and 150nM vincristine(L).

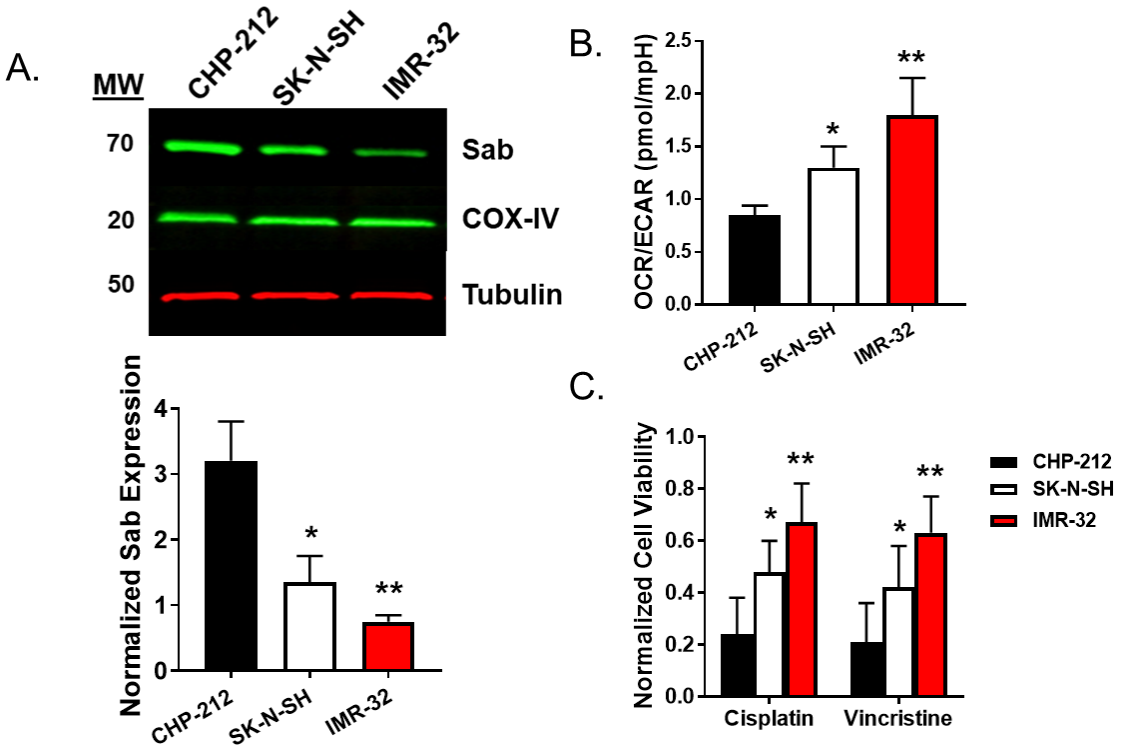

Figure 23. Metabolic and chemoresistant phenotypes correspond to Sab levels.

Three neuroblastoma lines were subjected to western blotting to detect the relative abundance of Sab (A), which was normalized to mitochondrial content (B). The oxidative character of the lines was determined using the OCR/ECAR ratio (C). Chemosensitivities for the three lines were assessed towards cisplatin and vincristine (D).

4. Discussion

The MOM scaffold protein Sab has been shown to affect mitochondrial dysfunction and apoptosis (J. W. Chambers and LoGrasso, 2011; T. P. Chambers et al., 2015). Our current study expanded the role of Sab-mediated signaling to include metabolic regulation in neuroblastoma. We found that Sab expression was reduced in neuroblastoma patients, and diminished Sab-mediated signaling

slowed cellular proliferation and decreased glycolysis, and enhanced PDH and complex I activities. Inhibiting Sab alters mitochondrial Bcl-2 proteins promoting resistance to chemotherapy-induced apoptosis. Meanwhile, over-expressing Sab induced proliferation, increased glycolysis, reduced oxidative metabolism, and enhanced sensitivity to chemotherapeutic drugs. We surmised that decreasing Sab expression may be part of oncogenesis in neuroblastoma.

The decrease in Sab expression in neuroblastoma patients was significant as indicated by the impact of Sab-JNK signaling on apoptosis. We believe that the lack of normal tissue controls, such as fetal brain tissue instead of ganglioneuroma in many studies, dampened the actual change in Sab expression between cancerous and non-transformed samples based on the impact of Sab inhibition and overexpression observed in the cell lines. We predict that Sab levels may be even lower in neuroblastoma cells than anticipated by this study.

The inhibition of Sab-mediated signaling impaired cellular proliferation and glycolysis (Figure 19) in neuroblastoma cells. Given that inhibition of Sab-mediated signaling has been shown not to affect nuclear JNK signaling (J. W. Chambers et al., 2011a), we surmised that the effects of Sab inhibition were post-translational, and this notion was supported by the lack of changes in glycolytic and respiratory protein levels (Figure 19 & 20). Additionally, we found a change in the relative abundance of phosphorylation on the Eα1 subunit of pyruvate dehydrogenase (Figure 20). The post-translational impact of JNK signaling has been linked to glycolysis before; wherein, JNK1 signaling events promote the activity of phosphofructokinase 1 (PFK1) (Deng et al., 2008). JNK phosphorylation of Bad

releases PFK-1 allowing for catalysis. Thus, JNK phosphoregulation of Bad and other glycolytic proteins may be a product of Sab-mediated signaling in neuroblastoma.

The decreased proliferation by impaired Sab-mediated signaling (Figure 19) stands in contrast to a study by Fey and colleagues, who found that Akt signaling inhibits JNK activation in SH-SY5Y cells (Fey et al., 2015). Thus, inhibiting JNK signaling, including Sab-mediated, may increase Akt-mediated proliferation. Unfortunately, Fey and colleagues did not investigate if this was an isoform-specific event, so it's possible that mitochondrial-specific JNK isoforms may not be affected by Akt signaling but could be by $TatSab_{KIM1}$. We also see parallels with our observations and Fey *et. al*. For example, suppression of nuclear JNK signaling by Akt is likely to decrease Sab expression in neuroblastoma. We recently demonstrated that cells lacking JNK have significantly lower Sab levels (T. P. Chambers et al., 2015). Akt inhibition of JNK may result in the decreased Sab expression observed in neuroblastoma patients. Thus, detangling the JNK isoforms and specific contributions of individual variants to neuroblastoma will be crucial.

We found that Sab-mediated signaling affects PDH phosphorylation in neuroblastoma cells (Figure 20A & 22F). This may indicate that active JNK signaling on Sab in neuroblastoma is contributing to aerobic glycolysis similar to the aging brain[30,42]. However, it should be noted that ERK1/2 and p38 isoforms have been found on mitochondria (Kim et al., 2006; Nowak et al., 2006), and the KIMs on Sab are MAPK-specific. Similarly, mitochondrial ERK signaling is linked

to complex I inhibition. Consequently, we cannot rule out the contributions of these two MAPKs to oxidative metabolism. Despite evidence indicating that mitochondrial JNK inhibits complex I and amplifies ROS production (J. W. Chambers and LoGrasso, 2011) through Src (Win et al., 2016), additional studies are needed to resolve the mechanism of complex I inhibition.

Recently, enhanced Sab-mediated signaling was linked to chemosensitization of cervical cancer cells (T. P. Chambers et al., 2015), which may have been facilitated the emigration of Bcl-2 proteins from mitochondria following cytotoxic stress (J. W. Chambers et al., 2011a). We found that Bcl-2 levels increased following Sab inhibition in SH-SY5Y cells (Figure 21). We propose that the increase in Bcl-2 and decrease in Bim in the absence of Sab-mediated signaling are due to diminished JNK phosphorylation of Bcl-2 and Bim (Putcha et al., 2003). The increased Bcl-2 will prevent Bax/Bak oligomerization and apoptosis. This may explain the chemo-resistance in neuroblastoma populations with low Sab expression. We correlated Sab levels to the metabolic phenotype and chemoresponsiveness of neuroblastoma cells (Figure 23). This result parallels clinical observations that indicate the robustness of cytotoxic JNK signaling could serve as a prognostic for neuroblastoma (Fey et al., 2015).

In summary, scaffold protein concentrations, such as Sab, at specific cellular locations represent the magnitude of the signaling event on an organelle influence the biological outcomes of signaling (Good et al., 2011). In that regard, we propose that the relative abundance of Sab on the MOM determines the robustness of JNK apoptotic signaling and the survival of neuroblastoma cells. Specifically, patients

with high Sab expression may be more susceptible to therapies and have a greater likelihood of survival. Chemo-sensitization in high Sab-expressing tumors would reduce drug doses and minimize the detrimental side-effects in patients. Ultimately, Sab concentrations ascertained from biopsies or emerging imaging techniques may be useful to discern appropriate treatment regimens for neuroblastoma patients.

5. References

Albino, D., Scaruffi, P., Moretti, S., Coco, S., Truini, M., Di Cristofano, C., Cavazzana, A., Stigliani, S., Bonassi, S., Tonini, G.P., 2008. Identification of low intratumoral gene expression heterogeneity in neuroblastic tumors by genome-wide expression analysis and game theory. Cancer 113, 1412–1422. doi:10.1002/cncr.23720

Asgharzadeh, S., Pique-Regi, R., Sposto, R., Wang, H., Yang, Y., Shimada, H., Matthay, K., Buckley, J., Ortega, A., Seeger, R.C., 2006. Prognostic significance of gene expression profiles of metastatic neuroblastomas lacking MYCN gene amplification. J. Natl. Cancer Inst. 98, 1193–1203. doi:10.1093/jnci/djj330

Biedler, J.L., Roffler-Tarlov, S., Schachner, M., Freedman, L.S., 1978. Multiple neurotransmitter synthesis by human neuroblastoma cell lines and clones. Cancer Research 38, 3751–3757.

Brunelle, J.K., Letai, A., 2009. Control of mitochondrial apoptosis by the Bcl-2 family. Journal of Cell Science 122, 437–441. doi:10.1242/jcs.031682

Certo, M., Moore, V.D.G., Nishino, M., Wei, G., Korsmeyer, S., Armstrong, S.A., Letai, A., 2006. Mitochondria primed by death signals determine cellular addiction to antiapoptotic BCL-2 family members. Cancer Cell 9, 351–365. doi:10.1016/j.ccr.2006.03.027

Chambers, J.W., Cherry, L., Laughlin, J.D., Figuera-Losada, M., LoGrasso, P.V., 2011a. Selective inhibition of mitochondrial JNK signaling achieved using peptide mimicry of the Sab kinase interacting motif-1 (KIM1). ACS Chem. Biol. 6, 808–818. doi:10.1021/cb200062a

Chambers, J.W., Howard, S., LoGrasso, P.V., 2013a. Blocking c-Jun N-terminal kinase (JNK) translocation to the mitochondria prevents 6-hydroxydopamine-

induced toxicity in vitro and in vivo. J. Biol. Chem. 288, 1079–1087. doi:10.1074/jbc.M112.421354

Chambers, J.W., LoGrasso, P.V., 2011. Mitochondrial c-Jun N-terminal kinase (JNK) signaling initiates physiological changes resulting in amplification of reactive oxygen species generation. J. Biol. Chem. 286, 16052–16062. doi:10.1074/jbc.M111.223602

Chambers, J.W., Pachori, A., Howard, S., Ganno, M., Hansen, D., Kamenecka, T., Song, X., Duckett, D., Chen, W., Ling, Y.Y., Cherry, L., Cameron, M.D., Lin, L., Ruiz, C.H., Lograsso, P., 2011b. Small Molecule c-jun-N-terminal Kinase (JNK) Inhibitors Protect Dopaminergic Neurons in a Model of Parkinson's Disease. ACS Chem Neurosci 2, 198–206. doi:10.1021/cn100109k

Chambers, J.W., Pachori, A., Howard, S., Iqbal, S., LoGrasso, P.V., 2013b. Inhibition of JNK mitochondrial localization and signaling is protective against ischemia/reperfusion injury in rats. J. Biol. Chem. 288, 4000–4011. doi:10.1074/jbc.M112.406777

Chambers, T.P., Portalatin, G.M., Paudel, I., Robbins, C.J., Chambers, J.W., 2015. Sub-chronic administration of LY294002 sensitizes cervical cancer cells to chemotherapy by enhancing mitochondrial JNK signaling. Biochemical and Biophysical Research Communications 463, 538–544. doi:10.1016/j.bbrc.2015.05.075

Chambers, T.P., Santiesteban, L., Gomez, D., Chambers, J.W., 2017. Sab mediates mitochondrial dysfunction involved in imatinib mesylate-induced cardiotoxicity. Toxicology 382, 24–35. doi:10.1016/j.tox.2017.03.006

Cheng, J., Fan, Y.-H., Xu, X., Zhang, H., Dou, J., Tang, Y., Zhong, X., Rojas, Y., Yu, Y., Zhao, Y., Vasudevan, S.A., Nuchtern, J.G., Kim, E.S., Chen, X., Lu, F., Yang, J., 2014. A small-molecule inhibitor of UBE2N induces neuroblastoma cell death via activation of p53 and JNK pathways. Cell Death and Disease 5, e1079–e1079. doi:10.1038/cddis.2014.54

Chonghaile, T.N., Sarosiek, K.A., Vo, T.T., Ryan, J.A., Tammareddi, A., Moore, V.D.G., Deng, J., Anderson, K.C., Richardson, P., Tai, Y.T., Mitsiades, C.S., Matulonis, U.A., Drapkin, R., Stone, R., DeAngelo, D.J., McConkey, D.J., Sallan, S.E., Silverman, L., Hirsch, M.S., Carrasco, D.R., Letai, A., 2011. Pretreatment Mitochondrial Priming Correlates with Clinical Response to Cytotoxic Chemotherapy. Science 334, 1129–1133. doi:10.1126/science.1206727

DeBerardinis, R.J., DeBerardinis, R.J., Mancuso, A., Mancuso, A., Daikhin, E., Daikhin, E., Nissim, I., Nissim, I., Yudkoff, M., Yudkoff, M., Wehrli, S., Wehrli, S., Thompson, C.B., Thompson, C.B., 2007. Beyond aerobic glycolysis:

Transformed cells can engage in glutamine metabolism that exceeds the requirement for protein and nucleotide synthesis. Proc Natl Acad Sci USA 104, 19345–19350. doi:10.1073/pnas.0709747104

Deng, H., Yu, F., Chen, J., Zhao, Y., Xiang, J., Lin, A., 2008. Phosphorylation of Bad at Thr-201 by JNK1 promotes glycolysis through activation of phosphofructokinase-1. Journal of Biological Chemistry 283, 20754–20760. doi:10.1074/jbc.M800024200

Fey, D., Halasz, M., Dreidax, D., Kennedy, S.P., Hastings, J.F., Rauch, N., Munoz, A.G., Pilkington, R., Fischer, M., Westermann, F., Kolch, W., Kholodenko, B.N., Croucher, D.R., 2015. Signaling pathway models as biomarkers: Patient-specific simulations of JNK activity predict the survival of neuroblastoma patients. Sci Signal 8, ra130–ra130. doi:10.1126/scisignal.aab0990

Filomeni, G., Aquilano, K., Rotilio, G., Ciriolo, M.R., 2003. Reactive oxygen species-dependent c-Jun NH2-terminal kinase/c-Jun signaling cascade mediates neuroblastoma cell death induced by diallyl disulfide. Cancer Research 63, 5940–5949.

Goldsmith, K.C., Gross, M., Peirce, S., Luyindula, D., Liu, X., Vu, A., Sliozberg, M., Guo, R., Zhao, H., Reynolds, C.P., Hogarty, M.D., 2012. Mitochondrial Bcl-2 Family Dynamics Define Therapy Response and Resistance in Neuroblastoma. Cancer Research 72, 2565–2577. doi:10.1158/0008-5472.CAN-11-3603

Goldsmith, K.C., Lestini, B.J., Gross, M., Ip, L., Bhumbla, A., Zhang, X., Zhao, H., Liu, X., Hogarty, M.D., 2010. BH3 response profiles from neuroblastoma mitochondria predict activity of small molecule Bcl-2 family antagonists. Cell Death Differ. 17, 872–882. doi:10.1038/cdd.2009.171

Good, M.C., Zalatan, J.G., Lim, W.A., 2011. Scaffold Proteins: Hubs for Controlling the Flow of Cellular Information. Science 332, 680–686. doi:10.1126/science.1198701

Hanahan, D., Weinberg, R.A., 2011. Hallmarks of Cancer: The Next Generation. Cell 144, 646–674. doi:10.1016/j.cell.2011.02.013

Janoueix-Lerosey, I., Lequin, D., Brugières, L., Ribeiro, A., de Pontual, L., Combaret, V., Raynal, V., Puisieux, A., Schleiermacher, G., Pierron, G., Valteau-Couanet, D., Frebourg, T., Michon, J., Lyonnet, S., Amiel, J., Delattre, O., 2008. Somatic and germline activating mutations of the ALK kinase receptor in neuroblastoma. Nature 455, 967–970. doi:10.1038/nature07398

Kim, B.-J., Ryu, S.-W., Song, B.-J., 2006. JNK- and p38 kinase-mediated phosphorylation of Bax leads to its activation and mitochondrial translocation

and to apoptosis of human hepatoma HepG2 cells. Journal of Biological Chemistry 281, 21256–21265. doi:10.1074/jbc.M510644200

Kristiansen, M., Hughes, R., Patel, P., Jacques, T.S., Clark, A.R., Ham, J., 2010. Mkp1 is a c-Jun target gene that antagonizes JNK-dependent apoptosis in sympathetic neurons. J. Neurosci. 30, 10820–10832. doi:10.1523/JNEUROSCI.2824-10.2010

Letai, A., Bassik, M.C., Walensky, L.D., Sorcinelli, M.D., Weiler, S., Korsmeyer, S.J., 2002. Distinct BH3 domains either sensitize or activate mitochondrial apoptosis, serving as prototype cancer therapeutics. Cancer Cell 2, 183–192. doi:10.1016/S1535-6108(02)00127-7

Magalhães, P.J., Andreu, A.L., Schon, E.A., 1998. Evidence for the presence of 5S rRNA in mammalian mitochondria. Mol. Biol. Cell 9, 2375–2382.

Maris, J.M., 2010. Recent advances in neuroblastoma. N Engl J Med 362, 2202–2211. doi:10.1056/NEJMra0804577

Matthay, K.K., Reynolds, C.P., Seeger, R.C., Shimada, H., Adkins, E.S., Haas-Kogan, D., Gerbing, R.B., London, W.B., Villablanca, J.G., 2009. Long-Term Results for Children With High-Risk Neuroblastoma Treated on a Randomized Trial of Myeloablative Therapy Followed by 13- cis-Retinoic Acid: A Children's Oncology Group Study. Journal of Clinical Oncology 27, 1007–1013. doi:10.1200/JCO.2007.13.8925

Nijboer, C.H., Bonestroo, H.J.C., Zijlstra, J., Kavelaars, A., Heijnen, C.J., 2013. Mitochondrial JNK phosphorylation as a novel therapeutic target to inhibit neuroinflammation and apoptosis after neonatal ischemic brain damage. Neurobiol. Dis. 54, 432–444. doi:10.1016/j.nbd.2013.01.017

Nowak, G., Clifton, G.L., Godwin, M.L., Bakajsova, D., 2006. Activation of ERK1/2 pathway mediates oxidant-induced decreases in mitochondrial function in renal cells. Am. J. Physiol. Renal Physiol. 291, F840–55. doi:10.1152/ajprenal.00219.2005

Porro, A., Haber, M., Diolaiti, D., Iraci, N., Henderson, M., Gherardi, S., Valli, E., Munoz, M.A., Xue, C., Flemming, C., Schwab, M., Wong, J.H., Marshall, G.M., Valle, Della, G., Norris, M.D., Perini, G., 2010. Direct and coordinate regulation of ATP-binding cassette transporter genes by Myc factors generates specific transcription signatures that significantly affect the chemoresistance phenotype of cancer cells. J. Biol. Chem. 285, 19532–19543. doi:10.1074/jbc.M109.078584

Putcha, G.V., Le, S., Frank, S., Besirli, C.G., Clark, K., Chu, B., Alix, S., Youle, R.J., LaMarche, A., Maroney, A.C., Johnson, E.M., 2003. JNK-mediated BIM phosphorylation potentiates BAX-dependent apoptosis. Neuron 38, 899–914.

Qing, G., Li, B., Vu, A., Skuli, N., Walton, Z.E., Liu, X., Mayes, P.A., Wise, D.R., Thompson, C.B., Maris, J.M., Hogarty, M.D., Simon, M.C., 2012. ATF4 Regulates MYC-Mediated Neuroblastoma Cell Death upon Glutamine Deprivation. Cancer Cell 22, 631–644. doi:10.1016/j.ccr.2012.09.021

Ren, P., Yue, M., Xiao, D., Xiu, R., Gan, L., Liu, H., Qing, G., 2015. ATF4 and N-Myc coordinate glutamine metabolism in MYCN-amplified neuroblastoma cells through ASCT2 activation. J. Pathol. 235, 90–100. doi:10.1002/path.4429

Rhodes, D.R., Kalyana-Sundaram, S., Mahavisno, V., Varambally, R., Yu, J., Briggs, B.B., Barrette, T.R., Anstet, M.J., Kincead-Beal, C., Kulkarni, P., Varambally, S., Ghosh, D., Chinnaiyan, A.M., 2007. Oncomine 3.0: genes, pathways, and networks in a collection of 18,000 cancer gene expression profiles. Neoplasia 9, 166–180.

Sandulache, V.C., Ow, T.J., Pickering, C.R., Frederick, M.J., Zhou, G., Fokt, I., Davis-Malesevich, M., Priebe, W., Myers, J.N., 2011. Glucose, not glutamine, is the dominant energy source required for proliferation and survival of head and neck squamous carcinoma cells. Cancer 117, 2926–2938. doi:10.1002/cncr.25868

Teitz, T., Wei, T., Valentine, M.B., Vanin, E.F., Grenet, J., Valentine, V.A., Behm, F.G., Look, A.T., Lahti, J.M., Kidd, V.J., 2000. Caspase 8 is deleted or silenced preferentially in childhood neuroblastomas with amplification of MYCN. Nat. Med. 6, 529–535. doi:10.1038/75007

Vander Heiden, M.G., Cantley, L.C., Thompson, C.B., 2009. Understanding the Warburg Effect: The Metabolic Requirements of Cell Proliferation. Science 324, 1029–1033. doi:10.1126/science.1160809

Waetzig, V., Wacker, U., Haeusgen, W., Björkblom, B., Courtney, M.J., Coffey, E.T., Herdegen, T., 2009. Concurrent protective and destructive signaling of JNK2 in neuroblastoma cells. Cell. Signal. 21, 873–880.

Wang, Q., Diskin, S., Rappaport, E., Attiyeh, E., Mosse, Y., Shue, D., Seiser, E., Jagannathan, J., Shusterman, S., Bansal, M., Khazi, D., Winter, C., Okawa, E., Grant, G., Cnaan, A., Zhao, H., Cheung, N.-K., Gerald, W., London, W., Matthay, K.K., Brodeur, G.M., Maris, J.M., 2006. Integrative genomics identifies distinct molecular classes of neuroblastoma and shows that multiple genes are targeted by regional alterations in DNA copy number. Cancer Research 66, 6050–6062. doi:10.1158/0008-5472.CAN-05-4618

Win, S., Than, T.A., Fernandez-Checa, J.C., Kaplowitz, N., 2014. JNK interaction with Sab mediates ER stress induced inhibition of mitochondrial respiration and cell death. Cell Death and Disease 5, e989–e989. doi:10.1038/cddis.2013.522

Win, S., Than, T.A., Min, R.W.M., Aghajan, M., Kaplowitz, N., 2016. c-Jun N-terminal kinase mediates mouse liver injury through a novel Sab (SH3BP5)-dependent pathway leading to inactivation of intramitochondrial Src. Hepatology 63, 1987–2003. doi:10.1002/hep.28486

Wu, M., Neilson, A., Swift, A.L., Moran, R., Tamagnine, J., Parslow, D., Armistead, S., Lemire, K., Orrell, J., Teich, J., Chomicz, S., Ferrick, D.A., 2007. Multiparameter metabolic analysis reveals a close link between attenuated mitochondrial bioenergetic function and enhanced glycolysis dependency in human tumor cells. AJP: Cell Physiology 292, C125–36. doi:10.1152/ajpcell.00247.2006

Yang, J., Liu, X., Bhalla, K., Kim, C.N., Ibrado, A.M., Cai, J., Peng, T.I., Jones, D.P., Wang, X., 1997. Prevention of apoptosis by Bcl-2: release of cytochrome c from mitochondria blocked. Science 275, 1129–1132.

Yang, L., Moss, T., Mangala, L.S., Marini, J., Zhao, H., Wahlig, S., Armaiz-Pena, G., Jiang, D., Achreja, A., Win, J., Roopaimoole, R., Rodriguez-Aguayo, C., Mercado-Uribe, I., Lopez-Berestein, G., Liu, J., Tsukamoto, T., Sood, A.K., Ram, P.T., Nagrath, D., 2014. Metabolic shifts toward glutamine regulate tumor growth, invasion and bioenergetics in ovarian cancer. Mol. Syst. Biol. 10, 728–728. doi:10.1002/msb.20134892

Zhou, Q., Lam, P.Y., Han, D., Cadenas, E., 2009. Activation of c-Jun-N-terminal kinase and decline of mitochondrial pyruvate dehydrogenase activity during brain aging. FEBS Letters 583, 1132–1140. doi:10.1016/j.febslet.2009.02.043

Zhou, Q., Lam, P.Y., Han, D., Cadenas, E., 2008. c-Jun N-terminal kinase regulates mitochondrial bioenergetics by modulating pyruvate dehydrogenase activity in primary cortical neurons. J. Neurochem. 104, 325–335. doi:10.1111/j.1471-4159.2007.04957.x

CHAPTER VI

Conclusion

1. Summary

Tumors of the central nervous system (CNS) remain some of the most difficult malignancies to treat because the blood brain barrier can limit the efficacy chemotherapeutic and immunotherapeutic approaches, but the physiology of these cancers has yet to be rigorously interrogated due to the difficulty of their locations. Only recently have techniques been developed to begin to address the biology of CNS tumors *in vivo*. By improving the collective understanding of CNS tumor physiology, one proposes that effective therapeutics can be designed to target unique aspects of a particular malignancy and improve the survival outcomes for patients. In our current study, we chose to take a stepwise approach to dissecting the complexities of tumor physiology and focused on aberrations of mitochondrial function. Mitochondria are critical to brain function, not only because they supply 90% of the ATP required by the organ, but because they are central mediators of neurotransmission and calcium buffering in neurons and modulators of clearance functions and detoxification reactions in glial cells. In CNS malignancies, mitochondrial induction of apoptosis may be altered accounting for the high rates of recurrence and resistance in these disorders. Based on the important roles for mitochondria in bioenergetic requirements for brain cells and mediating cell death responses, we focused our studies on these two aspects of CNS tumor cell physiology.

1.1 Chapter 3 Summary

In our first study (presented in Chapter 3), we examined the bioenergetic parameters and capacity for apoptosis in ten (10) distinct glioblastoma (GBM) cell

lines. Real-time metabolic profiling of the established cell lines revealed that there were no considerable differences in glycolysis and respiration. The metabolic similarities of the cell lines were corroborated by the examination of protein levels of glycolytic enzymes, glucose transporters, and monocarboxylate transporters. Next, we examined if the cell lines exhibited different responsiveness to the prevailing chemotherapeutic agent temozolomide (TMZ). We were able to characterize the 10 cell lines as either resistant, responsive, or sensitive to TMZ, and western blot analysis revealed that there was no difference in O-6-methylguanine-DNA methyltransferase (MGMT) levels (a proposed clinical biomarker) among the cell lines. This lead us to examine the relative abundance of anti-apoptotic and pro-apoptotic members of the Bcl-2 family of proteins. It has been previously shown that the concentrations of Bcl-2 family members can indicate the potential for cells to induce apoptosis as well as represent the relative sensitivity to therapeutic approaches in solid tumors. Our evaluation found that differences in the concentrations of anti-apoptotic Bcl-2 proteins (Bcl-2, Bcl-xL, and Mcl-1) and the pro-apoptotic BH3-only protein Bim correlated to the extent of resistance to TMZ. This observation was verified by inducing chemoresistance in U87 cells by exposing the cells to hypoxia for 18 hours. The hypoxic treatment increased the levels of anti-apoptotic Bcl-2 proteins and reduced the concentration of BIM in U87. Furthermore, pharmacological inhibition of both Bcl-2/Bcl-xL with ABT-737 (a BIM mimetic) and Mcl-1 with S63A45 effectively induced complete apoptosis in the 10 established cell lines at a dose of 1μM; however, individual treatments with either ABT-737 or S63A45 failed to alter cellular viability. To

determine if these observations corresponded to the apoptotic capacity of GBM in clinically relevant samples, we profiled expression of Bcl-2 proteins in glioma-like stem cells (GSCs) recently acquired from patient tumors. We found that with respect to TMZ exposure the four (4) GSC lines segregated across the same trend. Whereby, GSCs with high anti-apoptotic Bcl-2 levels and low Bim concentrations were resistant to TMZ, and cells with low anti-apoptotic proteins and elevated Bim levels were sensitive to TMZ. Likewise, we found that the GSCs were sensitive to a combination treatment of ABT-737 and SC63A45, but GSCs were far less susceptible to individual exposures to the drugs. Our results indicate that GBM tumors may be subject to BCl-2/BH3-only profiling and determining the apoptotic capacity of these tumors could represent a means to personalize treatments depending of the relative abundance of these proteins. Similarly, a combination of ABT-737 and S62A45 might be a useful approach to sensitize highly resistant tumors to contemporary therapy options.

1.2 Chapter 4 Summary

In our second study (Chapter 4), we examined the relative concentrations of the outer mitochondrial membrane (OMM) Sab, which based on our studies in gynecological cancers, facilitates c-Jun N-terminal Kinase (JNK) signaling on mitochondria. Increased JNK-Sab signaling was linked to diminished anti-apoptotic Bcl-2 levels and elevated BH3-only concentrations on mitochondria resulting in chemosensitive cancer cells. Our secondary analysis of GBM patient data revealed that Sab expression (mRNA) was decreased in tumor samples from patients, and this decrease was consistent across six independent studies. We

surveyed the 10 GBM cell lines to determine if Sab levels correlated to TMZ response, and there was absolutely no correlation between Sab concentration and the sensitivity of cells to TMZ. To determine if this was an artifact of prolonged cell culture, the GSCs were then analyzed for Sab concentrations, and again, there was no correlation between Sab abundance and chemoresponsiveness. However, we did notice the expression of a truncated version of Sab in the 10 established GBM cell lines that was not present in the GSCs. Using RT-PCR and sequencing, we found that a second transcript for Sab existed, which had lost the N-terminus of the protein (1-156). This matches the description for Sab isoform 2 identified previously in human gene expression studies. Because this splice variant lacks the original mitochondrial targeting sequence of Sab, we surmised that this variant may be impairing the ability of GBM cells to induce robust apoptosis. Therefore, we took SF268 cells and selected for clones that did not express the variant, and we found one clone (SF268-6) that expressed only full-length Sab. Our analysis revealed that there was no difference in chemosenstivity towards, TMX, irinotecan, or mitochondrial toxins. Immunofluerescence later revealed that the Sab-variant still localized to mitochondria, and this was confirmed by the presence of the variant protein in mitochondrial isolates. Therefore, the OMM signaling (including apoptosis) of Sab was still intact. However, previous studies have linked Sab-mediated signaling to inhibition of respiratory complex I. Previous topology studies in the Kaplowitz lab and recent studies in the Chambers lab suggest that the C-terminus of Sab is on the cytosolic face of mitochondria, and the N-terminal portions reside in the intermembrane space. This model places two coiled-coiled

motifs (CC-1 and CC-2) of Sab in the intermembrane space for protein-protein interactions. However, CC-1 is not present in Sab isoform 2 (the splice variant). Our examination of SF268 and SF268-6 reveal that SF268 had a faster proliferation rate than clone 6 (which expresses the full-length Sab only). Reflecting the increased proliferation rate, SF268 cells had a greater rate of glycolysis that SF268-6 clones. Further, cells expressing only full-length Sab (SF268-6) had a 30% higher basal respiratory rate that SF268 cells. Moreover, SF268 cells had a 60% lower respiratory capacity than clones with only full-length Sab. Pyruvate oxidation analysis reveal that the deficiency in oxidative phosphorylation occurs at the level of complex I. This would suggest that the loss of CC1 in the Sab variant releases a protein component capable of inhibiting respiration in mammalian cells. Future studies will be aimed at elucidating the molecular mechanisms of this novel form of metabolic control.

1.3 Chapter 5 Summary

In our final study, our goal was to determine if the observations in the previous two studies could be applied to other CNS malignancies, namely CNS-based neuroblastoma. Using secondary analysis of patient samples, we found that Sab expression in neuroblastoma was significantly lower than control samples. To determine if Sab abundance impacted mitochondrial capacity for apoptosis and cellular metabolism, we overexpressed Sab and a version of Sab (Sab^{KIML-A}) incapable of binding mitogen-activated protein kinases (MAPKs), such as JNK, as a negative control in human SH-SY5Y neuroblastoma cells. As expected, increasing Sab expression lead to a decrease in the levels of anti-apoptotic Bcl-2

proteins and elevated the concentrations of pro-apoptotic BH3-only proteins. This trend was not observed in the cells expressing Sab^{KIML-A} or red-fluorescent protein (RFP). The increased levels of Sab were sufficient to induce chemo-sensitization of Sab in the SH-SY5Y cells. With respect to metabolism, ectopic expression of Sab promoted increased glycolysis in SH-SY5Y cells; meanwhile, elevated Sab concentrations resulted in decreased respiration and spare respiratory capacity. The diminished respiration could be linked to inhibition of pyruvate dehydrogenase (PDH) by JNK phosphorylation on the E1α subunit. Additionally, increased Sab levels resulted in diminished complex I activity, which appear to be attributed to a loss of specific complex I components, namely NADH dehydrogenase component, NDUFS8. Inhibition of Sab mediated signaling with a small peptide (Tat-Sab_{KIM1}) was able to prevent the changes in Bcl-2 proteins and cellular metabolism. Finally, analysis of three (3) additional CNS-based neuroblastoma cell lines revealed, at least in this very small sample size, that Sab concentrations correlated to relative oxidative metabolism phenotypes and susceptibility to cisplatin and vincristine. These findings suggest that Sab-mediated signaling is a crucial modulator of cell vulnerability and metabolism in neuroblastoma cells; however, future studies in patient-derived samples and in mouse models will be useful in determining if these observations are clinically valid.

1.4 Conclusions

The results of our studies highlight that even in malignancies of the same organ the molecular mechanisms governing cancer pathogeneses are heterogeneous and unique among malignancies. While Sab-mediated signaling was not crucial to

chemo-susceptibility in GBM, Sab-facilitated events were crucial to the induction of apoptosis in neuroblastoma cells. However, and perhaps more interesting is the novel metabolic regulation observed in both GBM and neuroblastoma. The direct impact of Sab-mediated signaling on metabolism may represent a novel metabolic control point that may be exploited to weaken the bioenergetic capacity of CNS cancers, and perhaps creating a metabolic conflict may lead to apoptotic priming effectively rendering tumor cells more vulnerable to therapies. For these reasons, continued investigation of mitochondrial regulation in CNS cancers is likely to result in novel therapies capable of extending patient survival and cognitive health-spans.

2. Pitfalls and critical analysis

In the previous chapters, we have tried to highlight the weaknesses and pitfalls in our studies, and in doing so, we identified key limitations in our studies that could affect our analyses of the outcomes. There limitations include:

1. The experiments were not conducted in the context of the brain.
2. There are few cell lines and limited patient-derived samples used in the studies.
3. Many of the analyses conducted are based on endpoint analyses.
4. We were unable to transfect the Sab variant into clone SF268-6 to perform rescue experiments.

Each limitation will be addressed in more detail in the respective sections below.

2.1 Studies were performed in a cell autonomous setting.

The prevailing disconnect between the Sab expression studies in GBM patients and the lack of contribution of Sab to chemo-susceptibility or Bcl-2 protein levels in GBM cell lines or GSCs may be indicative of working with cells that have been adapted to culture or isolation of a particular cell population. It is well demonstrated that tumors are comprised of a very heterogeneous population of cells, and it is likely the culmination of the collective environment created by the different cell types that is ultimately responsible for the phenotypes of a particular tumor. Thus, any technique that isolates and enriches one type is probably not a true depiction of the tumor. Thereby, when we observe Sab protein levels that are easily detected by western blotting in cell culture, one may reason that the cells selected for in culture are not representative GBM tumor cells. Also, the tight correlation between Sab and the induction of apoptosis in neuroblastoma cells may also not be entirely reflective of neuroblastoma tumors cells. In fact, the culturing of cells from patient tumors and sustained culture of established cell lines can be viewed as a selection process for cells most adept at surviving in a particular set of growth conditions. Further complicating the use of cell lines is the nutrient-rich media, which in the right cells can lead to increased metabolism and elevated production of oxidants. These oxidizing compounds can lead to DNA damage and mutations that may alter the genetic background of the cell and remove it further from the original background in the patient tumor. Finally, the tumor microenvironment also plays a considerable role in the oncogenesis, progression, recurrence, and resistance. This complex environment is comprised of not only the tumor cells, but also

immune cells and additional support cells. Without the influence of these contributors and the products they secrete into the tumor microenvironment, it is highly unlikely that one could accurately reproduce cell physiology with a single cell type under robust growth conditions in culture. Therefore, our results should be taken with these limitations in mind, and our future studies will move to using in situ systems to better understand how Sab levels influence CNS tumor cell physiology in the brain.

2.2 Lack of sample numbers and patient context.

Another critical limitation to our studies would be the number of cell lines employed in the work. The ten GBM cell lines, the four GSC lines, and the four established CNS-neuroblastoma cell lines are insufficient to generate the statistical power needed to make relevant correlations between events. A limited number of cells were used in these studies because the ultimate goal was to move the studies into a patient-derived animal-based system once funding for the project became available. It was our intention to take the lessons learned from cell culture and apply them to the animal models to produce more clinically-relevant data. Unfortunately, the project was only funded recently, and now the patient derived animal studies will begin. This approach also highlights another limitation, and that is the lack of robust patient data related to our cells. Beyond genetic characterization, many of the patient-relevant information did not accompany the cells, even the NCI-60 panel. This information may support or contradict some of the findings, and this information would be crucial when making claims about personalization. Ultimately, switching into patient-derived in vivo models will fill this

gap, as our collaborators at Baptist Health South Florida will collect all relevant patient information, and (at the appropriate time) share it with our team. Thus, future studies will be supported by significant clinical insights into the samples.

2.3 Studies employed largely endpoint analyses.

Our studies focused primarily on the current state of existing cells lines, at time points well after the manipulation of Sab expression, or after a prolonged exposure to chemotherapeutic compounds. It is likely that the pathways we are measuring are very dynamic and under the controll of synchronized regulation. Therefore, the physiology of the cell may undergo multiple changes before arriving at the final measured state. It is possible that one of the intermediate phases may contribute greatly to the measured event. Perhaps, the manipulation of Sab expression and treatment with toxic compounds could serve as further selective pressures, and the resulting cells are a product of these artificial systems making the results less than reliable. Regardless, future endeavors should consider more kinetic-based approaches to assay what happens over the course of these treatments not simply what occurs when a drug is most potent or ectopic expression is at its highest point.

2.4 Inability to express Sab isoform 2 in SF268-6 cells.

Unfortunately, the major experiment missing from Chapter 4 is the ectopic expression of Sab isoform 2 in the SF268-6 cells (the clone that only expresses full-length Sab). Because time was limited, only two attempts were made at liposome-mediated transfection of a plasmid encoding Sab isoform 2. In the immediate future, I am anticipating using lentiviruses to introduce the plasmid to

the cells and reintroduce Sab isoform 2 into these cells and then monitor the impact on glycolysis and respiration, with emphasis on complex I.

3. Future directions

Future directions related to this study will primarily consist of using orthotopic xenografts of patient-derived tumor cells and monitoring mitochondrial physiology in these tumors. Additionally, perturbations in cancer-specific alterations in mitochondrial function will be exploited in order to improve therapeutic outcomes in patients.

APPENDICES

Supplementary information for chapter 3

Supplemental figure 1. Expression of metabolic enzymes in GBM cell lines. GBM cell lines were grown, lysed, and metabolic enzymes protein levels were assessed by western blot. Expression was normalized to the actin loading control.

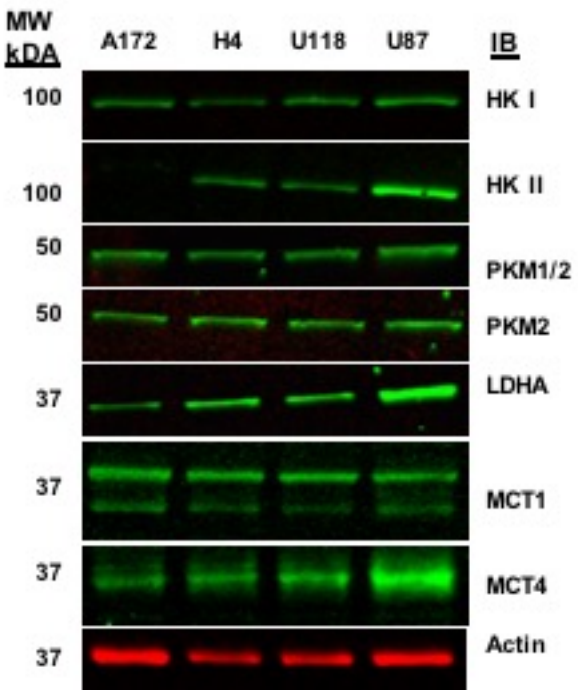

Supplemental Figure 2. Metabolic profiling. The respiratory profile of cells with and without the Sab splice variant was measured using the Seahorse XF-96 extracellular flux analyzer in the presence of Glucose, Glutamine, and or Pyruvate. (A) Basal respiration (B) maximum respiration (C) spare capacity (D) basal glycolysis, (E) maximum glycolysis (F) OCR/ECAR ratio. Comparisons between groups was performed using the Mann-Whitney test.

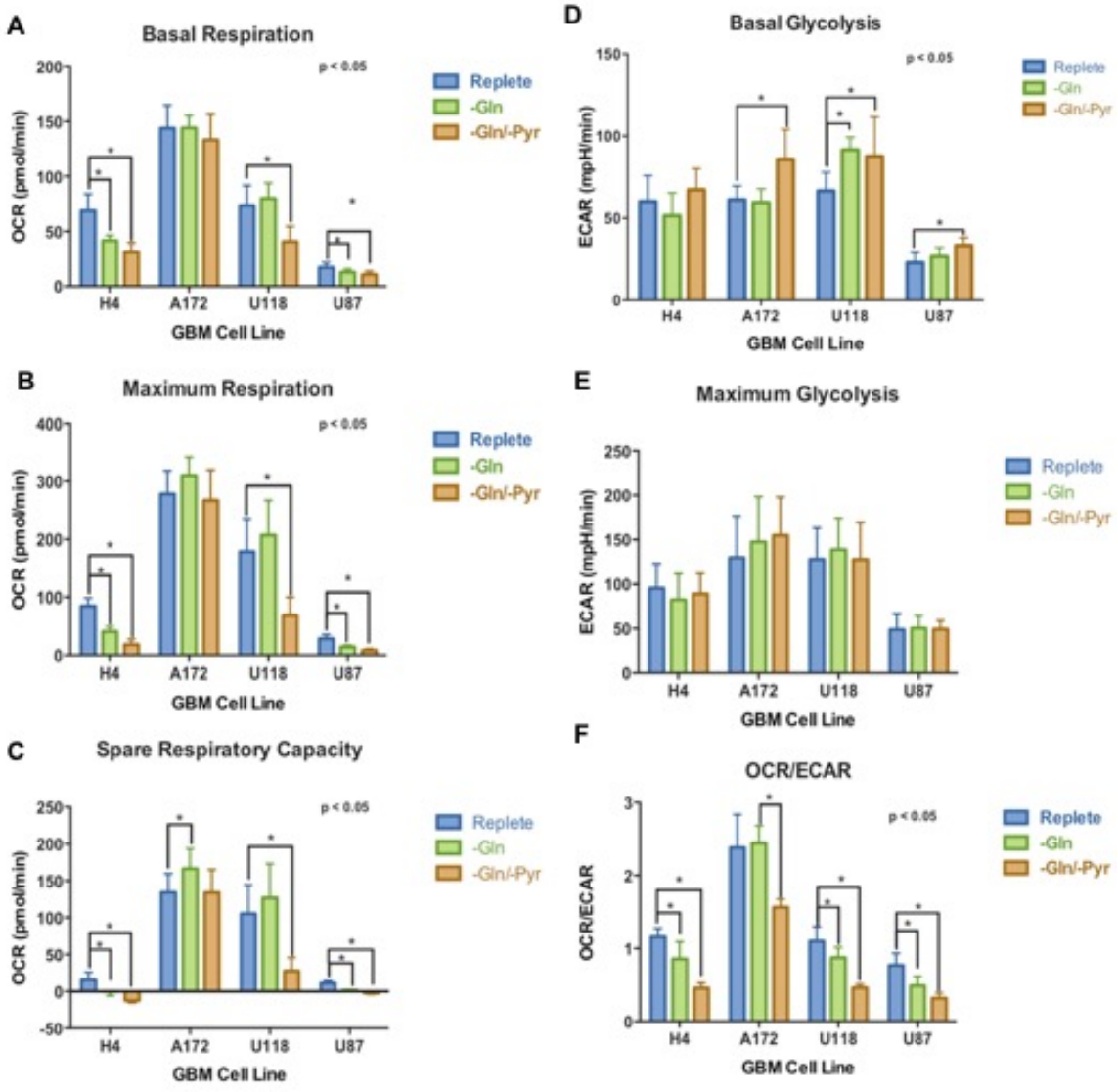

Supplemental Figure 3. MGMT expression in GBM cell lines. GBM cell lines were grown, lysed, and MGMT protein levels were assessed by western blot analysis for Bcl-2 family proteins. Expression was normalized to red Ponceau S staining. (A) Representative western blot. (B) Quantification of normalized protein expression.

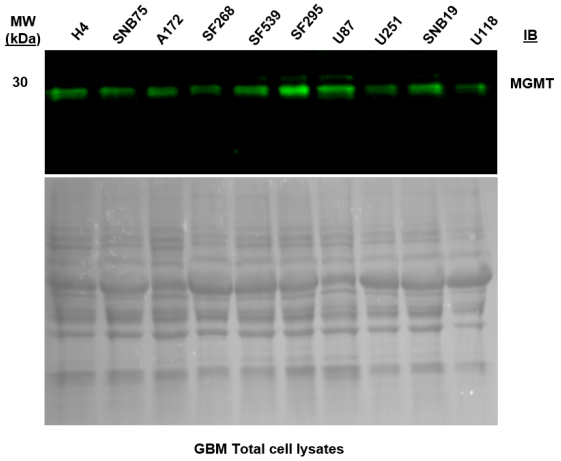

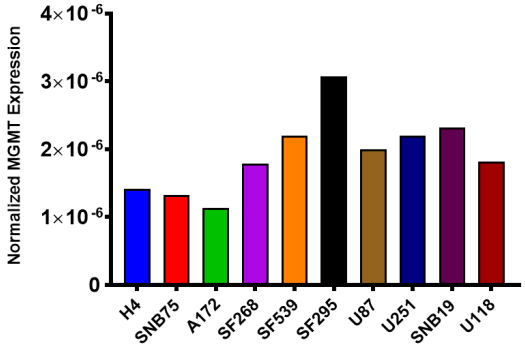

Supplemental Figure 4. Bcl-2 profiling of GBM cell lines. GBM cell lines were grown, lysed, and protein levels were assessed by western blot analysis for Bcl-2 family proteins. Expression was normalized to the actin loading control. (A) Representative western blot. Quantification of normalized protein expression of (B) Bcl-xL, (C) Bad, (D) Bid (E) Bik. One-way ANOVA was used to determine differences in protein expression between cell lines, $p<0.05$.

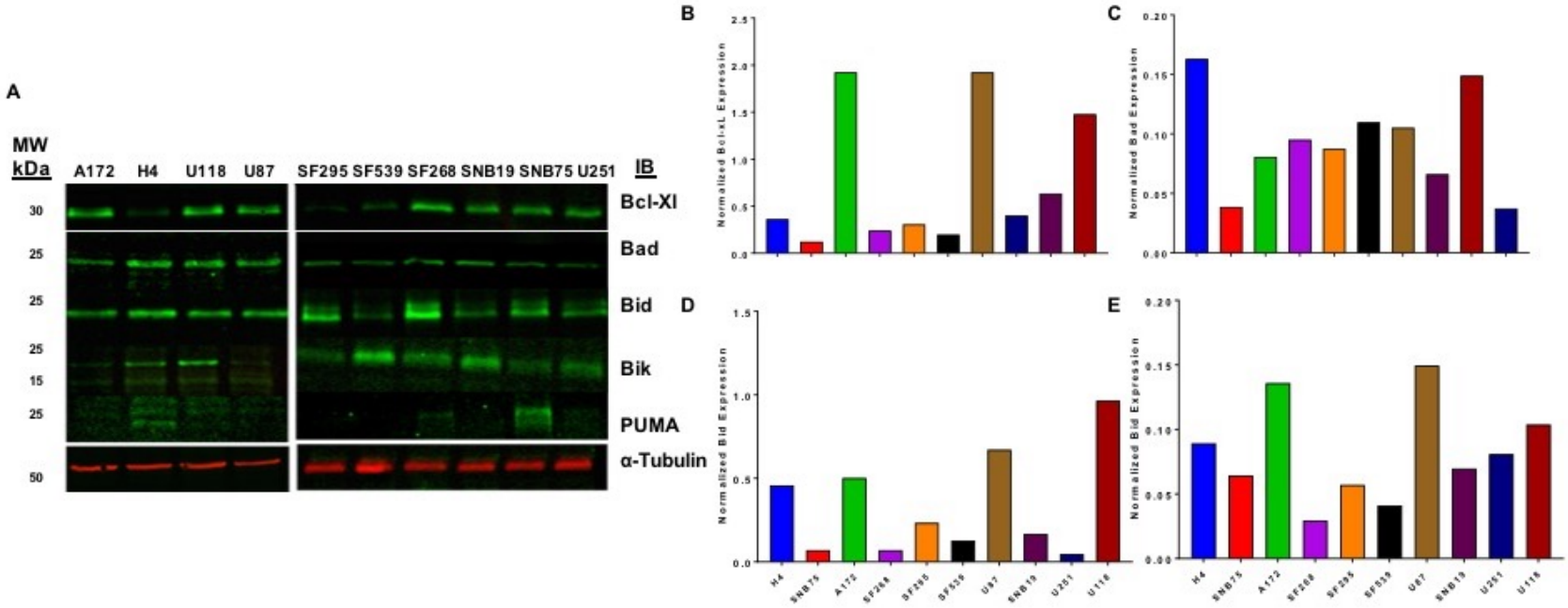

Supplemental Figure 5. Combination treatment of GBM cell lines with ABT-737 and chemotherapeutic drugs. GBM cell lines were incubated for 72 hours in the presence of 0-5μM of ABT-737, in combination with 125-250μM TMZ, 1-2.5 μM Irinotecan, or 35 μM Carboplatin. The cells were then fixed and stained with CellTag 700 stain to determine the number of cells. The fluorescence for each drug combination was plotted.

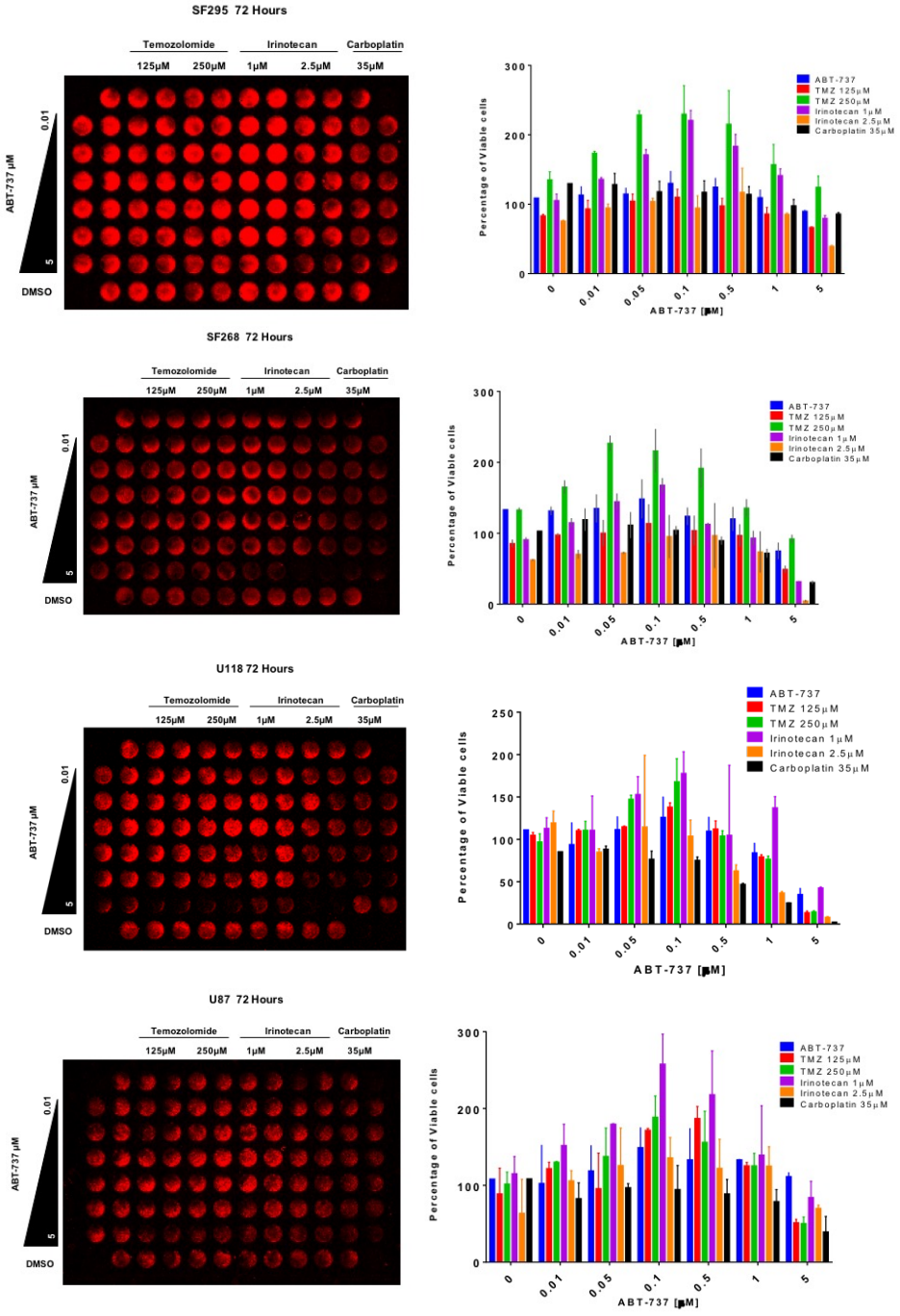

Supplemental Figure 6. Percentage of Cell Viability after treatment with Bcl-2 and Mcl-1 inhibitors in GBM Cell Lines. GBM cell lines were incubated for 72 hours in the presence of 0-10μM of ABT-737, 0-10μM S63845, or both. The cells were then fixed and stained with CellTag 700 stain to determine the number of cells (A) A172, SF268, (B) SF295, SF539, (C) U87, U118. The fluorescence for each TMZ dose was plotted (D, E, F, G, H, I) and comparisons between treatments was performed using ANOVA followed by Tukey's honest test. ***p<0.001, ****p<0.0001

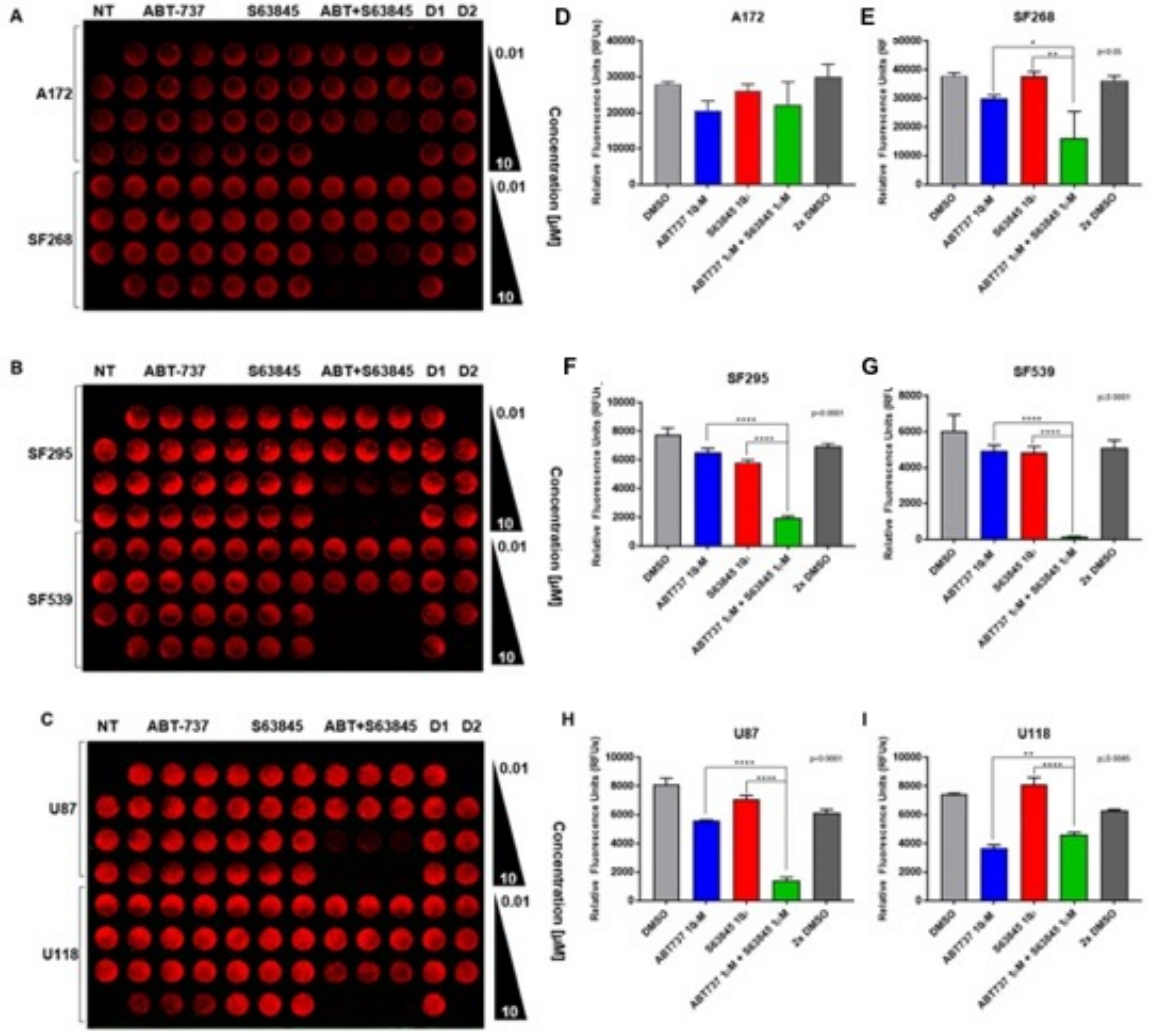

Supplemental Figure 7. Percentage of Cell Viability after treatment with Bcl-2 and Mcl-1 inhibitors in Glioma Stem Cells. GSCs were incubated for 72 hours in the presence of 0-10μM of ABT-737, 0-10μM S63845, or both. The cells were then fixed and stained with CellTag 700 stain to determine the number of cells. The fluorescence for each TMZ dose was plotted and comparisons between treatments was performed using ANOVA followed by Tukey's honest test. ***p<0.001, ****p<0.0001

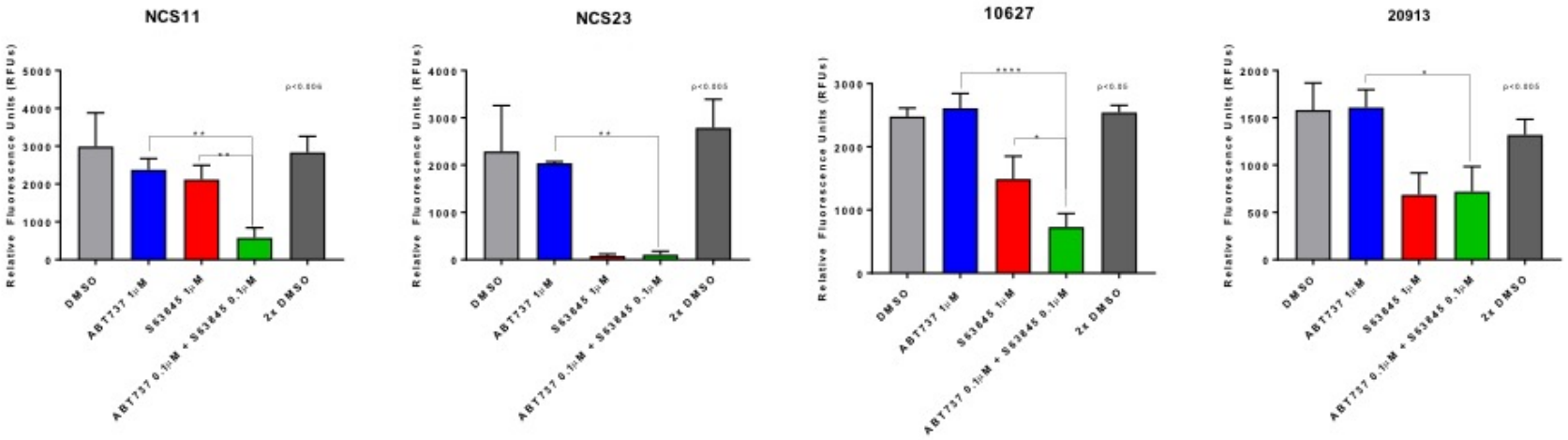

Supplementary information for chapter 4

Supplemental Figure 8. Sab expression in Glioma Stem Cells. GSCs were grown and lysed. Proteins (25μg) were quantified and resolved by SDS-PAGE. (A) Western blot analysis was used to detect Sab levels. Actin was used as loading control. (B) Quantification of expression levels.

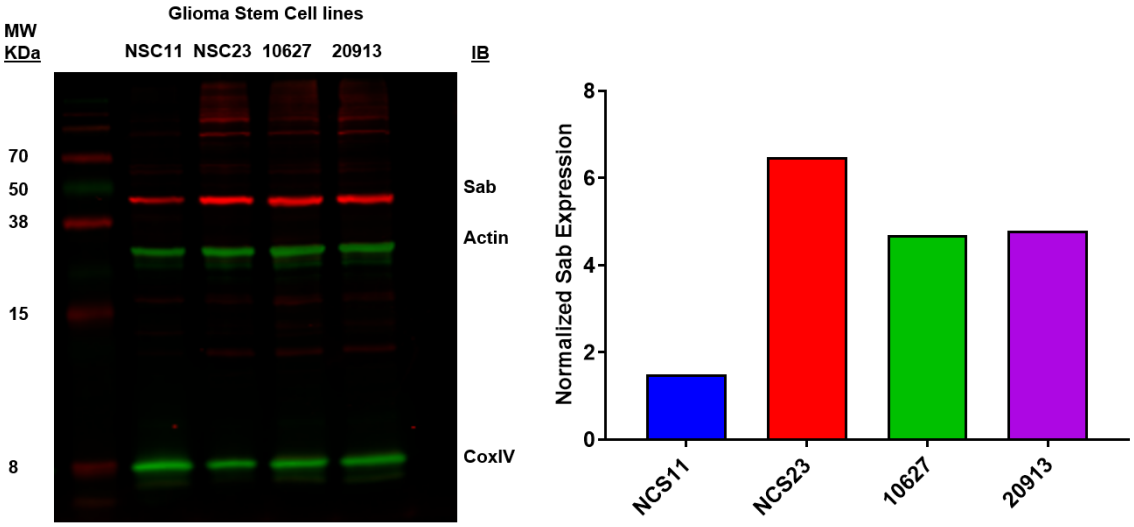

VITA

MONICA RODRIGUEZ SILVA

Born, Caracas, Venezuela

1997-2005	Lic. Biology Universidad Simon Bolivar Caracas, Venezuela
2013-2018	Doctoral Candidate Herbert Wertheim College of Medicine Florida International University Miami, Florida

FELLOWSHIPS, AWARDS AND HONORS

1. NIGMS-RISE Graduate Student Fellowship (2014-present). National Institutes of Health / National Institutes of General Medical Sciences. *NIH/NIGMS-R25-GM061347*
2. Summer Program in Neuroscience, Ethics and Survival (2016). National Institutes of Health / National Institutes of Mental Health. *NIH/NIMH-R25-MH055929*
3. ASCB MAC Graduate Student Award, sponsored by the ASCB Minority Affairs Committee, 2017.
4. Awarded Third Place Graduate Student Oral Presentation. MARC U*STAR and NIGMS RISE Student Biomedical Mini-Symposium, 2017.
5. Awarded First Place Graduate Student Oral Presentation. MARC U*STAR and NIGMS RISE Student Biomedical Mini-Symposium, 2016.
6. Recipient of ASBMB Graduate Student Award, sponsored by the ASBMB Minority Affairs Committee, 2016

PUBLICATIONS AND PRESENTATIONS

1. Rodriguez Silva M, Chinea A, Aberman Z, Colwell N, Gonzalez-Arias S, and Chambers J.W. *Bcl-2 profiling defines the therapeutic responsiveness in continuous glioblastoma cultures.* (Manuscript under preparation)
2. Rodriguez-Silva M, Portalatin G.M, Chambers T.P, Gonzales-Arias S, Chambers J.W. *Sab-mediated signaling influences metabolism and chemosusceptibility in human neuroblastoma cells.* (Manuscript under preparation)
3. Sodero A.O, Rodriguez-Silva M, Salio C, Sassoe-Pognetto M, Chambers J.W. *Sab is differentially expressed in the brain and affects neuronal activity.* Brain Research. 1670: 76-85. (2017).
4. Vanbellingen Q.P, Castellanos A, Rodriguez-Silva M, Paudel Iru, Chambers J.W, Fernandez-Lima F. *Analysis of chemotherapeutic drug delivery at the*

single cell level using 3D-MSI-TOF-SIMS. Journal of the American Society for Mass Spectrometry. 27(12): 2033-2040. (2016).

5. Vega V.L, Rodriguez-Silva M, Frey T, Gehrman M, Diaz J.C, Steinem C, Multhoff G, Arispe N, De Maio A. *Hsp70 Translocates into the Plasma Membrane after Stress and Is Released into the Extracellular Environment in a Membrane-Associated Form that Activates Macrophages. Journal of Immunology*. 180(6): 4299-307. (2008).
6. Ajami-Henriquez D, Rodríguez M, Sabino M, Castillo R.V, Müller A.J*, Boschetti-de-Fierro A, Abetz C, Abetz V, Dubois P. *Evaluation of cell affinity on poly(L-lactide) and poly(e-caprolactone) blends (PLLA/PCL) and on PLLA-b-PCL diblock copolymer surfaces*. *Journal of Biomedical Materials Research A.* 87(2): 405-17. (2008).
7. Rodriguez Silva M, and Chambers J.W. *A novel splice variant of Sab (SH3BP5) alters mitochondrial physiology.* (Poster Presentation). American Society for Cell Biology Meeting, ASCB/EMBO 2017, Philadelphia, PA, December 2-6,2017.
8. Wang W, Rodriguez Silva M, Chambers J.W. and Tse-Dinh Y. *Exth-09. Tdp1/top1 ratio as a predictive indicator for the response of glioblastoma cancer cells to irinotecan treatment.* (Poster Presentation). Society for Neuro-oncology Meeting, San Francisco, CA, November 16-19,2017.
9. Rodriguez Silva M, and Chambers J.W. *A novel splice variant of Sab (SH3BP5) alters mitochondrial physiology.* (Oral Presentation). MARC U*STAR and NIGMS RISE Student Biomedical Mini-Symposium, Miami, FL, October 12-13, 2017.
10. Rodriguez Silva M, and Chambers J.W. *Combined BH3 and Metabolic Profiling as Method to Define Chemoresponsiveness in Glioblastoma multiforme.* (Oral Presentation). MARC U*STAR and NIGMS RISE Student Biomedical Mini-Symposium, Miami, FL, October 3-4, 2016.
11. Rodriguez Silva M, Gonzalez-Arias S, and Chambers J.W. *Combined BH3 and Metabolic Profiling Define Chemoresponsiveness in Glioblastoma multiforme.* (Poster Presentation). Experimental Biology Meeting, EB2016, San Diego, CA, April 2-6. 2016.
12. Rodriguez Silva M, Chinea A, Aberman Z, Colwell N, Gonzalez-Arias S, and Chambers J.W. *Combined BH3 and Metabolic Profiling as a Method to Define Therapeutic Response and Resistance in Grade IV Astrocytomas.* (Poster Presentation). Society of Neuro-Oncology 20th Annual Scientific Meeting, San Antonio, TX, November 19-22, 2015.
13. Rodriguez Silva M, Aberman Z, Portalatin G.M., Chambers T.P., Gonzalez-Arias S, and Chambers J.W. *Sab-mediated signaling influences aerobic glycolysis and chemosusceptibility in human neuroblastoma cells*. (Poster Presentation). Society of Neuro-Oncology 20th Annual Scientific Meeting, San Antonio, TX, November 19-22, 2015.